Auxin signal in tobacco BY-2 cells

- Actin sensory role for auxin and auxin subcellular distribution

Zur Erlangung des akademischen Grades eines

DOKTORS DER NATURWISSENSCHAFTEN

(Dr. rer. nat.)

der KIT-Fakultät für Chemie und Biowissenschaften

des Karlsruher Instituts für Technologie (KIT)

genehmigte

DISSERTATION

von

Xiang Huang

aus

Jiangxi, China

Dekan: Prof. Dr. Willem Klopper

Referent: Prof. Dr. P. Nick

Korreferent: Prof. Dr. M. Bastmeyer

Tag der mündlichen Prüfung: 17.10.2017

Die vorliegende Dissertation wurde am Botanischen Institut des Karlsruher Instituts für Technologie (KIT), Botanisches Institut, Molekulare Zellbiologie, im Zeitraum von Oktober 2013 bis September 2017 angefertigt.

Hiermit erkläre ich, dass ich die vorliegende Dissertation, abgesehen von der Benutzung der angegebenen Hilfsmittel, selbstständig verfasst habe.

Alle Stellen, die gemäß Wortlaut oder Inhalt aus anderen Arbeiten entnommen sind, wurden durch Angabe der Quelle als Entlehnungen kenntlich gemacht.

Diese Dissertation liegt in gleicher oder ähnlicher Form keiner anderen Prüfungsbehörde vor.

Karlsruhe, im September 2017
Xiang Huang

Acknowledgments

I would like to take this opportunity to express my gratitude to all those people who helped me during my study.

First of all, I would like to thank Prof. Dr. Peter Nick for offering me the opportunity to start a new journey in Botanical Institute. His suggestions for the project, insights into questions, patience and kindness to other people, enthusiasm for life and science not just help and encourage me during my study period, but also will inspire my life in future.

I am grateful that Prof. Dr. Martin Bastmeyer agreed to be my co-examiner immediately and I really appreciate his time, devotion and expertise.

My special thanks to Prof. Dr. Ken-ichiro Hayashi from Okayama University of Science for providing the fluorescent auxin analogs, and Dr. Jan Petrášek from Institute of Experimental Botany, Academy of Sciences of the Czech Republic for providing the PIN1-GFP cell strain.

I would like to thank Dr. Jan Maisch, Dr. Qiong Liu, Dr. Michael Riemann, and Dr. Beatrix Zaban for their help and suggestions during my work. My special thanks to Dr. Qiong Liu for providing NtTPC1A-GFP cell strain. I appreciate the excellent technical support from Sabine Purper. My sincere thanks go to all the members who work in Botanical Institute for creating a happy, smooth and helpful working atmosphere. Also thanks to my Chinese friends working in the lab for their constant help and support in the daily life.

Finally, I would like to thank my dear parents who always understand, respect and support me for all these years.

This work is financially supported by the China Scholarship Council (CSC).

Xiang Huang

Table of Contents

Abbreviations

2,4-D: 2,4-dichlorophenoxyacetic acid

ABA: abscisic acid

ABP1: AUXIN BINDING PROTEIN 1

ADF2: actin-depolymerization factor 2

ARFs: AUXIN RESPONSE FACTORs

Aux/IAA: Auxin/INDOLE-3-ACETIC ACID

AUX/LAX: AUXIN1/LIKE-AUX1

BDM: 2,3-butanedione monoxime

BRs: brassinosteroids

BY-2: Bright Yellow 2

DMSO: dimethyl sulfoxide

ER: endoplasmic reticulum

FABD2: fimbrin actin-binding domain 2

GA: gibberellin

GFP: green fluorescent protein

IAA: indole-3-acetic acid

IAM: indole-3-acetamide

IAOx: indole-3-acetaldoxime

IPyA: indole-3-pyruvic acid

JA: jasmonic acid

MI: mitotic index

NAA: naphthalene-1-acetic acid

NBD: 7-nitro-2,1,3-benzoxadiazole

NtTPC1A: *Nicotiana tabacum* Two Pore Channel 1A

PA: phosphatidic acid

PIN: PIN FORMED

PIP2: phosphatidylinositol 4,5-bisphosphate

SCF: Skp1-Cullin-F-box

TIR1: TRANSPORT INHIBITOR RESPONSE1

TIR1/AFB: TRANSPORT INHIBITOR RESPONSE1/AUXIN SIGNALING F-BOX

Trp: tryptophan

WT: wild type

Zusammenfassung

Auxin spielt für die Steuerung von Wachstum und Entwicklung der Pflanze eine zentrale Rolle, indem es verschiedene äußere und innere Signale zu integrieren vermag. Viele Auxinantworten stehen Veränderungen des zellulären Auxinpegels in Zusammenhang und werden über Auxinbiosynthese, -metabolismus und polaren Transport moduliert. Der polare Auxintransport wird durch die polare Lokalisierung von Auxin-Efflux-Transportern bestimmt, die zwischen dem Zellinneren und der Plasmamembran in Abhängigkeit von Actin zirkulieren. Die Actindynamik beeinflusst, über die Wirkung auf den Auxintransport, auch den zellulären Pegel von Auxin und vermutlich auch die Auxin-Responsivität. Obwohl die Mechanismen von Auxintransport und auxinabhängiger Genexpression intensiv bearbeitet wurden, sind immer noch zentrale Fragen der Auxinbiologie unklar geblieben.

Um die mögliche Verbindung zwischen Auxin-Responsivität und Actindynamik zu untersuchen, wurden spezifische Entwicklungsantworten vergleichend zwischen einer untransformierten Tabak BY-2 Linie (Nicotiana tabacum L. cv Bright Yellow 2) und der transgenen BY-2 Linie GF11 charakterisiert. Bei dieser Linie wird eine GFP Fusion der Actinbindedomäne 2 von Fimbrin stabil exprimiert, was die Actindynamik leicht, aber signifikant vermindert. Die Entwicklungsantworten in der Zellkultur konnten in drei abgegrenzte Stadien unterteilt werden: Zellproliferation, Zellelongation und Zellfaden-Disintegration. Verschiedene Merkmale wurden in Antwort auf verschiedene Konzentrationen des natürlichen Auxins (Indol-3-Essigsäure, IES) quantifiziert. Durch Zugae von Auxin zur Wildtyp BY-2 Linie konnte die mitotische Aktivität stimuliert und verlängert werden, ebenfalls war der Übergang von der Proliferations- zur Elongationsphase verzögert. Beide Antworten waren in der GF11 Linie unterdrückt, konnten aber bei höheren Konzentrationen auch hier ausgelöst werden. Während der stationären Phase des Kultivationszyklus, beschleunigte Auxin im Wildtyp die Disintegration der Zellfäden.

Interessanterweise war diese Antwort in der GF11 Linie nicht unterdrückt, sondern in Richtung auf eine vollständigere Individualisierung der Zellen verstärkt Diese Antworten waren nicht von signifikanten Veränderungen in der Organisation von Actin begleitet. Diese Daten konnten durch ein Modell erklärt warden, wonach die reduzierte Actindynamik in der GF11-Linie eine Actinfunktion verändert, die nicht strukturell, sondern sensorisch ist und mit der Transduktion des Auxinsignals in Verbindung steht, was durch die Tatsache unterstützt werden, dass diese Antworten bei höherer Konzentration von Auxin ausgelöst werden konnten.

Diese Ergebnisse stellen eine Verbindung zwischen dem lokalen Auxinpegel und, vermittelt durch Actindynamik, der Auxin-Responsivität, her. Freilich weiß man noch sehr wenig über die subzelluläre Auxinverteilung. Um die Auxinverteilung und Bindeeigenschaften von Auxin in Tabak BY-2 Zellen untersuchen zu können, wurden fluoreszente Auxinanaloga [7-nitro-2,1,3-benzoxadiazole (NBD) konjugierte Naphthyl-1-Essigsäure (NBD-NAA) und NBD konjugierte Indole-3-Essigsäure (NBD-IAA)] eingesetzt, die über eine Kooperation mit der Gruppe von Prof. Dr. Hayashi von der Okayama University of Science verfügbar waren. Doppelvisualisierung mit fluoreszenten Markern für spezifische Organellen zeigte, dass NBD-NAA mit dem Endoplasmatischen Reticulum (ER) und dem Tonoplasten assoziiert war, während NBD-IAA nur an das ER gebunden vorlag. Um die Spezifität der Bindung zu überprüfen wurden Kompetitionsexperimente mit unmarkierten Auxinen (IES, NAA, 2,4-D) durchgeführt und über eine Kreuzkorrelationsanalyse quantifiziert. Hierbei konnte NAA sehr wirksam sowohl mit NBD-NAA als auch mit NBD-IAA um die Bindestellen konkurrieren. Hingegen konnten IAA und 2,4-D, wenn auch weniger wirksam als NAA, nur mit NBD-NAA konkurrieren. Diese Befune zeigen, dass es zwei unterschiedliche Typen von Auxinbindestellen auf dem ER gibt, die sich hinsichtlich ihrer Affinität für NAA und IES unterscheiden. Ebenfalls gibt es zwei Bindestellen auf dem Tonoplasten, die NAA und 2,4-D mit unterschiedlicher Affinität binden. Jedes Organell ist daher mit unterschiedlichen Auxinbindestellen ausgestattet, die unterschiedliche Auxine mit unterschiedlicher

Affinität zu binden vermögen, was auf unterschiedliche Auxin-Signalwege hindeutet.

Abstract

Auxin plays a central role in the regulation of plant growth and development by integrating external and internal stimuli into auxin signal pathway. Many auxin responses are closely connected with modulations of cellular auxin level, which is under the control of auxin biosynthesis, metabolism, and polar transport. The polar auxin transport depends on the polar localization of auxin-efflux carriers. The cycling of these carriers between cell interior and plasma membrane depends on actin. The dynamics of actin, by affecting auxin transport, also change intracellular auxin level and, presumably, control the auxin-responsiveness. Although the mechanisms of auxin transport and auxin regulation of gene expression have been intensively studied, there are still many fundamental questions of auxin biology to be elucidated.

To study the potential link between auxin-responsiveness and actin dynamics, specific developmental responses were investigated and compared between the non-transformed tobacco BY-2 (*Nicotiana tabacum* L. cv Bright Yellow 2) cell line and the transgenic BY-2 line GF11, which could stably express a GFP-fimbrin actin-binding domain 2 construct causing slightly but significantly decrease actin dynamicity. The developmental responses in the cell line could be divided into three distinct stages: cell cycling, cell elongation and file disintegration. Several characters were quantitatively monitored in response to different concentrations of exogenous natural auxin (indole-3-acetic acid, IAA). By application with auxin to wild type BY-2 cell line, the mitotic activity was stimulated and prolonged, and the exit from the proliferation phase was delayed. In contrast, both responses were suppressed in the GF11 line, but could be observed at higher concentrations. Likewise, during the stationary phase of the cultivation cycle, auxin strongly accelerated the cell file disintegration in wild type BY-2 cell line. Interestingly, this response was not suppressed but progressed to a more complete disintegration in the GF11 line. These responses were not accompanied by significant alternations in the organization of

actin filaments. These data could be explained by a model, where the reduced dynamics of actin in the GF11 line altered a function of actin that is not structural, but sensory and linked with auxin signaling as indicated by the fact that these responses could be elicited at higher concentrations of auxin.

As shown by these results, local auxin level, through actin dynamics, links with auxin-responsiveness. However, the understanding of subcellular auxin distribution in is still limited. To probe subcellular auxin distribution and binding characteristics in the tobacco BY-2 cell, fluorescent auxin analogues [7-nitro-2,1,3-benzoxadiazole conjugated naphthalene-1-acetic acid (NBD-NAA) and NBD conjugated indole-3-acetic acid (NBD-IAA)] were employed which were available through a cooperation with the group of Prof. Dr. Hayashi in Okayama University of Science. Through dual-labeling with fluorescent markers tagged to specific organelles, it was found that NBD-NAA was localized to the endoplasmic reticulum (ER) and the tonoplast, whereas NBD-IAA was only localized to the ER. In addition, non-labelled auxin (NAA, IAA, 2,4-D) was used in competition experiments with NBD-NAA or NBD-IAA to probe specificity of binding of the fluorescent analogues for the binding sites. To quantify the binding, cross-correlation analysis was employed. Here, NAA could very efficiently compete with both NBD-NAA and NBD-IAA for the binding sites. However, IAA and 2,4-D, while being less efficient as NAA, could still affect NBD-NAA binding to the binding sites. These findings reveal that there are two types of distinct auxin binding sites at the ER with distinct affinity for NAA and IAA binding; likewise, there are two types of distinct auxin binding sites at the tonoplast for NAA and 2,4-D binding. Thus, each organelle harbors auxin-binding sites that allow recognizing different types of auxins with different sensitivity, indicative of different transduction chains.

1. Introduction

1.1 What is signal

All living creatures are surrounded by the ocean of signals. At any place and any time, from the simplest living unit like bacteria to the most complex living creature like human are all receiving and processing signals from the external and internal. “To be or not to be”, the life of living organism depends on the capability of perceive and process signals. So, what is signal? It is not easy to precisely define the conception of signal. Anything providing information can be perceived by some organisms is a signal. The signal can represent the resource of food, danger of predator, change of temperature, release of chemicals, some voices for communication, and so on. The sources of signals, the forms of signals are various.

The signals occur at the spatial level and the temporal level. In the simplest way, something complete new suddenly appeared can be a signal for the living creature. For instance, the sight of carnivore coming close can alert herbivores preparing to run away from danger. In plant, when touched by animals, the compound leaves of *Mimosa pudica* fold inward and droop to protect themselves from harm (Amador-Vargas *et al*., 2014). Even the unicellular organisms, like *Euglena gracilis*, possess a cellular structure identified as the eyespot to assist the movement in response to light (James *et al.*, 1992). Another kind of signal is the quantity change of something already exists. As an organism, it is impossible to react to every stimulus which is quite uneconomical. So, nothing would happen until the stimulus passes the threshold. A well-known example is the action potential in neurons, as the first direct recording of the electrical changes across the neuronal membrane by Hodgkin and Huxley (Hodgkin and Huxley, 1939). The action potentials are generated by ion channels forming the permeation pathways to across the neuronal membrane. Neurons maintain a voltage difference between the exterior and interior of the cell by pumping

Na^+ out and K^+ in. Initial stimulation of sensory nerve leads to a local depolarizing response, opening a few Na^+ channels to increase inflowing of Na^+. As a result, the resting membrane potential around -60 to -70 mV approaches to the ‘‘threshold’’ value around -45 mV, then it causes a rapid recruitment of all the Na^+ channels open leading to the fast reach of the full action potential. After that, the K^+ channels open and outflowing of K^+ brings the membrane potential back (Barnett and Larkman, 2007). Even more complex form of signal could be the pattern change of stimuli. A famous example is plant photoperiodism, which plants require the relative lengths of day and night periods in order to flower (Garner and Allard, 1920). Later, it was found out that the length of night was the critical factor (Hamner and Bonner, 1938; Hamner, 1940): when the night length is shorter than the critical photoperiod, long-day plants flower; for the short-day plants require a continuous period of darkness exceeding their critical photoperiod, short nights or pulse of some light for several minutes during the night prevent short-day plants flower (Aus ń *et al*., 2005). As above pointed out, it is clear that the signals to the living organisms exhibit vast diversity, and correspondingly the creatures have to develop plentiful solutions while facing the survival challenge.

1.2 Architecture basis for signal perception and transduction

As in nature, there are plenty of signals existing all the time. How to distinguish the useful signals from the noise, which accounts for the majority part? Therefore, the organisms have to evolve special mechanisms to precisely receive and transduce the desired signals to survive during the evolution. The process of proceeding signals occurs in the organisms, which actually always happen at subcellular level with special molecular reactions. For instance, a more or less symmetric zygote can divide and generate an embryo with clear axis and polarity, which will then develop into an independent and complex organism. This is only possible, because signals from the environment or the neighboring cells orient subcellular architecture of the cell as the basic structural and functional unit of development. This means that some

components of subcellular architecture must be able to perceive and process orienting signals, and to transduce them into a morphogenetic response. In the following sections, architecture basis for signal perception and transduction about how cells sense and respond to signals will be introduced.

1.2.1 Receptor

The most common basics for signal sensing are receptors, which are protein molecules being able to sense signals. According to their location, receptors could be classified into transmembrane receptors and intracellular receptors. As the plasma membrane separate the interior of cell from the outside environment, many receptors are embedded in the membrane in order to receive first sign from extracellular signaling. In plant pathogen defense, plant cells could recognize many molecules produced by microbial pathogens, so called elicitors, which trigger innate immune responses in plants (Jones and Dangl, 2006). Classical examples include the hepta-beta-glucoside-binding protein for oomycete glucans in soybean (Cheong and Hahn, 1991; Umemoto *et al*., 1997), FLS2 protein for bacterial flagellin in *Arabidopsis thaliana* (Gomez-Gomez and Boller, 2000), EFR protein for bacterial EF-Tu in *Nicotiana benthamiana* (Zipfel *et al*., 2006), CEBiP protein for fungal chitin in suspension-cultured rice cells (Kaku *et al*., 2006), and LeEix protein for fungal ethylene-inducing xylanase (EIX) in tomato *Lycopersicon esculentum* (Ron and Avni, 2004).

Some other receptors locating at cytoplasm can not only response to signals, but might also be part of signaling itself by changing the spatial distribution. In mammalian cells, the glucocorticoid receptor will, upon binding of glucocorticoid ligands, translocate into the nucleus to regulate the transcription of specific genes (Rhen and Cidlowski, 2005). Likewise, in plant cells, phytochromes are a class of photoreceptor to detect the light environment and synthesized in the inactive Pr form in the cytosol. The Pr form phytochrome can convert to the biologically active Pfr

form under red light irradiation. Conversely, the Pfr form can convert back to the inactive Pr form by absorbing far-red light (Devlin *et al.*, 2007). Then the light-activated phytochrome shift into the nucleus and activate the transcriptional regulator Phytochrome-Interacting Factor (Leivar and Quail, 2011; Casal *et al*., 2014). In addition, some receptors are retained in the nucleus. One unique property of nuclear receptor is the capability to directly bind to DNA, causing the regulation of gene expression. For example, thyroid hormone receptor in mammalian cells (Oppenheimer *et al*., 1972; Flamant *et al*., 2006) and TRANSPORT INHIBITOR RESPONSE1 (TIR1) protein for auxin receptor in plant cells (Dharmasiri *et al*., 2005a; Kepinski and Leyser, 2005).

1.2.2 Cytoskeleton

The cytoskeleton is found underlying the cell membrane in the cytoplasm and provides scaffolding structure for membrane proteins to anchor. Besides, the cytoskeleton elements interact extensively and communicate bidirectionally with cellular membranes (Doherty and McMahon, 2008). The main role of the cytoskeleton in animal cells is to control cell shape. Since the cytoskeleton consists of elements able to confer compression forces (microtubules), and of elements able to confer traction forces (actin filaments), it can act as tensegral structure integrating mechanic forces over the entire cell and is central for this signal-dependent morphogenetic response. For example, focal adhesion formation (actin filaments involved) at the front of the cell and disassembly (microtubules involved) at the rear are important for the migration of adherent cells (Ezratty *et al*., 2005). Whereas cytoskeletal tensegrity of animal cells is used to maintain cellular structure (Ingber, 2003), the situation is different in plant cells, where the architectural functions of the cytoskeleton are partially adopted by the plant cell wall, providing the potential for a functional shift of the cytoskeleton. Considering the highly dynamic properties of cytoskeleton, the composition and decomposition of cytoskeleton elements also provide the functional basis for other non-structure role. Here, cytoskeletal tensegrity

might be used for sensing or signal processing (Nick, 2013).

Several environmental signals, such as sound vibrations, osmotic stress, cold and heat, act by exerting a mechanical force upon the plasma membrane (Los and Murata, 2004; Mishra *et al*., 2016). Only in a second step, these mechanical forces are translated into biochemical signals, which in walled plant cells involve the cytoskeleton–plasma membrane–cell wall continuum (Wyatt and Carpita, 1993; Pont-Lezica *et al*., 1993; Baluška *et al*., 2003). This functional unit has also been demonstrated for tobacco BY-2 cells (Gens *et al*., 2000), and is thought to perceive, integrate and process mechanical stimuli, and transduce them into appropriate responses of growth. These morphogenetic responses seem to be linked with cortical microtubules that establish and reinforce the axis of cell division and cell expansion by guiding the direction of cellulose deposition (Li *et al*., 2015). In addition to morphogenetic responses, external stimuli can cause other developmental responses of the target cells that are rather linked with the second component of the plant cytoskeleton, actin filaments, including actin microfilament rearrangements (Mishra *et al*., 2016). The importance of actin remodeling is also well established during programmed cell death (Gourlay and Ayscough, 2005; Smertenko and Franklin-Tong, 2011). When actin filaments rapidly detach from the cell membrane and contract into dense cables, this is often a hallmark for ensuing cell death (Guan *et al*., 2013; Chang *et al*., 2015). Another example is auxin, as endogenus plant signal, is directionally transported depending on the polar localization of auxin-efflux carriers (Robert and Friml, 2009). The cycling of these carriers between cell interior and plasma membrane depends on actin (Zhu and Geisler, 2015). Actin, in turn, is remodeled depending on auxin constituting a self-referring feedback loop that can act as oscillatory signaling hub (Nick, 2010). This actin-auxin oscillator involves auxin-dependent recruitment of actin-associated proteins such as actin depolymerization factor 2 (Durst *et al*., 2013), but also integrates stress-related signals, such as superoxide ions generated by the membrane located NADPH oxidase RboH (Chang *et al.*, 2015). Auxin employs these superoxide anions to trigger signaling across the membrane signals, involving activation of

phospholipase D producing phosphatidic acid (PA) and phosphatidylinositol 4,5-bisphosphate (PIP_2). Since PA sequesters actin-capping proteins, and PIP2 the actin-depolymerization factor, exogenous auxin will modulate actin dynamics and bundling (Eggenberger *et al*., 2017). The bidirectional relationship between signaling and cellular organization is reflected in a dual role of the cytoskeleton as central element of cytoplasmic architecture.

1.3 auxin as the most cardinal signal molecules for plant

Plant hormones, as endogenous signal molecules, have very wide impact on plant growth, although their concentrations in plant tissue or cells are extremely low. They are used as molecular messengers to control physiological processes during the plant development and stimuli response. Auxin, known as the first-identified plant hormone, is synthesized in the young and growing plant tissue, transported and induced a growth response in other plant tissues (Bonner and Bandurski, 1952; Bartel, 1997; Woodward and Bartel, 2005; Tanaka *et al*., 2006). According to Charles Darwin's observation on phototropism of *Phalaris canariensis* coleoptiles, he proposed the existence of signal molecules transmitted from the tip of coleoptile downward, causing phototropic curvature (Darwin, 1880). Since then, many efforts have been made to try to elucidate the mechanism and finally it was identified light-mediated asymmetric redistribution of auxin from the sunny side to the shaded side, causing differential growth rate and phototropic curvature (Enders and Strader, 2015). In addition to auxin, there are other major classes of natural plant hormones: cytokinins, abscisic acid (ABA), ethylene, gibberellins (GAs), brassinosteroids (BRs), and jasmonic acid (JA). Every kind of hormone can regulate a vast amount of cellular and developmental processes; meanwhile multiple hormones often control a common single process. For example, cytokinins play a central role during cell division, leaf growth and shoot formation, as well as induce resistance against pathogen infection (Skoog and Miller, 1957; Werner *et al*., 2001; Choi *et al*., 2011). When plants are under stress, like cold temperature, salt and drought stress, ABA acts as an inhibitory

chemical compound, causing plant adaptive behaviors, such as seed and bud dormancy and stomatal closure (Schroeder *et al*., 2001; Finkelstein *et al*., 2002; Zhu, 2002; Kermode, 2005). As for GAs, they are also associated with several plant growth and development processes, such as seed germination, stem elongation, and flowering, as well as linked to stress tolerance, including cold, salt and osmotic stress (Reid, 1993; Blazquez *et al*., 1998; Gomi and Matsuoka, 2003; Colebrook *et al*., 2014). One of the most important plant research applications related to the GA is the "green revolution". Those dwarf mutants, such as gene *sd1* in rice and gene *Rht* in wheat, are involved in the biosynthesis and signaling pathways of GA (Peng *et al*. 1999; Sasaki *et al*. 2002).

Besides these natural auxins, many compounds with clear auxin functional activity were synthesized. Such as, 2,4-dichlorophenoxyacetic acid (2,4-D) (Sharp and Gunckel, 1969), naphthalene-1-acetic acid (NAA) (Beyer and Morgan, 1970), 4-amino-3,5,6-trichloropicolinic acid and 2,4,5-Trichlorophenoxyacetic acid (2,4,5-T) (Hamaker *et al.*, 1963). These synthetic auxins are used as herbicide to kill broadleaf weeds by mimicking the action of natural auxin, which results in an uncontrolled way of plant growth and eventually causes susceptible plant death (Grossmann, 2010; Song, 2014).

The regulate functions of plant hormones are not isolated from each other; instead there are close and active interaction among them. For instance, ethylene or JA can rapidly promote *ERF1* expression, which encodes a transcription factor to regulate the expression of pathogen defense genes, and treatment with both of them synergistically activates *ERF1* (Lorenzo *et al*., 2003). In contrast, hormones also show antagonistic interactions. In the formation of lateral roots, auxin promotes the process while cytokinins application suppresses root formation and reverses the auxin effect (Zhang and Hasenstein, 1999; Casimiro *et al*., 2001; Woodward and Bartel, 2005). What is even more interesting is the way of interaction between hormones can be altered by extra factors: under unstressed condition, auxin and cytokinins act antagonistically to

maintain the root meristem. However, aluminum-induced stress causes a synergistic way of both hormones to mediate root growth inhibition in *Arabidopsis* (Yang *et al*., 2017). Despite these hormones exhibit extensive cross-talk and signal integration with each other during plant developmental signaling pathways, the details about these molecular coordinated regulations are still far from clear.

1.3.1 Auxin manipulate plant development and and gene experession

The term “auxin” is derived from the Greek word “auxein” meaning “to grow”. Auxin, including natural and synthetic auxins, plays an important and central role in the regulation of plant growth and development at cellular level and plant organ level. For example, cell division (Stals and Inze, 2001; Campanoni and Nick, 2005), cell elongation (Rayle and Cleland, 1992; Campanoni and Nick, 2005), cell differentiation (Dello Ioio *et al*., 2008; Ishida *et al*., 2009), embryonic axis development (Weijers *et al*., 2006; Ueda *et al*., 2011), plant apical dominance and shoot branching (Shimizu-Sato *et al*., 2009), vascular system development (Mattsson *et al*., 1999), and phyllotaxis formation (Reinhardt *et al*., 2003).

The natural auxin indole-3-acetic acid (IAA), as major intrinsic developmental signal, has a wide effect on plant growth and development. Auxin control plant morphogenesis by manipulating auxin-related gene expression. This manipulation is strongly relied on the auxin intracellular level. When the concentration of IAA is below a threshold level, the activity of transcription factors, AUXIN RESPONSE FACTORs (ARFs), is repressed by Auxin/INDOLE-3-ACETIC ACID (Aux/IAA) repressor proteins (Tiwari *et al*., 2004; Chapman and Estelle, 2009; Wang and Estelle, 2014); whereas in the presence of high concentration of IAA, IAA molecule promotes the binding of an Aux/IAA protein and a TRANSPORT INHIBITOR RESPONSE1/AUXIN SIGNALING F-BOX (TIR1/AFB) protein, forming a co-receptor for IAA (Dharmasiri *et al*., 2005a; Kepinski and Leyser, 2005; Chapman and Estelle, 2009). As a result, it leads to the ubiquitination of Aux/IAA through the

Skp1-Cullin-F-box (SCF) ubiquitin ligase complex with TIR1/AFB protein and degradation of Aux/IAA via the proteasome (Gray *et al.*, 2001; Zenser *et al.*, 2001; Liscum and Reed, 2002; Dharmasiri *et al*., 2003; Kepinski and Leyser, 2004; Woodward and Bartel, 2005). The degradation of Aux/IAA repressor relieves the repression of the ARF transcription factor that can either activate or repress transcription of auxin-responsive target genes (Ramos *et al.*, 2001; Tiwari *et al.*, 2003; Dreher *et al*., 2006; Boer *et al*., 2014). When the concentration of IAA decreases, the affinity of SCF^{TIR1} complex for binding Aux/IAA proteins also goes down, so the number of repressor Aux/IAA proteins increases, enhancing the repression of ARFs (Peer, 2013).

The Aux/IAA protein family and the TIR1/AFB protein family have multiple members, which display different binding affinities for different auxins, including the natural auxin and synthetic auxin (Calderón-Villalobos *et al*., 2012; Lee *et al*., 2014; Winkler *et al*., 2017). There are 29 Aux/IAA members, distributed in the five chromosomes, and 6 TIR1/AFB members in *Arabidopsis* that may form the auxin co-receptor complex (Liscum and Reed, 2002; Dharmasiri *et al.*, 2005b; Parry *et al.*, 2009). In another model plant of rice, the Aux/IAA family has 31 members (Jain *et al*. 2006). Based on the presence of particular member of Aux/IAA proteins and TIR1/AFB proteins, the complex exhibits varying affinities. Together with the specific kind of auxin, the auxin-receptor complex regulates a vast number of various plant development activities. Additionally, the diversity of ARF proteins family, such as 22 identified ARF proteins in *Arabidopsis* (Guilfoyle and Hagen, 2007) and 28 members in the ARF family of rice (Wang *et al*. 2007), contributes to the abundance of auxin-induced responses. As a consequence, the responses of plant to auxin display the specific properties depending on organ and auxin concentration – while IAA stimulates growth in coleoptiles linked with actin being organized in form of fine strands (rice: Wang and Nick, 1998; Holweg *et al*., 2004; Nick *et al*., 2009; maize: Waller *et al*., 2002), it inhibits growth in roots correlated with bundling of actin (Rahman *et al.*, 2007). This apparent discrepancy has to be seen in the differential

auxin sensitivity and the bell-shaped dose-response curve for auxin-dependent responses: Roots are more sensitive to auxin with the endogenous levels of auxin already being beyond the optimum, such that even relatively low concentrations of exogenous auxin inhibit root growth (Foster *et al*., 1952; Foster *et al.*, 1955). In contrast, shoots and coleoptiles are less sensitive, such that exogenous auxin is stimulating growth. In fact, when the concentrations are raised progressively in maize coleoptiles beyond the optimum of growth, actin is bundled as well which and actin is repartitioned from a soluble into a sedimentable state (Waller *et al*., 2002).

It is clear that the interaction between Aux/IAAs and SCF^{TIR1} is central to auxin biology, modulating auxin-responsive gene transcription. The tight regulation of intracellular auxin level is therefore required for the correct plant growth and development.

1.3.2 Cellular auxin homeostasis

As auxin plays an important role in the regulation of plant development, influencing many essential processes in plant, the plant have to tightly control its cellular auxin homeostasis through several strategies: *de novo* biosynthesis, conversion, storage (Korasick *et al*. 2013; Enders and Strader, 2015), oxidation and degradation (Meudt and Gaines, 1967; Gazarian *et al*., 1998; Ljung *et al.*, 2002), and transport (Benková *et al*. 2003; Carrier *et al*. 2008). The intracellular auxin pool includes a mixture of free auxin, conjugated auxins, and some inactive auxin precursor (Korasick *et al*. 2013).

Compared with abundant knowledge of the IAA physiology effects and molecular mechanism of gene regulation, the IAA biosynthetic pathway is not fully understood. Researchers have identified two main kinds of biosynthesis pathways for natural IAA: tryptophan (Trp)-dependent and Trp-independent pathways (Zhao, 2010; Korasick *et al*. 2013). The Trp-dependent auxin biosynthesis pathways include the

indole-3-acetaldoxime (IAOx) pathway (Mikkelsen *et al*., 2000; Zhao *et al*., 2002), the indole-3-acetamide (IAM) pathway (Pollmann *et al*., 2009), and the indole-3-pyruvic acid (IPyA) pathway (Tao *et al*., 2008; Zhao, 2012), which is considered as the main biosynthetic pathway of IAA (Zhao, 2012). The IPyA pathway, conversing Trp to IAA, is a simple, two-step process: the TRYPTOPHAN AMINOTRANSFERASE OF ARABIDOPSIS (TAA) family of Trp aminotransferases catalyzes the formation of IPyA from Trp, and the YUCCA (YUC) family of flavin monooxygenases converts IPyA to IAA (Tao *et al*., 2008; Stepanova *et al*., 2008; Yamada *et al.*, 2009; Mashiguchi *et al.*, 2011; Dai *et al.*, 2013). In addition to Trp-dependent pathways, the mutants in *Arabidopsis* and maize lacking tryptophan as a metabolic intermediate, it is still possible for IAA biosynthesis to occur (Wright *et al*., 1991; Normanly *et al*., 1993), indicating there is a route of IAA biosynthesis independent of tryptophan.

Since the IAA biosynthesized from *de novo*, intracellular IAA either can start to play a role in IAA-related physiological activities, or be transformed into inactive form and stored in plant cell. In fact, only a small fraction of IAA exists in the free IAA form, around up to 25% of the total amount of IAA; while the rest of IAA exists in the conjugated form (Ludwig-Müller, 2011). Auxin conjugates can be divided into three major forms, including ester conjugates with sugar moieties, amide conjugates with amino acids, and amide conjugates with peptide and protein (Bajguz and Piotrowska, 2009). For example, the *iaglu* gene in maize, encoding (uridine 5'-diphosphate-glucose:indol-3-ylacetyl)-3-D-glucosyl transferase, conjugates IAA to glucose to form IAA-glucose (Szerszen *et al*., 1994). Several amide conjugates with amino acids have been identified, such as IAA-Asp in Scots pine *Pinus sylvestris* L. (Anderson and Sandberg, 1982), IAA-Glu in cucumber *Cucumis sativus* L. (Sonner and Purves, 1985), IAA-Ala in spruce *Picea abies* (Östin *et al.*, 1992), and IAA-Leu in *Arabidopsis thaliana* (Bartel and Fink, 1995). Thus, the compositions of IAA conjugates with amino acids depend on plant species. The last form is IAA conjugate with peptide and protein. For instance, a peptide from *Phaseolus vulgaris* seed has

been extracted and analyzed, and found it was bound with 2 indole-3-acetyl moieties in amide linkage per peptide (Bialek and Cohen, 1986). In strawberry, peptide fragment analysis indicates IAA could bind to either a chaperonin related to the hsp60 class of proteins or an ATP synthase (Park *et al.*, 2006). In addition IAA conjugates, IAA also can be converted to its non-active methyl ester form, MeIAA (Yang *et al*., 2008). Besides, the precursor of IAA is another way of IAA storage form. When necessary, the precursor of IAA can be converted to IAA in a short time and start to play its role (Korasick *et al.*, 2013). IBA, an auxin precursor, is converted into active IAA by peroxisomal beta-oxidation to promote root hair and cotyledon cell expansion in *Arabidopsis thaliana* seedling development (Strader *et al*., 2010).

In addition to maintain auxin homeostasis through the regulation of auxin *de novo* biosynthesis and conjugation, peroxidase-catalysed IAA oxidation and degradation occurs as well (Meudt and Gaines, 1967; Gazarian *et al*., 1998). In another way, IAA can first be converted to IAA conjugates, then IAA conjugates be the subject to oxidation and degradation. For instance, feeding high level of IAA promoted IAA conversion to IAA-Asp in *Arabidopsis*, refeeding of IAA further oxidized IAA-Asp to Ox-IAA–Asp and OH-IAA–Asp and none of IAA-Asp conjugates were hydrolyzed back to IAA (Östin *et al.*, 1998).

In mature plant, not every cell can synthesize auxin, but every cell is under the control of auxin. Therefore, auxin transport plays a critical role in regulate the auxin level among the cells in the same tissue or different tissues. This will be introduced in the next section.

1.3.3 Intercellular auxin transport

Auxin transport had been observed in the test of *Avena sativa* coleoptile curvature by Went at 1928, but until 1934, IAA was isolated from human urine for the first time (Enders and Strader, 2015). From the very early stage of auxin study, auxin transport

phenomenon is familiar to researchers, while the molecular mechanism beneath it has been uncovered until recent decades.

Young and fast growing tissues, like shoots, young leaves, and roots meristem, can synthesize auxin (Ljung *et al*., 2001), and transport of auxin from its biosynthesis sites to distant sites is critical for plant normal development. For instance, embryonic apical-basal axis development (Friml *et al*., 2003; Weijers *et al*., 2006; Ueda *et al*., 2011), lateral root growth (Bhalerao *et al*., 2002), and vascular development (Gälweiler *et al*., 1998; Mattsson *et al*., 1999). The polar transport property is unique for auxin among plant hormones. This directional movement of auxin in plant tissue is the result of numerous cell-to-cell auxin transport, which is a very complex process involving multiple auxin carriers to guide auxin movement.

IAA is a weak acid (Pacifici *et al*., 2015). In extracellular matrix, mildly acidic environment, auxin can enter the cytoplasm in two different ways: the non-charged IAA and protonated form of the IAA (IAAH) use passive diffusion to across the plasma membrane, and the anionic form IAA^-, majority form IAA, relies on active transport by influx carriers (Swarup *et al*., 2001; Friml, 2010; Swarup and Péret, 2012). AUXIN1/LIKE-AUX1 (AUX/LAX) are major auxin influx carriers. The AUX1/LAX family members include AUX1, LAX1, LAX2, and LAX3 (Marchant *et al*., 1999; Swarup *et al*., 2004; Yang *et al*., 2006; Péret *et al*., 2012). However, inside the cytoplasm (pH 7.0), the anionic IAA^- form cannot freely move out of the cell and relies on active auxin efflux carriers (Friml, 2010). The efflux carriers include PIN FORMED (PIN) and ATP-BINDING CASSETTE GROUP B (ABCB/MDRPGP) (Chen *et al*., 1998; Sidler *et al*., 1998; Paponov *et al*., 2005; Carraro *et al*., 2012; Balzan *et al*., 2014). In particularly, PIN proteins are asymmetric distributed and polarly localized at plasma membrane. Therefore, they play a critical role in the polar auxin transport and form the auxin directional movement and auxin gradient along the tissue (Ljung *et al*., 2005; Wisniewska *et al*., 2006; Grieneisen *et al*., 2007; Robert and Friml, 2009). These auxin gradients, providing spatiotemporal information, are

used to maintain correct plant development (Ikeda *et al*., 2009; Robert *et al.*, 2013). For instance, the maximal concentration of auxin located in distal cells of the Arabidopsis root apex, which was necessary for correlate root pattern (Sabatini *et al.*, 1999; Kramer and Bennett, 2006). In contrast, the mutants of efflux carriers cause abnormal plant morphology, due to lack of proper auxin gradient. The reduction of polar auxin transport in *Atpin1* mutants altered the formation of vascular tissue and formed the pin-shaped phenotype (Okada *et al*., 1991; Gälweiler *et al*., 1998).

The polar localization of PIN proteins is dynamic, recycling between the plasma membrane and endosomal compartments, such as endoplasmic reticulum (ER) (Geldner *et al.*, 2001; Dhonukshe *et al.*, 2007; Mravec *et al.*, 2009; Bosco *et al*., 2012). PIN3 is expressed in gravity-sensing tissues, and the change of gravity stimulus caused quickly relocalization of PIN3 (Friml *et al*., 2002). The process of relocalization of PIN proteins is an actin-dependent manner (Friml *et al.*, 2002; Hou *et al.*, 2003; Sun *et al.*, 2004; Zhu and Geisler, 2015). Thus, PIN proteins cycling links between actin, polar auxin transport and eventually modulates auxin signal spatiotemporal distribution in plant cell.

1.4 Scope of the dissertation

The *Nicotiana tabacum* L. cv. Bright Yellow 2 (BY-2) has been used as a model system in plant cell biological field (Nagata *et al*., 1992). BY-2 cells can be stably cultured in a Murashige and Skoog medium (Murashige and Skoog, 1962). Compared with whole plant organism, BY-2 suspension cells grow in a relatively short cultivation cycle with certain degree of synchronization (Nagata and Kumagai, 1999). Last but not least, BY-2 cells have been routinely transformed through biolistic or *Agrobacterium*-mediated transformation, so numerous transgenic BY-2 cell lines have been created for various specific research purpose. Like a transgenic line, GF11 cell line, is stably expressing the actin binding domain 2 of plant fimbrin in fusion with green fluorescent protein (GFP), which leads to slightly but significantly decrease

actin dynamicity (Sano *et al.*, 2005; Holweg, 2007; Zaban *et al.*, 2013).

This dissertation can be separated into two main parts. The first section deals with the question: what is the role of actin for auxin-dependent developmental responses? The second part is: based on fluorescent auxin analogs, investigate fluorescent auxin analogs and auxin spatiotemporal behavior, including binding properties and subcellular distribution.

1.4.1 Role of actin in auxin-dependent responses of tobacco BY-2

Actin is remodeled depending on auxin constituting a self-referring feedback loop that can act as oscillatory signaling hub (Nick, 2010). This actin-auxin oscillator model predicts that even slight changes of actin dynamics should alter the cellular responses to auxin. There are some indications supporting this prediction: Actin marker lines of Arabidopsis expressing the actin marker actin-binding domain of plant fimbrin (GFP-FABD2) showed a significant reduction in auxin transport (Holweg, 2007), and the auxin-dependent regeneration of tobacco protoplasts was affected leading to a high frequency of cells with an aberrant additional polarity (Zaban *et al*., 2013).

In this section study is to test, whether developmental responses to auxin are dependent on actin dynamics in walled cells as well. Although developmental responses of suspension cells are limited to cell proliferation, cell expansion, and synchronization into pluricellular chains, this developmental sequence is clearly under control of auxin in a very specific manner (Campanoni and Nick, 2005). One specific aspect of these auxin responses is a pronounced bell-shaped dose-response curve, i.e. at high (>10 µM) concentrations, the response is less pronounced than for a lower (1-2 µM) level of auxins (Foster *et al*., 1955). This is classically interpreted as manifestation of a two-point attachment towards a receptor (Foster *et al.*, 1952). Therefore, it is important to include also such high concentrations, although they exceed the endogenous level of auxin by an order of magnitude. To address the

potential link between auxin-responsiveness and actin dynamics, it is considered to choose the transgenic line GF11, stably expressing the actin binding domain 2 of plant fimbrin in fusion with GFP (Sano *et al*., 2005). This domain is used as state-of-the art marker for plant actin, but also causes a slight, but significant decrease of actin dynamicity (Holweg, 2007; Zaban *et al*., 2013). What are the phenotypes of this GF11 line to different concentrations of exogenous natural auxin, IAA, in comparison to the non-transformed BY-2 wild type? From the findings of these specific phenotypes, if there are differences between GF11 line and BY-2 wild type, what role of actin plays in auxin signaling, except the structural functions of actin, such as the role of actin for nuclear migration?

1.4.2 Characteristic of fluorescent auxin analogs and auxin at the subcellular level in tobacco BY-2 cells

The auxin gradients has been established by local auxin biosynthesis (Cheng *et al*., 2006; Stepanova *et al*., 2008) and intercellular polar auxin transport (Ljung *et al*., 2005; Wisniewska *et al*., 2006), which are both tightly connected with internal and external signals. The development of specialized cells in the gametophyte is controlled by maintaining auxin gradient, as positional information for the proper pattern formation in the embryo sac (Pagnussat *et al*., 2009). Gravitropism in the root is caused by the accumulation of auxin at the lower side of root (Ottenschläger *et al*., 2003; Swarup *et al*., 2005). Therefore, the modulation of auxin distribution is used as a means to efficiently integrate signals by plant, and the spatiotemporal auxin distribution is as the direct signal to trigger plant developmental programs to respond to those integrated signals.

To visualize auxin spatial distribution with high resolution is still a challenge until recently. There are some indirect methods to monitor auxin distribution. For instance, immunolocalization by using anti-IAA antibody (Benková *et al*., 2003), auxin responsive promoters (such as DR5) ligated to the *GUS* (β-glucuronidase) gene or

GFP gene (Ulmasov *et al.*, 1997; Blilou *et al.*, 2005; Vanneste and Friml, 2009), auxin carriers tagged with fluorescent protein, such as GFP (Wisniewska *et al*., 2006; Mravec *et al*., 2008), auxin measurements by gas chromatography-mass spectrometry (GC-MS) (Ljung, *et al*., 2001). Additionally, radiolabeled auxin can be used as reporter to directly reflecting its own localization (Reed *et al*., 1998; Petrášek *et al*., 2006), such as labelled with ^{13}C (Liu *et al*. 2012), ^{14}C (Rashotte *et al*. 2003), or ^{3}H (Hošek *et al*. 2012). However, these indirect or direct methods require multiple and time consuming steps. Spatiotemporal resolutions of these reporter systems are also not precise enough at cellular level, and cannot provide available information about auxin subcellular localization.

Better reporter system is required, with simple and fast procedure as well as high spatial resolution. One possible method for tracking auxin *in vivo* at the cellular level is to develop fluorescent labeled auxin. Some small fluorophores with low molecular weight make them suitable for labeling certain molecules to trace target molecules, minimizing effects on their biological activity. A remarkable example of small fluorophores is NBD (7-nitro-2,1,3-benzoxadiazole) and other related benzoxadiazole compounds, widely applied in cell biological research (Chattopadhyay, 1990; Lace and Prandi, 2016). Hayashi *et al*. (2014) synthesized fluorescently labeled auxin analogs (NBD-NAA and NBD-IAA), which are designed to be active for auxin transport system but inactive for auxin signaling and metabolism, reflecting the native auxin gradient and transport sites. With these new tools of fluorescent auxin analogs, for the first time, it is possible to directly investigate what is their subcellular spatial distribution by employing some fluorescent markers tagged to specific organelles. Because these fluorescent auxin analogs are active for auxin transport system, they can be used as competitors for native auxins. Therefore, they could be used to probe specificity of auxin binding sites, and quantify the fluorescent signal of auxin analogs to calculate the binding affinity. All these differences between different fluorescent auxin analogs and native auxins could be cues to different auxin receptors, which remain one of the most fundamental questions of auxin biology.

2. Materials and Methods

2.1 Tobacco cell cultivation

Wild-type (WT) BY-2 (*Nicotiana tabacum* L. cv Bright Yellow 2) suspension cell lines (Nagata *et al*., 1992) were cultivated in liquid medium containing 4.3 g/L Murashige and Skoog salts (Duchefa Biochemie, Haarlem, The Netherlands), 30 g/L sucrose (Carl Roth GmbH, Karlsruhe, Germany), 200 mg/L KH_2PO_4 (Merck Chemicals GmbH, Darmstadt, Germany), 100 mg/L (myo)-inositol (Carl Roth GmbH, Karlsruhe, Germany), 1 mg/L thiamine (Sigma Aldrich, St. Louis, USA), and 0.2 mg/L (0.9 µM) of 2,4-dichlorophenoxyacetic acid (2,4-D; Fluka Chemie GmbH, Buchs, Switzerland), adjusted to pH 5.8. The cells were subcultivated weekly, inoculating 1.0 mL of stationary cells into fresh medium (30 mL) in 100 mL Erlenmeyer flasks corresponding to 10^5 cells·mL^{-1}. Preparatory studies had shown that the progression of the different developmental stages was dependent on the initial density of the culture. The cells were incubated at 26 ℃ under constant shaking on a KS260 basic orbital shaker (IKA Labortechnik) at 150 rpm. Every three weeks, the stock BY-2 calli were subcultured on media solidified with 0.8% (w/v) agar (Carl Roth GmbH, Karlsruhe, Germany).

The transgenic BY-2 strains were cultivated in the same media as non-transformed wild-type cultures (WT BY-2), but supplemented with specific antibiotics. The cells were subcultivated weekly, inoculating 1.5 mL of stationary cells into fresh medium (30 mL). The GF11 line, stably transformed BY-2 cells with a GFP-fimbrin actin-binding domain 2 (GFP-FABD2) construct (Sano *et al*., 2005), were supplemented with 30 mg/L Hygromycin. The NtTPC1A-GFP, stably transformed BY-2 cells with an NtTPC1A (*Nicotiana tabacum* Two Pore Channel 1A) -GFP construct (Kadota *et al*., 2004), were supplemented with 100 mg/L Kanamycin. The NtTPC1A-GFP cell strain was kindly provided by Dr. Q. Liu (Botanical Institute,

Karlsruhe Institute of Technology, Germany). The PIN1-GFP, stably transformed BY-2 cells with a fusion construct of PIN1 (pin-formed protein 1, from *Arabidopsis thaliana*) and GFP (Benková *et al.*, 2003), were supplemented with 40 mg/L Hygromycin. The PIN1-GFP cell strain was kindly provided by Dr. J. Petrášek (Institute of Experimental Botany, Academy of Sciences of the Czech Republic, Prague, Czech Republic).

2.2 Fluorescent auxin analogs

Two kinds of fluorescent auxin analogs, NBD-NAA (7-nitro-2,1,3-benzoxadiazole conjugated to NAA) and NBD-IAA, have been recently reported (Hayashi *et al.*, 2014). These two auxin analogs are designed to remain active for auxin transport system, but inactive for auxin signaling and metabolism. Therefore, it can provide the potential to visualize auxin transport and distribution, without disturbing auxin signaling pathway. The NBD-NAA and NBD-IAA were kindly provided by Prof. Dr. K. Hayashi (Department of Biochemistry, Okayama University of Science, Japan).

Each tube of chemical contained 100 μg NBD-NAA or NBD-IAA. To make 5 mM long term stock solution, 100 μg NBD-NAA was dissolved in 48.97 μL dimethyl sulfoxide (DMSO; Carl Roth GmbH, Karlsruhe, Germany) and 100 μg NBD-IAA was dissolved in 44.31 μL DMSO. The 5 mM NBD-NAA or NBD-IAA DMSO stock solutions were divided into four aliquots. The 5 mM stock solutions were stored at deep freezer (-80C°). For the experimental concentration was suggested between 2 - 5 μM, 2 μM was chosen as the final experimental concentration after some preliminary tests. Therefore, the 0.5 mM short term stock solution was prepared by diluting 5 mM stock solutions with DMSO. Then 4 μL 0.5 mM NBD-NAA or NBD-IAA was transferred into a 2 mL sterile Eppendorf tube. The 0.5 mM stock solutions were also stored at deep freezer (-80C°).

2.3 Auxin (IAA) long term treatment

After inoculation of the WT and GF11 cell strains, indole-3-acetic acid (IAA; Carl Roth GmbH, Karlsruhe, Germany) was added directly into the cell culture medium to final concentrations of 2 µM, 8 µM, 16 µM or 32 µM (to probe for a potential bimodality of the dose-response relation), using filter-sterilized stocks of 5 mM, 20 mM, 40 mM or 80 mM IAA dissolved in 96% ethanol, respectively. The concentration of 2 µM for the (easily oxidized) IAA is physiologically equivalent to the 0.9 µM of the (very stable) 2,4-D used as complement in this part of experiments. A cell culture without any added IAA was used as control group. Preparatory experiments using solvent controls with corresponding concentrations of ethanol did not show any significant effects. The effects of IAA were tested only over the first culture cycle, i.e. the inoculum was always coming from cells that had been cultivated under control conditions (i.e. in the absence of exogenous IAA).

In all of this part experiments, the same, basal level of 2,4-D (0.9 µM) were present, required to sustain proliferation activity. In a control experiment targeted to detect a potential influence of 2,4-D on IAA-dependent responses, the cells were cultivated either in 32 µM of exogenous IAA alone (i.e. omitting any 2,4-D), in 32 µM of 2,4-D alone, or in a combination of 31.1 µM IAA and the usual basal level (0.9 µM) of 2,4-D: After inoculation of the WT cell strain, IAA or 2,4-D was added directly into the cell culture medium to final concentration of 32 µM, using filter-sterilized stocks of 80 mM IAA or 2,4-D dissolved in 96% ethanol, respectively. Another cell culture with normal culture medium (with 0.9 µM 2,4-D), adding 77.75 mM IAA stock solution (dissolved in 96% ethanol) to final concentration of 31.1 µM, was employed as control group.

2.4 Fluorescent auxin analogs short term treatment

After 1 day of cell subcultivation, aliquots of 1 mL WT cells were incubated with 4

μL 0.5 mM fluorescent auxin analogs (NBD-NAA or NBD-IAA) for 20 min on a rotor (IKA-WERK, Staufen, Germany) at 200 rpm. Then each sample was transferred into custom-made staining chambers using mesh with a pore-size of 70 μm as bottom (Nick *et al.*, 2000) to remove the medium, and wash twice with fresh medium to remove unbounded fluorescent auxin analogs. For the transient transgenic NtTPC1A-RFP strain or protoplasts of NtTPC1A-GFP strain and PIN1-GFP strain, samples were prepared and selected 1 mL samples with the same procedure as WT cells.

For the fluorescent auxin analogs localization experiments, aliquots of 1 mL 1-day-old WT BY-2 cells were pre-incubated with 4 μL 0.5 mM fluorescent auxin analogs for 20 min on a rotor at 200 rpm. After that, 1 μL 1 mM ER-Tracker (ER-Tracker™ Red dye, Thermo Fisher Scientific, USA) dissolved in DMSO was employed, incubating for 1 min on a rotor at 200 rpm. Then the cells were washed twice with fresh medium as mentioned above. For the co-treatment of fluorescent auxin analogs and auxin (NAA, IAA and 2,4-D) experiments, aliquots of 1 mL 1-day-old WT BY-2 cells were incubated with 4 μL 0.5 mM fluorescent auxin analogs and 4 μL auxin stocks of 0.5 mM, 5 mM or 25 mM (IAA and 2,4-D dissolved in 96% ethanol, NAA dissolved in 5 mM KOH). After 20 min incubation, the cells were washed twice with fresh medium as mentioned above. For the weighted colocalization coefficients of NBD-NAA experiments, aliquots of 1 mL 1-day-old WT BY-2 cells were first incubated with 4 μL 0.5 mM NBD-NAA and 4 μL IAA (or 2,4-D) stocks of 0.5 mM or 25 mM for 20 min on a rotor at 200 rpm, subsequently added 1 μL 1 mM ER-Tracker for another 1 min incubation. Then the cells were washed twice with fresh medium as mentioned above.

2.5 Agrobacterium-mediated transient expression of NtTPC1A-RFP

Transient cell line expressing NtTPC1A-RFP was gained through method developed by Buschmann *et al*. (2010) with minor modifications. First, 100 μl electro-competent

A. tumefaciens (strain LBA 4404; Invitrogen Corporation, Paisley, UK) was incubated with 100 ng vectors containing NtTPC1A-RFP on ice for 20 min. The mixture was then transferred into electroporation cuvette with 2 mm electrode gap (Peqlab, Erlangen, Germany) for electric pulses of 2.5 kV, 200 Ω for 5 ms (Gene Pulser Xcell™ electroporator, Bio-Rad, Laboratories, Hercules, CA, USA). After electric pulse incubation, *A. tumefaciens* were plated onto solid LB (Lennox Broth, Carl Roth GmbH, Karlsruhe, Germany) agar medium containing antibiotics (100 μg/mL rifampicin, 300 μg/mL streptomycin and 100 μg/mL spectinomycin) and incubated for 3 days at 28 ℃ in the darkness. The colonies grew to proper size and selected single colony to inoculate to 5 mL liquid LB medium containing the same selective antibiotics for overnight incubation at 28 ℃ in the darkness. Certain amount of the overnight culture was inoculated into 5 mL of fresh liquid LB medium (without antibiotics) to reach an OD_{600} of 0.15. When the OD_{600} reached 0.8, transformed *A. tumefaciens* were harvested by centrifugation at 8000 g (Heraeus Pico 17 Centrifuge, 600 Thermo Scientific, Langenselbold, Germany) for 7 min at 28 ℃. The *A. tumefaciens* were then re-suspended in 180 μL washing medium (4.3 g/L Murashige and Skoog salts, 10 g/L sucrose, pH 5.8).

1.5 mL of 7-day-old WT BY-2 cells was used for subcultivation. After 3 days growth, collected 3 flasks of WT BY-2 cells together and washed twice with 200 mL of washing media (4.3 g/L Murashige and Skoog salts, 10 g/L sucrose, pH 5.8) each time using a scientific Nalgene® filter holder (Thermo Scientific, Langenselbold, Germany) combined with Nylon mesh with pores of diameter of 70 μm. The washed cells were then suspended in washing medium again, harvesting 5- to 6- fold concentrated cell suspension. These concentrated cells were incubated with transformed *A. tumefaciens* in a falcon tube on an orbital shaker at 100 rpm for 5 min till fully mixed. After mixture, the cells were dropped onto petri dishes containing washing medium solidified with 0.5 % (w/v) Phytagel (Sigma P8169) on which a single layer of sterile filter paper was placed in advance. These plates were sealed with parafilm and incubated at 22 ℃ in the darkness. After 4 days, the cells could be used for

observation under microscope.

2.6 Generation of protoplasts

The protocol was adapted from Kuss-Wymer and Cyr (1992), Zaban *et al*. (2013) and Brochhausen *et al*. (2016) with minor modifications. Aliquots of 4 mL were harvested under sterile conditions 1 d after subcultivation and digested for 1 h at 26 ℃ in 4 mL enzyme solution of 1% (w/v) cellulase YC (Yakuruto, Tokyo) and 0.1% (w/v) pectolyase Y-23 (Yakuruto, Tokyo) in 0.4 mol/L mannitol at pH 5.5 under constant shaking on a KS260 basic orbital shaker (IKA Labortechnik) at 100 rpm in Petri dishes of 90 mm diameter.

After digestion, protoplasts were harvested by centrifugation at 500 rpm for 5 min in fresh reaction tubes. The protoplast sediment was carefully re-suspended in 10 mL of FMS wash medium containing 4.3 g/L Murashige and Skoog salts (Duchefa Biochemie, Haarlem, The Netherlands), 100 mg/L (myo)-inositol (Carl Roth GmbH, Karlsruhe, Germany), 0.5 mg/L nicotinic acid (Carl Roth GmbH, Karlsruhe, Germany), 0.5 mg/L pyroxidine- HCl (Sigma Aldrich, St. Louis, USA), 0.1 mg/L thiamin (Sigma Aldrich, St. Louis, USA) and 10 g/L sucrose (Carl Roth GmbH, Karlsruhe, Germany) in 0.25 M mannitol (Carl Roth GmbH, Karlsruhe, Germany) (Kuss-Wymer and Cyr 1992; Wymer *et al*. 1996).

After three washing steps, protoplasts were transferred into 4 mL FMS-store medium, which was the same like FMS wash medium but complemented with 0.1 mg/L 1-naphthaleneacetic acid (NAA, Sigma Aldrich, St. Louis, USA) and 1 mg/L benzylaminopurine (BAP, Sigma Aldrich, St. Louis, USA). Then the protoplasts could be used for observation under microscope.

2.7 Quantification of morphology and pattern

2.7.1 Determination of mitotic indices and cell viability

To determine mitotic indices, 0.5 mL aliquots of cell suspension were collected daily from day 1 to day 5 after inoculation and fixed in Carnoy fixative (3 : 1 [v/v] 96% [v/v] ethanol : glacial acetic acid) complemented with 0.25% (v/v) Triton X-100, and then stained with 2'-(4-hydroxyphenyl)-5-(4-methyl-1-piperazinyl)-2,5'-bi(1H-benzimid-azole) trihydrochloride (Hoechst 33258, Sigma-Aldrich), which was prepared as a 0.5 mg/mL filter-sterilized stock solution in distilled water and used at a final concentration of 1 µg/mL. Cells were viewed under an AxioImager Z.1 microscope (Zeiss, Jena, Germany) using the filter set 49 DAPI (excitation at 365 nm, beam splitter at 395 nm, and emission at 445 nm). Mitotic indices were calculated as the number of cells in mitosis divided by the total number of cells counted. The values reported are based on the observation of 1,500 cells from three independent experiments.

To quantify cell viability, 0.5 mL aliquots of cell suspension were collected daily from day 1 to day 5 after inoculation. Each sample was transferred into custom-made staining chambers using mesh with a pore-size of 70 µm as bottom (Nick *et al.*, 2000) to remove the medium, and then the cells were incubated in 2.5% (w/v) Evans Blue for 3 min according to Gaff and Okong'O-Ogola (Gaff and Okong'O-Ogola, 1971). The Evans Blue was eliminated by washing twice with fresh medium. The frequency of the unstained (viable) cells was determined as well as the cell number per milliliter using a Fuchs-Rosenthal hematocytometer under bright-field illumination.

2.7.2 Determination of cell density and estimation of doubling times

As first step, time courses of cell density were established over the proliferation phase of the culture, by collecting 0.5 mL aliquots of the cell suspension daily from day 0

till the day 3, when proliferation activity began to weaken, and counting cells using a Fuchs-Rosenthal hematocytometer under bright-field illumination. Based on these time courses for cell density and the assumption of first-order kinetics:

$$\frac{dn}{dt} = k \cdot n$$

with n number of cells, and k the time constant of exponential growth, the natural logarithm

$$\ln\big(n(t)\big) = \ln\big(n(t=0)\big) + kt$$

should follow a straight line with a slope of k that could be approximated by linear regression. From the estimated value of k, doubling time τ (= duration of the cell cycle) could be estimated as based on the equation:

$$\ln\big(2 \cdot n(t=0)\big) = ln\big(n(t=0)\big) + k\tau$$

as

$$\tau = \ln(2) / k.$$

The correlation coefficients for this estimates were >0.95 in most cases. The values reported are based on the observation of 1,500 cells from three independent experimental series.

2.7.3 Determination of cell number per file frequency distributions

Aliquots of 0.5 mL cell suspension were collected daily from days 0 to 5 after inoculation and immediately viewed under an AxioImager Z.1 microscope (Zeiss, Jena, Germany) equipped with an ApoTome microscope slider for optical sectioning, and recorded by a cooled digital CCD camera (AxioCam MRm). Differential interference contrast images were obtained by a digital imaging system (AxioVision; Zeiss, Jena) and frequency distributions over the number of cells per individual file were constructed using the MosaiX function. For each picture, the MosaiX function of the AxioVision software was used to cover a 4 x 4 mm area with 121 single pictures at an overlay of 10 %. Each data point represents 1,500 individual cell files, respectively collected from three independent experimental series.

2.8 Microscopy and image analysis

2.8.1 Microscopy image acquisition

For morphological studies, BY-2 cells were examined under an AxioImager Z.1 microscope (Zeiss, Jena, Germany) equipped with an ApoTome microscope slider for optical sectioning and a cooled digital CCD camera (AxioCam MRm; Zeiss). GFP fluorescence from fluorescent auxin analogs were recorded through the filter set 38 HE (excitation at 470 nm, beamsplitter at 495 nm and emission at 525 nm). For mitotic indices, cells were viewed under an AxioImager Z.1 microscope (Zeiss, Jena, Germany) using the filter set 49 DAPI (excitation at 365 nm, beam splitter at 395 nm, and emission at 445 nm). For cell viability, cell density, and frequency distributions of cell number per file, cells were observed in the differential interference contrast (DIC) using a 20x objective (Plan-Apochromat 20x/0.75) and the MosaiX function of the imaging software (Zeiss).

For observation of individual cells in more details and colocalization analysis of NBD-NAA and ER-Tracker, cells were viewed under the AxioObserver Z.1 (Zeiss, Jena, Germany) inverted microscope equipped with a laser dual spinning disk scan head from Yokogawa (Yokogawa CSU-X1 Spinning Disk Unit, Yokogawa Electric Corporation, Tokyo, Japan), a cooled digital CCD camera (AxioCam MRm; Zeiss) and two laser lines (488 nm and 561 nm, Zeiss, Jena, Germany) attached to the spinning disk confocal scan head. Images were taken using a Plan-Apochromat 63x/1.44 DIC oil objective operated via the ZEN 2012 (Blue edition) software platform.

2.8.2 Colocalization analysis

The protocol was adapted from Zeiss Company with minor modifications (https://www.zeiss.com/content/dam/Microscopy/Downloads/Pdf/FAQs/zen-aim_colo

calization.pdf). Zeiss ZEN 2012 (Blue edition) software provides the “Co-localization” function to analyze any two channel image. Colocalization analysis is performed on a pixel by pixel basis. Every pixel in the image is plotted in the scatter diagram based on its intensity level from each channel.

To accurately set the scatterplot crosshairs, single label control samples must be prepared. In this study, a NBD-NAA-only control sample and an ER-Tracker-only control sample were prepared. To begin with, the double label (NBD-NAA and ER-Tracker) experimental samples were imaged under the AxioObserver Z.1 inverted microscope equipped with a laser dual spinning disk scan head , a cooled digital CCD camera and two laser lines (488 nm and 561 nm) using a Plan-Apochromat 63x/1.44 DIC oil objective. Then, the NBD-NAA-only control sample and the ER-Tracker-only control sample were imaged with the exact same microscope settings as the double label experimental samples. For the NBD-NAA-only control sample, both the NBD-NAA channel and the ER-Tracker channel were imaged. By using the tool to select the region of cell and examining the scatterplot of NBD-NAA-only control sample, the pixel distribution of NBD-NAA-only population could be examined. The horizontal crosshair could be set just above this population. For the ER-Tracker-only control sample, the process was repeated to set the vertical crosshair. Once the exact (X, Y) coordinates are determined by using the NBD-NAA-only control sample and the ER-Tracker-only control sample, they must be kept the same for analysis of the double label (NBD-NAA and ER-Tracker) experimental samples.

The software can automatically analyze many different measurements from the scatterplot. In the calculation for the colocalization coefficients, every pixel has the same value in the equations. The weighted colocalization coefficients are calculated by summing the pixels with taking into account intensity value in the colocalized region and then dividing by the sum of pixels with taking into account intensity value either in the NBD-NAA channel or the ER-Tracker channel.

2.8.3 Fluorescence intensity measurement

ImageJ software can be used for measuring the fluorescence intensity in a selected region. The protocol was adapted from McCloy *et al*. (2014) with several modifications. Samples of cells incubated with NBD-NAA were imaged under an AxioImager Z.1 microscope equipped with an ApoTome microscope slider, a cooled digital CCD camera and the filter set 38 HE (excitation at 470 nm, beamsplitter at 495 nm and emission at 525 nm) using a Plan-Apochromat 20x/0.75 objective. First, cell regions were selected using the drawing/selection tools. Second, selected "Set Measurements" from the analyze menu, choosing AREA, INTEGRATED DENSITY and MEAN GRAY VALUE. Third, selected the "Measure" from the analyze menu and the software would automatically measure values. Forth, selected a region next to the cells without fluorescence and repeated the measure process, which would be the background.

Once the measurement of all cells from one sample was finished, a formula was used to calculate the corrected total cell fluorescence (CTCF):

$$\text{CTCF} = \text{Integrated Density} - \begin{matrix}(\text{Area of selected cell} \times \text{Mean fluorescence} \\ \text{of background readings})\end{matrix}$$

For each sample, the mean value of cell fluorescence could be calculated as the corrected single cell fluorescence (CSCF):

$$\text{CSCF} = \frac{\text{CTCF}}{\text{cell number}}$$

3. Results

In this dissertation, the results will be presented in two main parts. The first part is about the role of actin dynamicity in auxin-dependent responses, namely how actin participate in auxin signal to modulate BY-2 cell development process. This process includes three distinct stages: cell cycling, cell elongation and file disintegration. With the treatment of different concentrations of auxin (IAA), the cell phenotypes at different distinct stages are analyzed between transgenic BY-2 cell and wild type. The second part focuses on auxin spatial distribution and binding characteristic. First, fluorescent auxin analogs are employed to visualize spatial localization. Then, combinations of fluorescent auxin analogs and auxin applications are aimed to discriminate potential auxin binding sites and binding property.

3.1 The impact of actin organization on auxin-dependent responses in tobacco BY-2 cells

3.1.1 BY-2 cells in suspension pass a sequence of three stages

In order to address the role of actin in the regulation of auxin-dependent cellular responses, a framework is needed to describe and compare these responses on a quantitative level. During their cultivation cycle, BY-2 cells undergo an ordered developmental process that can be subdivided into three distinct stages: cell cycling, cell elongation and file disintegration (Fig. 3.1). After inoculation, cells enter a cycling phase. During this period, cells divide in a fast pace in several cycles giving rise to cell files composed of 6 to 8 cells. The first division (duration τ_1) is longer than the subsequent (usually two) divisions (durations τ_2 and τ_3). After a few days, cells exit from the cycling stage (t_{ex}), and begin to elongate. Soon after, at t_{dis}, the last stage of the culture cycle, file disintegration, initiates. Hereby, after cell expansion, the connection between some cells in the same cell file becomes loose, and the cell file is

divided into two shorter files. These smaller cell files decay further, until only unicellular and bicellular files are left at the end of the cultivation cycle. It should be noted that not all files have reached the terminal unicellular state by the end of the cultivation cycle, but continue their decay after subcultivation, i.e. at a time when the singular cells already enter the next round of cycling. Thus, during the first day of the culture cycle, a transition from a unicellular to a bicellular situation (by division, with a duration of τ_1), and a transition from incompletely disintegrated bicellular files into single cells (with a duration of τ_d) proceed in parallel. In the attempt to reach a more complete disintegration, subcultivation intervals beyond 7 days had been tested. However, after day 7, viability dropped rapidly and drastically (data not shown), such that this approach was not meaningful. It should be mentioned that the progression and completeness of the developmental pattern described above was dependent on the initial density of the culture. When the inoculum was chosen higher than the 10^5 cells·mL^{-1} used here, the lag phase between subcultivation and onset of proliferation was shortened, the exit from proliferation was delayed, and the disintegration of files at the end of the culture cycle was incomplete. On the other hand, when cell density was too low, this resulted in a prolonged lag phase and reduced proliferation.

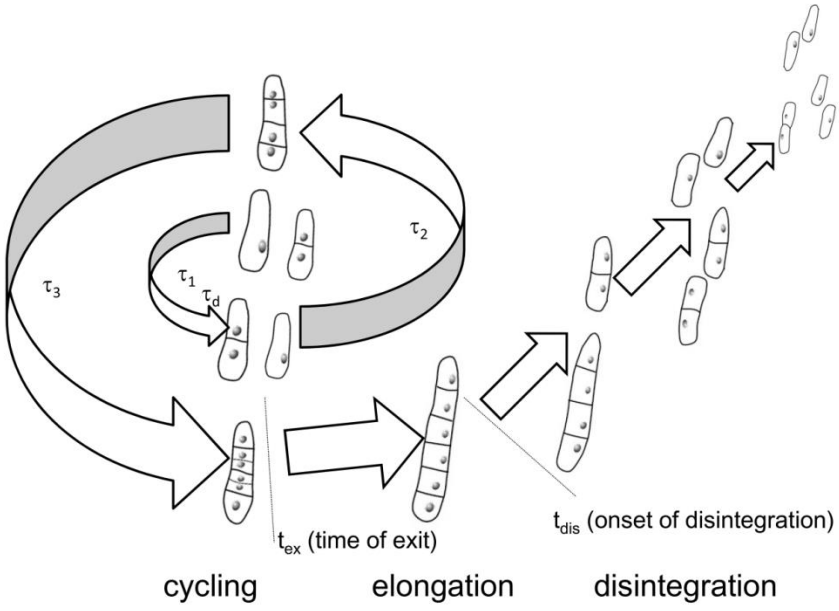

Fig. 3.1 Schematic representation of the cultivation cycle and the parameters used for its quantitative description. The cycle is divided into three stages: cell cycling, cell elongation and

cell disintegration with τ_1, τ_2 and τ_3 representing the duration of the first, second and third cell cycle, respectively, and τ_d the time constant for the decay of files that are still bicellular at subcultivation. The transition from cycling to elongation is described by t_{ex}, the onset of file disintegration by t_{dis}.

3.1.2 The progression of mitotic activity is modulated by natural auxin (IAA)

The mitotic index (MI) over time were measured in the non-transformed BY-2 cell line (WT) and the transformed GF11 actin-marker line to define the temporal pattern of cell division. In the absence of exogenous IAA, mitotic index in the WT increased progressively reaching a peak at day 3 with almost 4% of cells encountered in mitosis, followed by a sharp decline to less than 1% at day 5 (Fig. 3.2A). In contrast, the mitotic index in the transgenic GF11 line was already high from day 1 and persisted at this level till day 3, when it declined in the same way as in the WT (Fig. 3.2A).

This temporal pattern was modulated by IAA in a dose-dependent manner: The presence of IAA (2 μM) prolonged the rise of MI in the wild type by one additional day, such that a (higher) maximum of almost 5% was reached at day 4 (Fig. 3.2B). Again, this was followed by a sharp decline, but even at day 5, MI was significantly higher as compared to the untreated control (Fig. 3.2A). For GF11, 2 μM of IAA was not promoting mitotic activity, but in contrast caused a slight, but significant reduction, if compared to the situation without IAA (compare Figs. 3.2A and 3.2B). As a consequence, mitotic index in the transgenic line was consistently lower compared to the wild type, and did also not increase over time, but dropped sharply from day 4 (i.e. from the same time point, when also MI in the WT declined). Treatment with medium concentrations of IAA (8 μM and 16 μM) produced the same pattern as 2 μM (data not shown). However, for a high concentration of IAA (32 μM, included to test whether the dose-response was bell-shaped), the MI for the WT cells was persistently at 3.5% between days 1 and 3 (Fig. 3.2C), which is close to the peak activity reached

in the IAA-free control at day 3 (Fig. 3.2A). Instead, the decline after day 3 was very mild - at day 5, still 3% of the cells were found in mitosis (Fig. 3.2C), compared to less than 1% in the experiment without exogenous IAA (Fig. 3.2A). Under this high concentration of IAA, the transgenic GF11 behaved almost identically as the WT. The only difference was a significantly stronger decline of mitotic index following day 3 compared to the WT (Fig. 3.2C). It should be noted that the peak of the MI was now again at day 3 (as in the IAA-free control), and not at day 4 (as in the experiment with 2 μM of IAA). It should be mentioned that a basal level of 2,4-D (0.9 μM) was present in all experiments - this was required to sustain a stable level of cell proliferation.

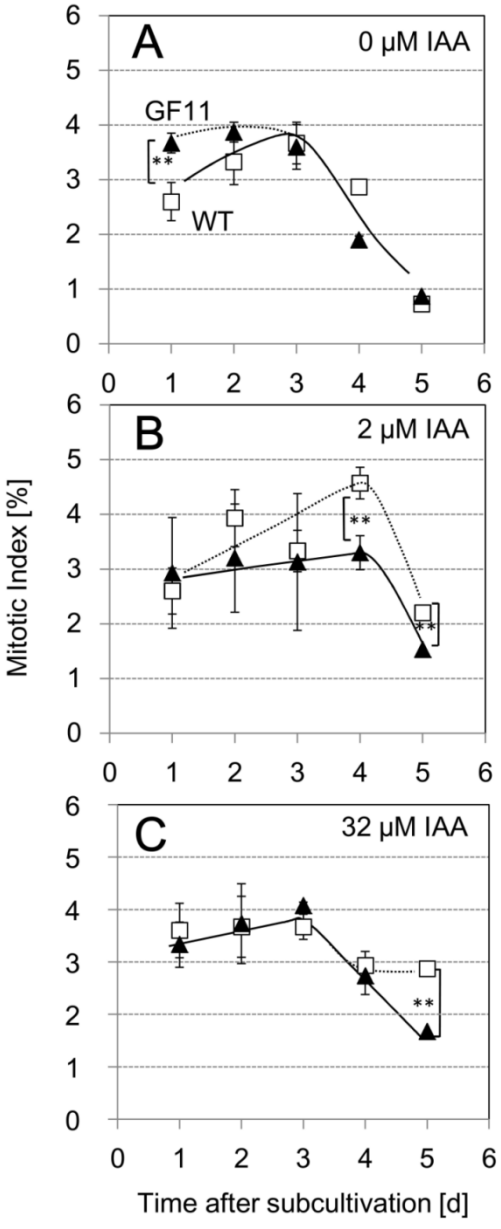

Fig. 3.2 Mitotic index of the non-transformed BY-2 cell line (WT, white squares) and the GFP-FABD2 overexpressor (GF11, black triangles) over time after subcultivation in the absence of (A), or in presence of 2 μM (B), or 32 μM (C) IAA. Each point is based on 1,500 individual cells from three independent experimental series. Error bars indicate SE of the mean. Asterisks represent statistically significant differences (Student's t-test) with $P<0.01$.

In order to understand these effects of IAA on actin filaments, the organization of actin filaments were also observed in the GF11 line through the culture cycle from day 1 until day 5 on a daily basis, either in untreated controls or in cells cultivated in presence of 2 µM or 32 µM IAA, respectively. It was not able to detect any significant difference of the actin filaments for any of these treatments (Fig. 3.3).

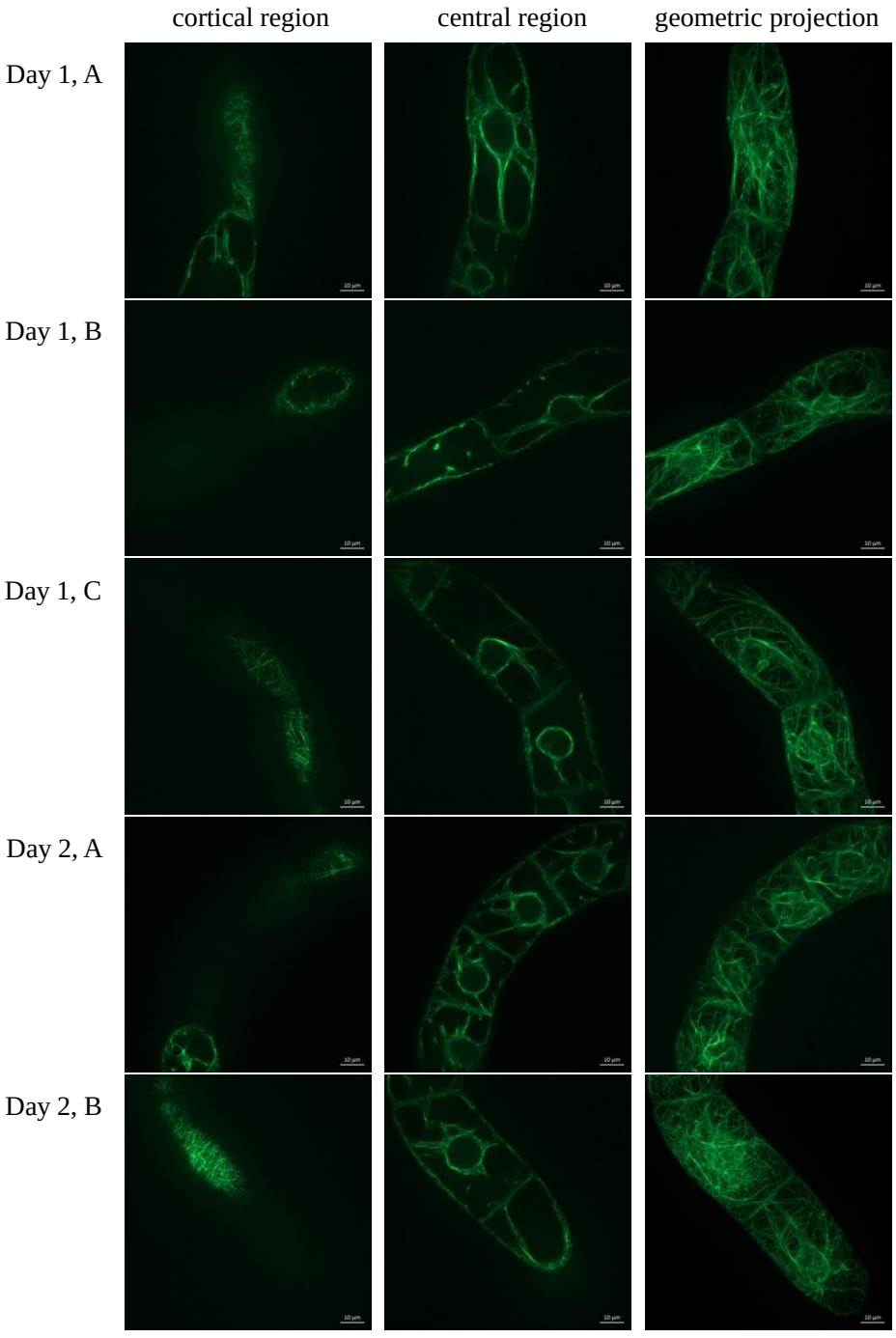

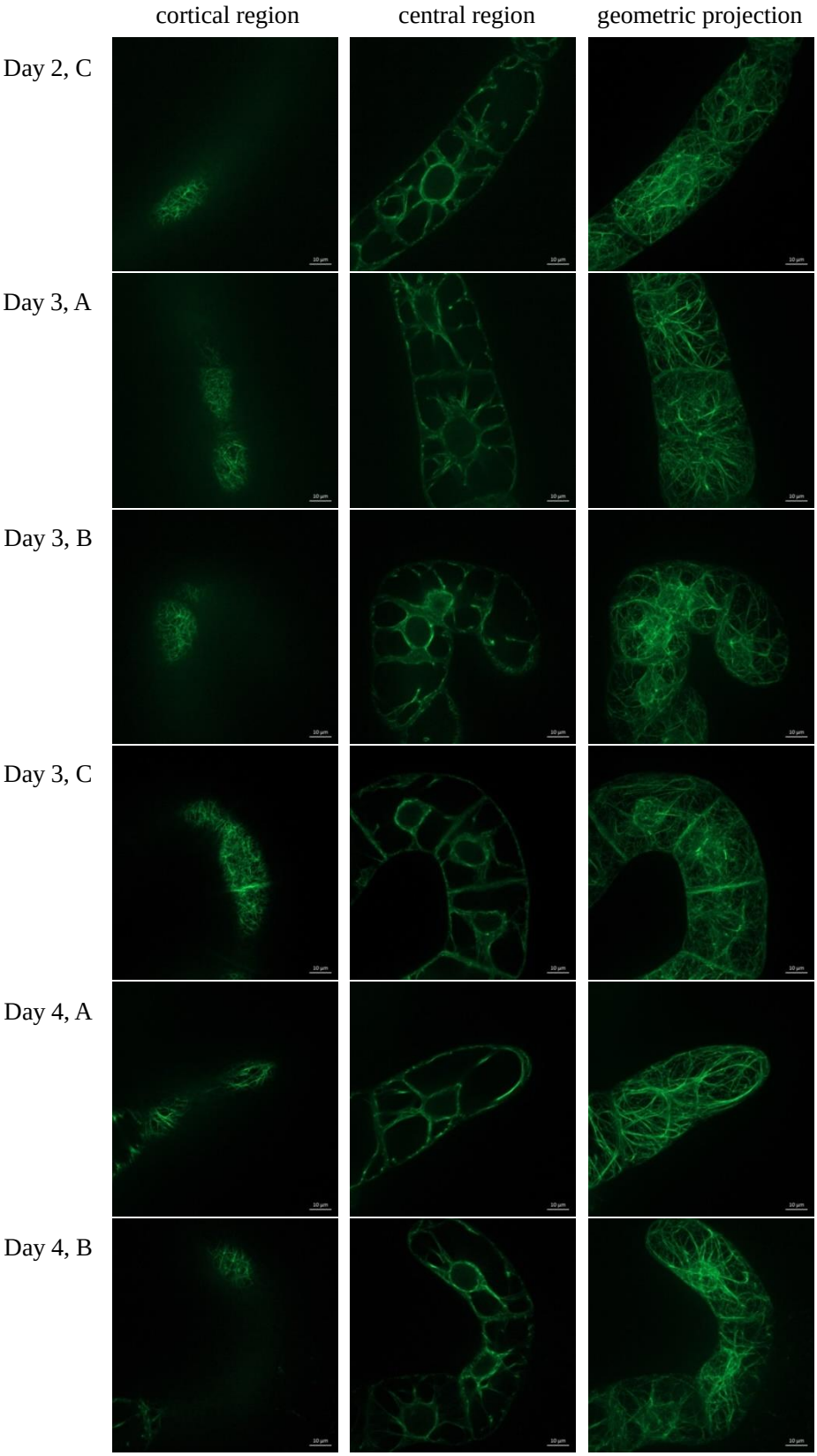
cortical region
central region
geometric projection
Day 2, C
Day 3, A
Day 3, B
Day 3, C
Day 4, A
Day 4, B

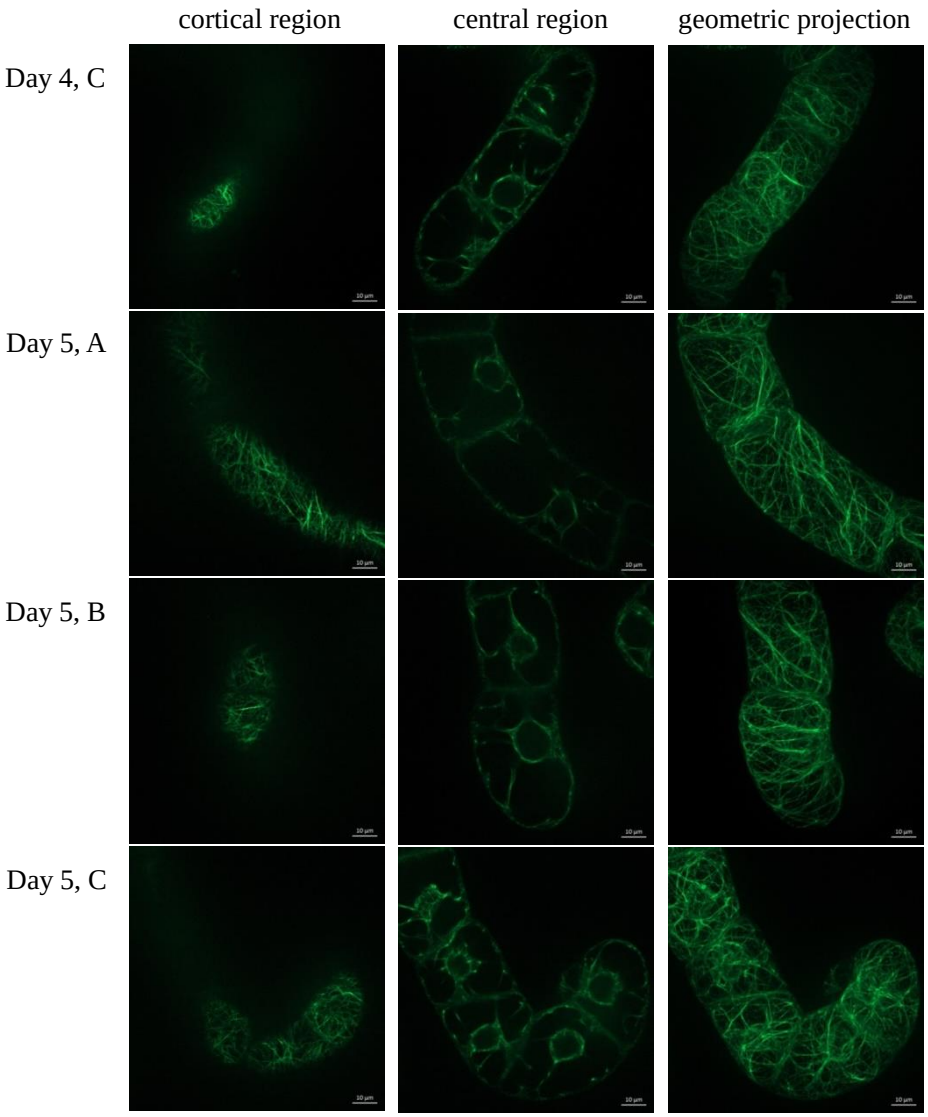

Fig. 3.3 Representative cells of the GF11 strain recorded at days 1 through 5 during cultivation without supplementary IAA (A), or with 2 µM (B), or with 32 µM (C) IAA. Confocal sections in the cortical region (left column), in the central region (central column), and geometric projections of the entire z-stack (right column) are shown (scale bar represents 10 µm).

3.1.3 Auxin and actin increase doubling times in a synergistic manner

The duration of the plant cell cycle is under control of phytohormonal signals, and therefore it can be addressed the effect of auxin on doubling times in both cell lines based on time courses of cell density. In both WT and the GFP-FABD2 overexpressor GF11 cell lines, doubling was slow immediately after subcultivation, but then accelerated to around 20 - 25 h per cycle (Fig. 3.4). For both lines, cell cycle duration was almost identical, and remained unchanged in presence of 2 µM IAA. Interestingly, a qualitative difference was observed for high auxin (32 µM IAA, roughly ten times above the typical endogenous levels). Here, the cell cycle became extremely slow in GF11 during day 1 (Fig. 3.4B), whereas in the WT there was no change compared to the auxin-free control (Fig. 3.4A). For the subsequent days, this initial difference vanished completely - for these later time points, the doubling time in GF11 was the same as in the WT and it was also the same as without auxin. This means that high auxin and overexpression of the GFP-FABD2 marker acted synergistically in slowing down the first cell division, but did not show such a synergy for the subsequent days.

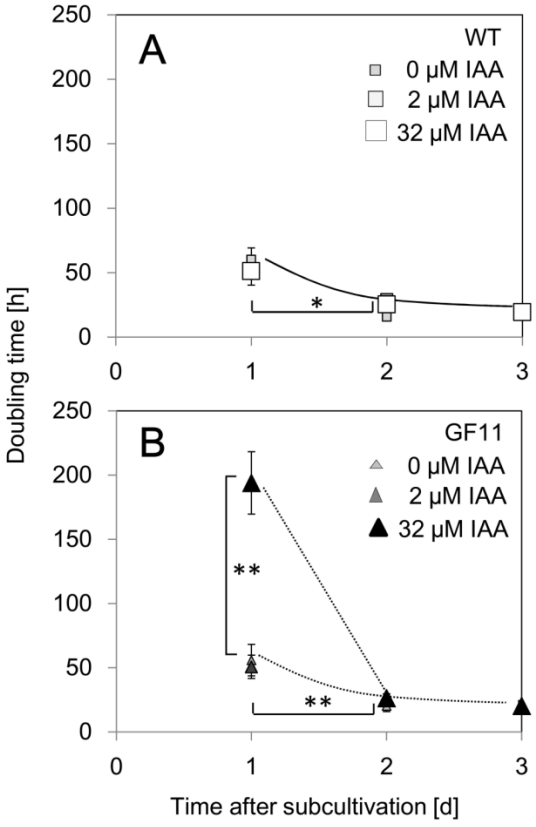

Fig. 3.4 Doubling time in the non-transformed BY-2 cell line (WT, A) and the GFP-FABD2 overexpressor (GF11, B) over time after subcultivation in the absence of IAA or in presence of 2 or 32 µM IAA, respectively. Each point is based on three independent experimental series. Error bars indicate SE of the mean. Asterisks represent statistically significant differences (Student's t-test) with $P<0.05$ (*) and $P<0.01$ (**), respectively.

3.1.4 File disintegration is delayed by auxin depending on actin

Cell division leads to pluricellular files that disintegrate into smaller units during the later phase of the cultivation cycle. To investigate the influence of auxin on the formation and disintegration of these supracellular structures, the frequency distributions over number of cells per file were constructed, and the mean cell number per file were determined to monitor the temporal pattern of file formation and decay in response to different concentrations of IAA. As long as the build-up of files by cell cycling is stronger than the decay of files, the mean value should increase reaching a maximum, when both processes are in balance, and it should decrease again, when file decay exceeds cell division in the non-decaying files.

Under control conditions, in the absence of supplementary IAA, the maximum value was reached one day earlier in the WT as compared to GF11 (Fig. 3.5A). When added 2 µM (Fig. 3.5B) or 32 µM (Fig. 3.5C) IAA, it did not change the timing of this peak in GF11. Only the amplitude was decreased slightly, but not significantly. In contrast, in the wild type, the peak was delayed by one day for 2 µM of IAA (Fig. 3.5B), and for 32 µM of IAA this delay was accompanied by a significant increase of amplitude (Fig. 3.5C). It should be noted that the maximum file length was reached at a time point, when mitotic index was still increasing (compare Fig. 3.2 and Fig. 3.5). This means that disintegration of cell files initiates at a time point, when cells are still cycling. In the WT, auxin delays the onset of disintegration in parallel to prolonging the cycling stage of the culture. In the GF11 line, auxin cannot induce such a delay of disintegration (Fig. 3.5C), and it also does not prolong the cycling stage of the culture (Fig. 3.2C).

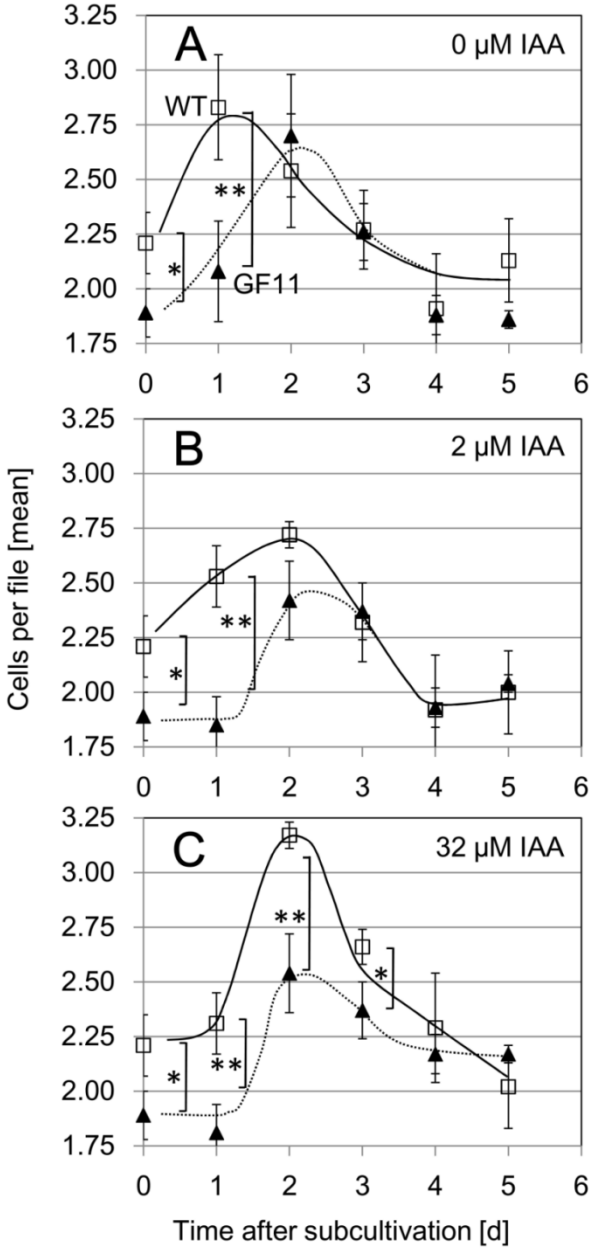

Fig. 3.5 Mean cell number per file over time in the non-transformed BY-2 cell line (WT, open squares) and the GFP-FABD2 overexpressor (GF11, black triangles) over time after subcultivation in the absence of IAA (A), or in presence of 2 µM (B) or 32 µM (C) IAA. Each point is based on 1,500 individual cell files from three independent experimental series. Error bars indicate SE of the mean. Asterisks represent statistically significant differences (Student's t-test) with $P<0.05$ (*) and $P<0.01$ (**), respectively.

To get insight into the role of actin stabilization for responses that depend on polar auxin transport, frequency distributions of cell number per file were constructed over the cultivation cycle for both cell strains and for different concentrations of exogenous IAA. The third cell cycle in a file (leading to the transition from n = 4 to either n = 5 in case of asynchrony, or from n = 4 to n = 6 in case of synchrony) depends on polar auxin transport (Campanoni *et al.*, 2003; Maisch and Nick, 2007). It showed that the GF11 line performed a priori a significant reduction of this synchrony (Fig. 3.6), and this low synchrony did not significantly change when the concentration of exogenous

IAA was raised over 2 µM, 8 µM, 16 µM till 32 µM. In contrast, the synchrony in the wild type dropped with increasing IAA concentration till it was as low as in GF11.

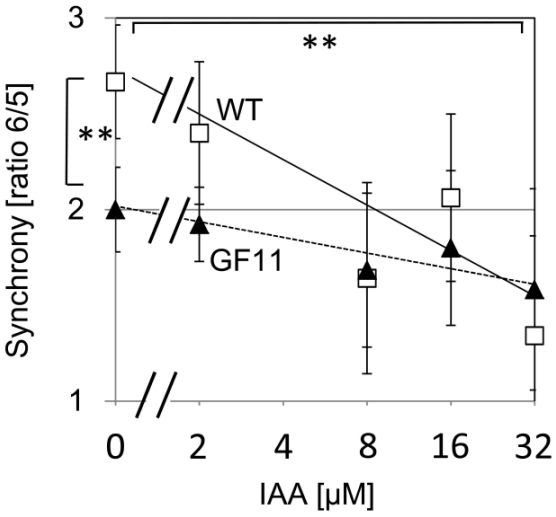

Fig. 3.6 Ratio of hexacellular over pentacellular files at day 3 of the cultivation cycle in dependence of exogenous IAA in non-transformed wild type (WT, white squares) versus the GFP-FABD2 overexpressor GF11 (black triangles). This ratio monitors the synchrony of the third division cycle within a file and depends on polar auxin flux. Each point is based on 1,500 individual cell files from three independent experimental series. Error bars indicate SE of the mean. Asterisks represent statistically significant differences (Student's t-test) with $P<0.01$ (**).

To address a potential influence of the basal level (0.9 µM) of the non-transportable artificial auxin 2,4-D, a supplementary experiment was conducted (Fig. 3.7). In this experiment, WT BY-2 cells were cultivated either in 32 µM IAA (without 2,4-D), in a combination of 31.1 µM IAA with the usual basal level (0.9 µM) of 2,4-D, or with 32 µM 2,4-D alone, i.e. in the absence of exogenous IAA. Then, the frequencies of cell number per file were determined at day 2 after subcultivation. The distribution patterns between IAA alone and the combination of low 2,4-D and IAA were almost identical (Fig. 3.7). The only difference was a slightly (but significantly) reduced frequency of bicellular files in the absence of 2,4-D. In contrast, cells that had been exclusively treated with 32 µM 2,4-D, showed a conspicuous increase in the proportion of bicellular files, while the proportion of quadricellular file was strongly decreased as compared to the situation with 0.9 µM of 2,4-D and 31.1 µM IAA given in combination. These data show that the pattern of division synchrony is almost exclusively controlled by IAA, while 2,4-D only plays a very marginal role.

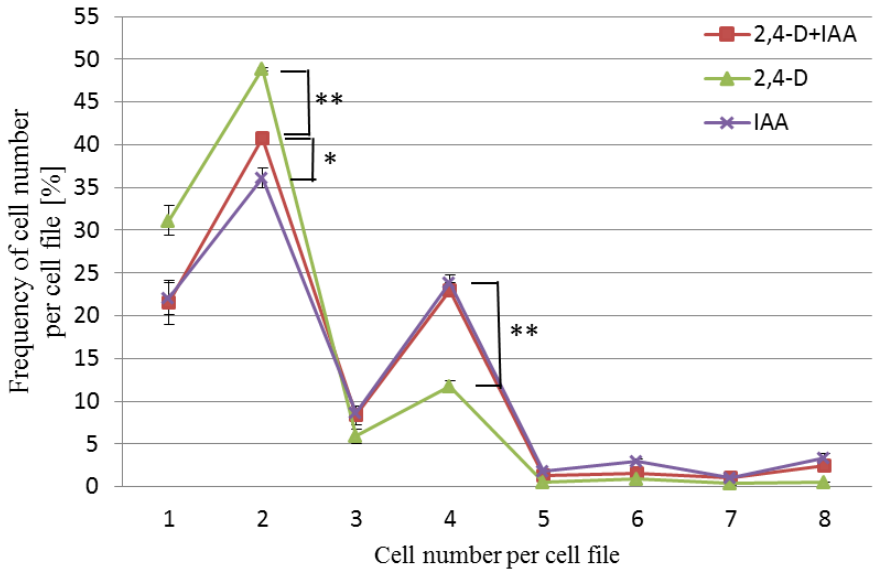

Fig. 3.7 The frequencies of cell number per file at day 2 of the WT BY-2 cultivation with the same total concentration on solely IAA (32 µM), solely 2,4-D (32 µM), and combination of 2,4-D (0.9 µM) and IAA (31.1 µM). Each point is based on 1,500 individual cell files from three independent experimental series. Error bars indicate SE of the mean. Asterisks represent statistically significant differences (Student's t-test) with $P<0.01$ (**), and $P<0.05$ (*).

3.1.5 Auxin delays the exit from the cycling stage

At the late stage of cell cultivation, cell cycling activity weakens progressively, and file disintegration becomes dominant (see Fig. 3.1). When the time course of mitotic index (see Fig. 3.2) is compared with the time course of mean cell number per file (see Fig. 3.5), it becomes clear that file disintegration already initiated at a time, when cells still underwent mitotic cycling. To estimate the exit time from the cycling stage, the mitotic index data are calculated and set the maximal MI as 100%. Then fit a linear regression to the MI values of the following days. From the regression, the 50% of the maximal MI value is set as the exit point, i.e. the time, when 50% of the previously cycling population has stopped cycling. This exit point was delayed by around one day for 2 µM, 8 µM and 16 µM of IAA, as compared to the control (0 µM). Both WT and GFP-FABD2 overexpressor behaved identically with respect to this exit point (Fig. 3.8). However, for 32 µM of IAA, the cycling stage for the WT

was strongly prolonged, which was not seen in the GF11 line. Thus, in analogy with the delay of file disintegration, the response of exit from cycling to high levels of IAA seems to be suppressed in the GFP-FABD2 overexpressor line.

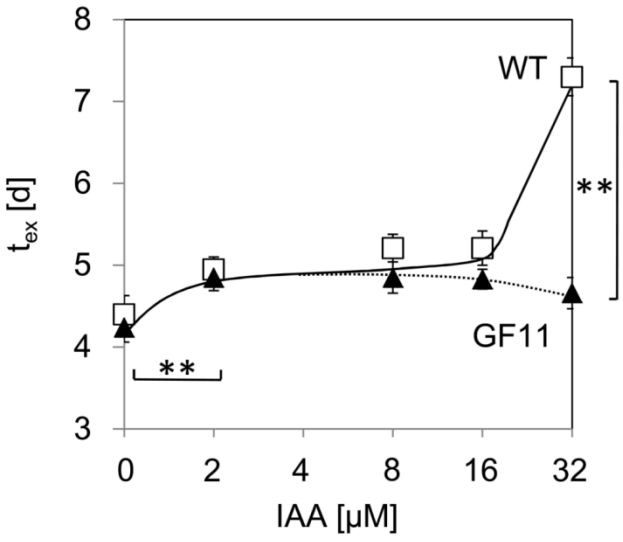

Fig. 3.8 Time of exit from the cycling stage in the WT (open squares) and the GFP-FABD2 overexpressor GF11 (black triangles) over the concentration of supplementary IAA. Each point is based on 1,500 individual cells from three independent experimental series. Error bars indicate SE of the mean. Asterisks represent statistically significant differences (Student's t-test) with $P<0.01$ (**).

3.1.6 Auxin stimulates initial cell file decay depending on actin

In the whole population of BY-2 cells, not all the cells are synchronized. At the end of the cultivation cycle, there are still some cell files not reaching the terminal unicellular or bicellular files. After subcultivation, a new wave of vigorous cell division initiates (see Figs. 3.1 and 3.2). However, there is still a significant proportion (around 40%) of bicellular files that have not completely decayed to the unicellular stage. These bicellular files should produce a large frequency of quadricellular files during day 1 and 2. When followed the frequency distributions of cell number per file on a daily base time point after subcultivation, it turned out that there were high proportions of unicellular and bicellular files during days 0, 1 and 2 (data not shown). This means that most bicellular files must still undergo decay, whereas the completely disintegrated single cells already begin to enter a new cell cycle.

If one neglects (the small frequency) files composed of more than two cells, it is possible to calculate the decay rates (from bicellular to singular) for WT and GF11 over day 1. For the wild type in the absence of auxin, around 48 h were required to get from a bicellular to a unicellular situation (Fig. 3.9), but this was accelerated to around 24 h in presence of 2 µM or 32 µM IAA. This decay was considerably faster in the GFP-FABD2 overexpressor GF11. Here, in the absence of auxin, the rate was 18 h in absence of auxin and decreased to 6 h at 2 µM, and 4 h at 32 µM of IAA (Fig. 3.9). This means that auxin stimulates the decay of residual bicellular files and that this auxin response is accentuated in the GFP-FABD2 overexpressor. The fact that the time constant for the decrease of bicellular files is higher than that for doubling, also means that the vast majority of bicellular files first decays before entering a new cycle of mitosis.

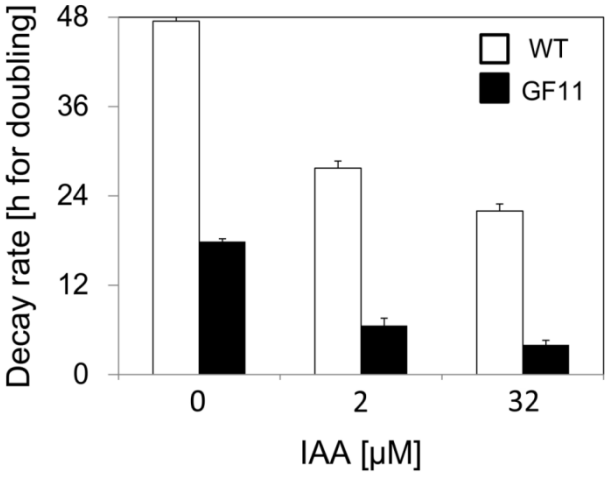

Fig. 3.9 Initial decay of cell files in the WT (white bars) and the GFP-FABD2 overexpressor GF11 (black bars) during day 1 after subcultivation in the absence of, or in presence of 2 µM or 32 µM IAA, respectively. Each point is based on 1,500 individual cell files from three independent experimental series. Error bars indicate SE of the mean. Asterisks represent statistically significant differences (Student's t-test) with $P<0.01$ (**).

3.2 The characteristic of fluorescent auxin analogs and auxin at the subcellular level in tobacco BY-2 cells

3.2.1 The different distribution patterns of NBD-NAA and NBD-IAA at the subcellular level

To investigate the subcellular distribution pattern of fluorescent auxin analogs, wild type BY-2 cells were incubated with NBD-NAA (2 μM) or NBD-IAA (2 μM) for different time periods, after that using cell culture medium wash the cells to remove unbounded NBD-NAA or NBD-IAA. As auxin can cross the plasma membrane to enter the cytoplasm by passive diffusion and influx carriers, 1 min and 20 min were selected for the incubation time. The results showed NBD-NAA presented a dot-like distribution after 1 min incubation (Fig. 3.10 C), while the 20 min incubation turned to be a membrane-like distribution (Fig. 3.10 F). However, the results of NBD-IAA distribution pattern were consistent, independent of incubation time. NBD-IAA always exhibited a dot-like distribution (Fig. 3.10 I and L). These findings suggest that NBD-NAA need to take some time to target to its final position, NBD-IAA could localize to the final position in a very short time, and the subcellular distribution patterns of NBD-NAA and NBD-IAA are different.

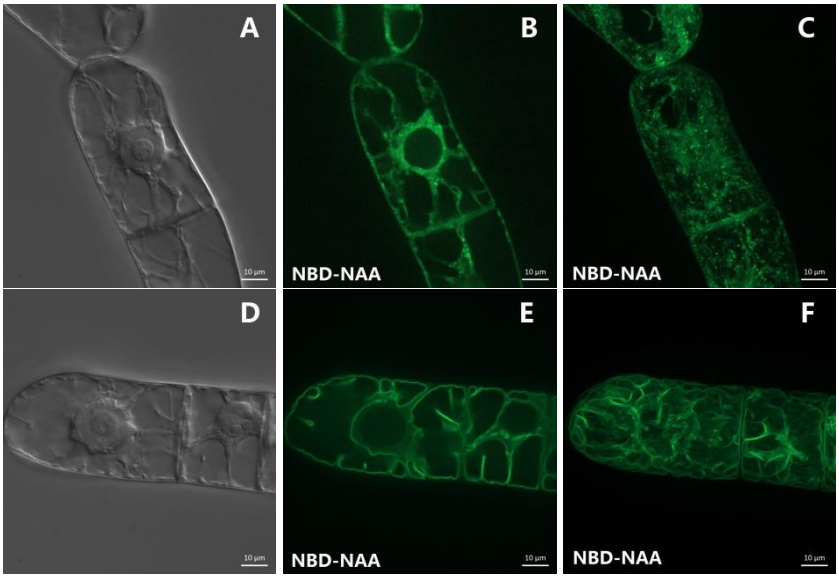

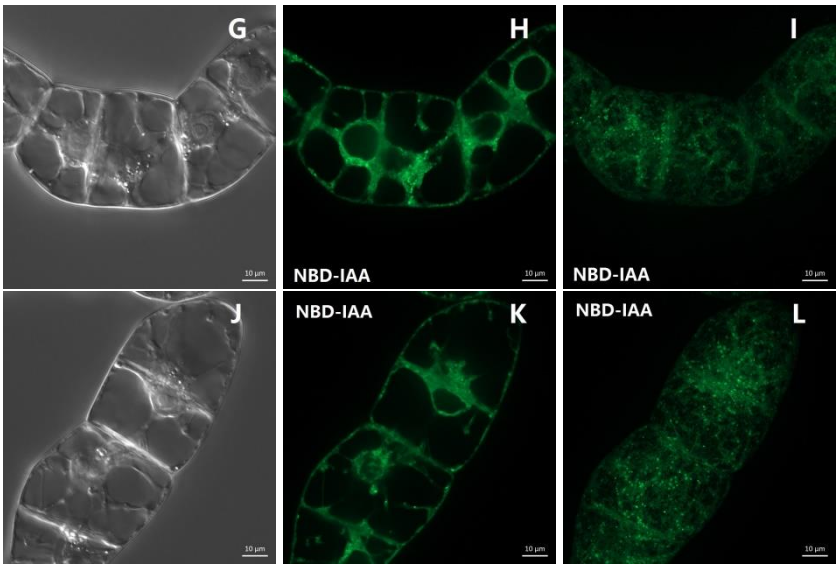

Fig. 3.10 Subcellular distribution pattern of NBD-NAA and NBD-IAA in WT BY-2 cells. The images of cells with NBD-NAA (2 μM) treatment were recorded after 1 min incubation (A-C). Confocal sections in the central region (A and B), and geometric projections of the z-stack (C) are shown. The images of cells with NBD-NAA (2 μM) were recorded after 20 min incubation (D-F). The images of cells with NBD-IAA (2 μM) were recorded after 1 min incubation (G-I). The images of cells with NBD-IAA (2 μM) were recorded after 20 min incubation (J-L). Scale bar represents 10 μm.

3.2.2 NBD-NAA localized to the endoplasmic reticulum (ER) and the tonoplast, NBD-IAA localized to the ER

As mentioned above the distribution patterns of fluorescent auxin analogs are different, when the incubation time was long enough (see Fig. 3.10 F and L). In order to figure out the exact subcellular localization of NBD-NAA and NBD-IAA, several fluorescent markers were employed to test colocalization of NBD-NAA or NBD-IAA.

To examine whether the fluorescent auxin analogs were localized to the ER, the WT BY-2 cells were incubated with NBD-NAA (2 μM) and ER-Tracker (1 μM). The results showed that areas around the nucleus and near the plasma membrane were yellow, indicating in these areas NBD-NAA were colocalized with ER-Tracker (Fig.

3.11 C). However, it also clearly showed that there were some NBD-NAA did not colocalized with ER-Tracker (Fig. 3.11 C and F). In contrast, the cells incubated with NBD-IAA (2 μM) and ER-Tracker (1 μM), the results exhibited completely colocalization of these two fluorescent compounds. These evidences indicated NBD-NAA and NBD-IAA were localized to the ER, and NBD-NAA also localized to other cellular compartment.

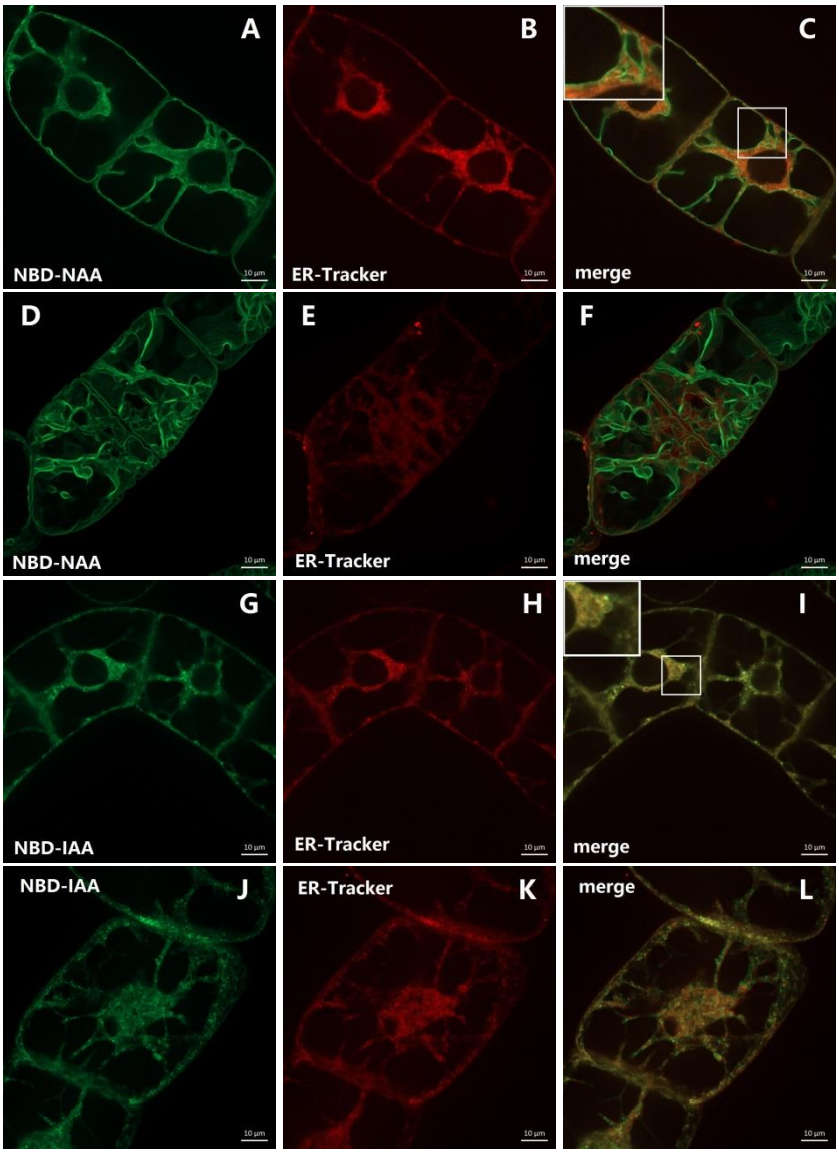

Fig. 3.11 Subcellular localization of NBD-NAA in WT BY-2 cells (A–F). The cells were pre-incubated with 2 μM NBD-NAA for 20 min, and then incubated with 1 μM ER-Tracker for 1 min. Images of NBD-NAA (A and D) and ER-Tracker (B and E) were merged (C and F). Subcellular localization of NBD-IAA in tobacco WT BY-2 cells (G–L). The cells were incubated

with 2 μM NBD-IAA for 20 min, after that treated with 1 μM ER-Tracker for 1 min. Images of NBD-IAA (G and J) and ER-Tracker (H and K) were merged (I and L). Confocal sections in the central region (A-C and G-I) and geometric projections of the z-stack (D-F and J-L) are shown. Scale bar represents 10 μm.

To further investigate the subcellular localization of NBD-NAA, the BY-2 cells were transiently *Agrobacterium*-mediated transfected, expressing NtTPC1A-RFP, in order to test its colocalization with NBD-NAA. NtTPC1A-RFP is encoding calcium channels in BY-2 cells (Kadota *et al.*, 2004; Kurusu *et al.*, 2012b), targeting to the tonoplast. The treatment with NBD-NAA (2 μM) displayed a colocalization between NtTPC1A-RFP and NBD-NAA (Fig. 3.12 C and F). In order to further confirm it, the protoplasts of BY-2 cell were harvested by digesting cell wall with enzyme solution of cellulose and pectolyase. When the cell wall was removed, the turgor pressure would turn protoplast into a global shape, so that the plasma membrane can be separated from tonoplast. Applied with NBD-NAA (2 μM), the distribution pattern of NBD-NAA in WT BY-2 was quite similar to the pattern of NtTPC1A-GFP (Fig. 3.12 H and J). Additionally, the protoplast of PIN1-GFP was generated. PIN1-GFP is auxin efflux carrier fused with GFP protein, locating to the plasma membrane. It showed a clear difference between the distribution pattern of PIN1-GFP and the distribution pattern of NBD-NAA (Fig. 3.12 H and L). These results implied that NBD-NAA can localize to tonoplast.

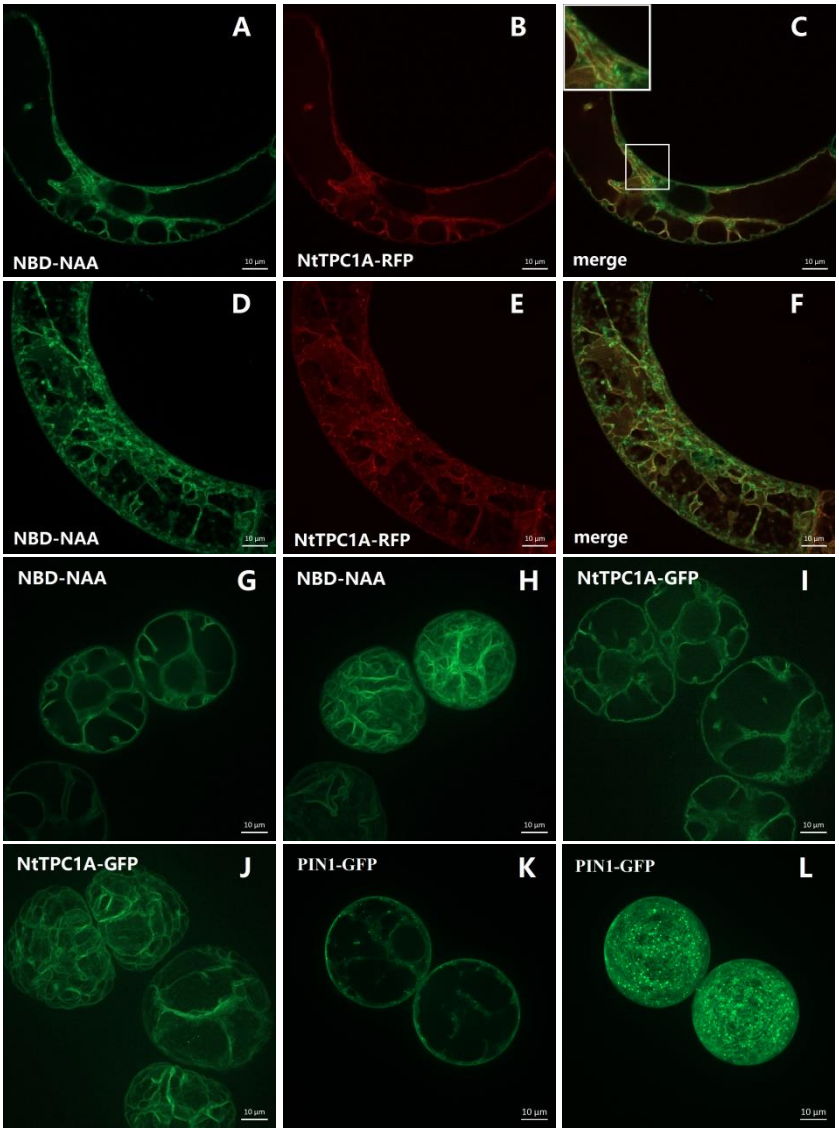

Fig. 3.12 The transient *Agrobacterium*-mediated transformation of BY-2 cells with NtTPC1A-RFP fusion proteins (B and E) were incubated with 2 μM NBD-NAA (A and D) for 20 min (A–F). Images of NBD-NAA and NtTPC1A-RFP were merged (C and F). The protoplasts of WT BY-2 cells were treated with 2 μM NBD-NAA for 20 min (G and H). The protoplasts of NtTPC1A-GFP (I and J) and PIN1-GFP (K and L) were generated. Scale bar represents 10 μm.

3.2.3 The binding characteristic of fluorescent auxin analogs and auxin in tobacco BY-2 cells

Since the subcellular localization of fluorescent auxin analogs have been demonstrated (see Fig. 3.11 and Fig. 3.12), they have the potential to monitor the

binding characteristic of themselves and auxin, in this part of study, including NAA, IAA, and 2,4-D. First, it is necessary to find out whether NBD-NAA (or NBD-IAA) can compete with auxin (NAA, IAA and 2,4-D) for the same binding sites. If so, then the fluorescent alteration of NBD-NAA (or NBD-IAA) can reflect some binding characteristic of auxin, which is invisible.

3.2.3.1 NBD-NAA can high efficiently compete with NAA for the same binding sites, low efficiently compete with IAA and 2,4-D

To investigate whether NBD-NAA and NAA bind to the same binding sites and this binding process was reversible or not, some WT BY-2 cells had been treated by two steps: first NAA incubation for 20 min, then NBD-NAA (2 μM) incubation for another 20 min (Fig. 3.13 A-D). Other WT BY-2 cells were treated with NBD-NAA (2 μM) and NAA together for 20 min (Fig. 3.13 E-H). Several concentrations of NAA were selected: 2 μM (Fig. 3.13 A, B, E, and F), 20 μM (data not shown), and 100 μM (Fig. 3.13 C, D, G, and H). The results exhibited the same trend of NBD-NAA fluorescent fading with the increment of NAA concentration. These findings suggested NBD-NAA and NAA could bind to the same binding sites, and the binding process was a reversible process. In the following experiments, NBD-NAA (or NBD-IAA) and auxin (NAA, IAA, and 2,4-D) were always added to the cells at the same time, incubating for 20 min.

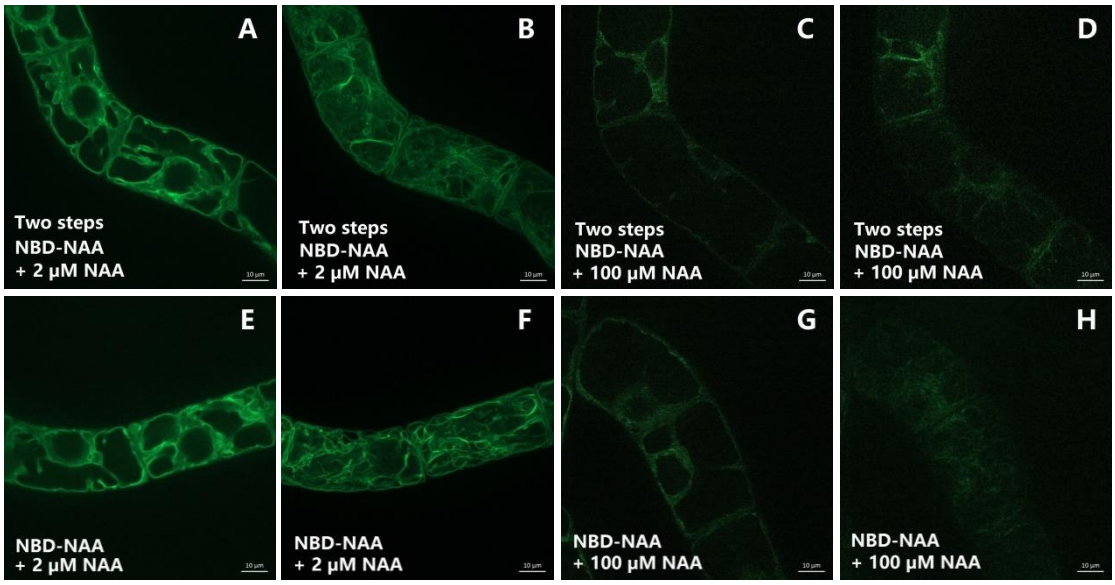

Fig. 3.13 NBD-NAA and NAA compete for the same binding sites. Cells were incubated with NBD-NAA and NAA by two steps treatments (A-D). The cells were pre-incubated with 2 μM (A and B) or 100 μM (C and D) NAA for 20min, and then treated with 2 μM NBD-NAA for another 20 min. The cells were treated with 2 μM (E and F) or 100 μM (G and H) NAA, together with 2 μM NBD-NAA for 20 min. Scale bar represents 10 μm.

In order to test whether NBD-NAA and IAA (or 2,4-D) also bind to the same binding sites or not, wild type BY-2 cells were treated with NBD-NAA (2 μM) and IAA (or 2,4-D) for 20 min (Fig. 3.14 A-H). Several concentrations of IAA (or 2,4-D) were selected: 2 μM, 20 μM (data not shown), and 100 μM. Unlike NAA (see Fig. 3.13), these auxin (IAA or 2,4-D) could not induce an dramatically decrement of NBD-NAA fluorescent, even under high concentration of 100 μM (Fig. 3.14 A-H). However, the treatment of 100 μM 2,4-D altered the distribution pattern of NBD-NAA, from membrane-like pattern to dot-like pattern (Fig. 3.14 H). To find out whether the alteration of NBD-NAA distribution pattern was related to 100 μM 2,4-D, the NtTPC1A-GFP transgenic cell strain was treated with 2 μM, 20 μM (data not shown), or 100 μM 2,4-D (Fig. 3.14 I-L). The results showed that the membrane-like structure of NtTPC1A-GFP was maintained, even under 100 μM 2,4-D treatment. All this part results implied that NBD-NAA cannot efficiently compete with IAA or 2,4-D for binding to the same sites.

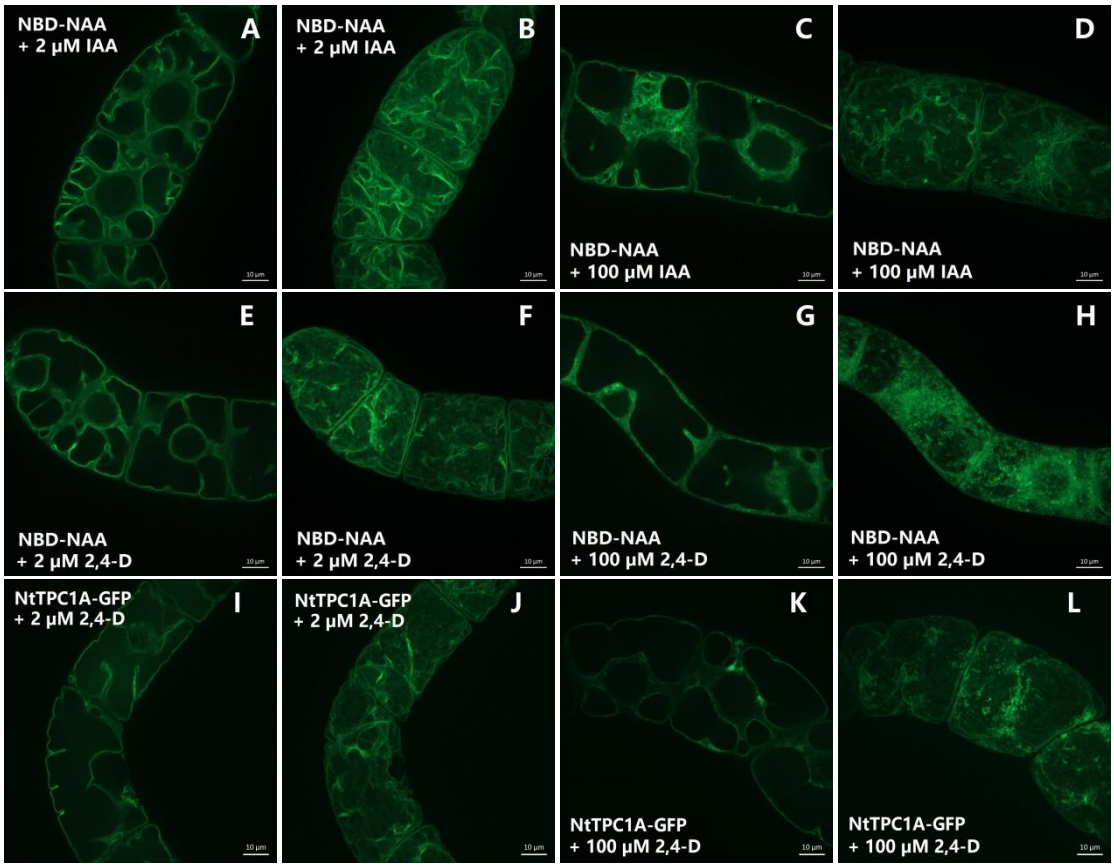

Fig. 3.14 Distribution of NBD-NAA in WT BY-2 cells with IAA or 2,4-D treatment (A-H). The cells were co-incubated with 2 µM NBD-NAA and 2 µM (A and B) or 100 µM (C and D) IAA for 20 min. The cells were treated with 2 µM (E and F) or 100 µM (G and H) 2,4-D, together with 2 µM NBD-NAA for 20 min. The tonoplast-targeted NtTPC1A-GFP transgenic cells under 2,4-D treatment (I-L). The transgenic cells were incubated with 2 µM (I and J) or 100 µM (K and L) 2,4-D for 20 min. Scale bar represents 10 µm.

3.2.3.2 NBD-IAA also can high efficiently compete with NAA for the same binding sites, low efficiently compete with IAA and 2,4-D

As the binding characteristic of NBD-NAA has been figured out above (see Fig. 3.13 and Fig. 3.14), what is the binding characteristic of NBD-IAA? To examine whether NBD-IAA can compete with auxin, including IAA, NAA and 2,4-D, for their binding sites, wild type BY-2 cells were incubated by NBD-IAA (2 µM) and auxin with different concentrations: 2 µM, 20 µM (data not shown), and 100 µM (Fig. 3.15). The results showed that with 2 µM or 20 µM auxin treatments, none of these three kinds

of auxin could induce significant alteration of NBD-IAA fluorescent. However, with 100 μM auxin treatment, not IAA but NAA could induce a significant reduction of NBD-IAA fluorescent distribution, and 2,4-D was unable to affect NBD-IAA fluorescent distribution. These findings suggested NBD-IAA could not efficiently compete with IAA and 2,4-D for the same binding sites. And strangely, NBD-IAA could compete with NAA for the same binding sites. Perhaps, due to NBD moiety was conjugated to IAA, this NBD moiety induced some changes in NBD-IAA binding properties.

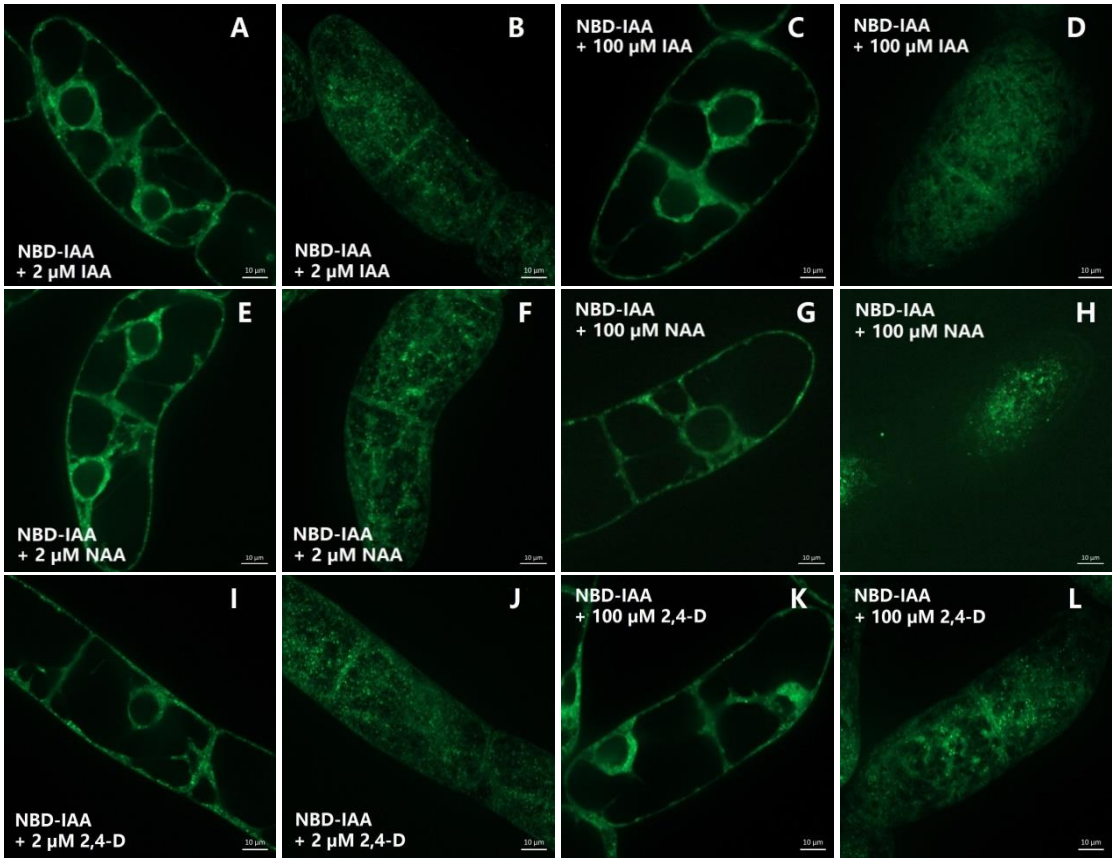

Fig. 3.15 Effects of auxin (IAA, NAA and 2,4-D) on NBD-IAA distribution in WT BY-2 cells. The wild type BY-2 cells were incubated with 2 μM (A and B) or 100 μM (C and D) IAA and 2 μM NBD-IAA together for 20 min. The cells were co-treated with 2 μM (E and F) or 100 μM (G and H) NAA and 2 μM NBD-IAA for 20 min. The cells were treated with 2 μM (I and J) or 100 μM (K and L) 2,4-D, together with 2 μM NBD-IAA for 20 min. Scale bar represents 10 μm.

3.2.3.3 IAA and 2,4-D can affect NBD-NAA binding to the binding sites although in different ways

The NBD-NAA can precisely compete with NAA for their binding sites, but not so efficient for IAA or 2,4-D binding sites (see Fig. 3.13 and Fig. 3.14). Although the fluorescent alteration of NBD-NAA under IAA or 2,4-D treatment was not obvious through the naked eye, it is still possible to quantify the changes of fluorescent by Zeiss ZEN software. After the WT BY-2 cells were incubated with NBD-NAA (green fluorescent molecule) and ER-Tracker (red fluorescent molecule), images of cell sample were recorded under microscope with two channels. These images can be analyzed for colocalization, based on a pixel by pixel basis and the intensity level from each channel. The weighted colocalization coefficients are calculated by summing the pixels with intensity value in the colocalized region and then dividing by the sum of pixels with intensity value either in the NBD-NAA channel or the ER-Tracker channel.

In order to investigate whether IAA or 2,4-D can affect NBD-NAA binding to the binding sites, WT BY-2 cells were incubated with NBD-NAA and ER-Tracker, in the absence or in the presence of IAA or 2,4-D. Then the weighted colocalization coefficients of NBD-NAA were calculated. In the absence of IAA or 2,4-D, the values of NBD-NAA weighted colocalization coefficients were around 35 – 45% (left black columns, Fig. 3.16), and the values of ER-Tracker weighted colocalization coefficients were nearly 100% (right black columns, Fig. 3.16). These results were consistent with the findings mentioned above: the subcellular localizations of NBD-NAA are the ER and the tonoplast (see Fig. 3.11 and Fig. 3.12). Again, the weighted colocalization coefficients of NBD-NAA proved that only parts of NBD-NAA were localized to the ER.

Meanwhile, the values of weighted colocalization coefficients were differently altered,

according to the presence of IAA or 2,4-D. Provided 2 µM or 100 µM IAA, the NBD-NAA weighted colocalization coefficients were reduced (left grey columns, Fig. 3.16 A and B). In contrast, 100 µM 2,4-D enhanced the weighted colocalization coefficients of NBD-NAA (left grey columns, Fig. 3.16 D), while 2 µM 2,4-D did not alter the values of NBD-NAA weighted colocalization coefficients (left grey columns, Fig. 3.16 C). However, the values of ER-Tracker weighted colocalization coefficients were still almost 100% (right grey columns, Fig. 3.16). These results implied that IAA and 2,4-D can also affect NBD-NAA binding to its binding sites, although not as efficient as NAA (see Fig. 3.13).

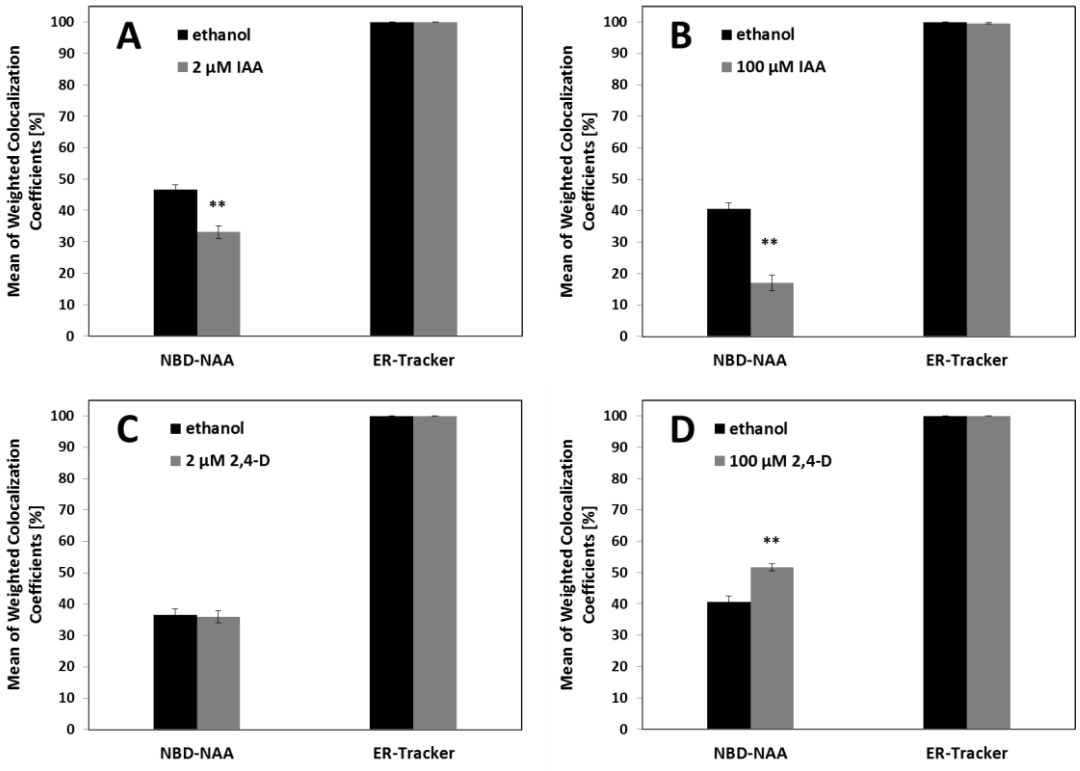

Fig. 3.16 Mean values of weighted colocalization coefficients of NBD-NAA or ER-Tracker in WT BY-2 cells. Cells were treated with 2 µM NBD-NAA (and same amount of ethanol solution as the other treatments) as control (black columns) for 20 min, and then added 1 µM ER-Tracker for 1 min. Cells were co-incubated with 2 µM NBD-NAA and 2 µM IAA (A), 100 µM IAA (B), 2 µM 2,4-D (C), or 100 µM 2,4-D (D) for 20 min, respectively, then treated with 1 µM ER-Tracker for 1 min (grey columns). Each mean value represents in each case averages from 50 individuals. Error bars indicate SE. Asterisks represent statistically significant differences (Student's Independent two-sample t-test) with $P<0.05$ (*) and $P<0.01$ (**), respectively.

3.2.3.4 Dissociation constant (Kd) of NAA was determined by quantifying fluorescent alteration of NBD-NAA

As there were competitive binding between NBD-NAA and NAA for the same binding sites (see Fig. 3.13), the quantitative treatments of NBD-NAA and NAA competition were conducted, applying constant concentration of NBD-NAA (2 µM) combining with different concentrations of NAA. Then the fluorescent alteration of NBD-NAA was quantified by ImageJ software, and determined the affinity of the binding sites to NAA using the Michaelis-Menten formula. The results showed that with the increasing concentrations of NAA, the values of relative fluorescence intensity (the same value as the corrected single cell fluorescence, CSCF) were progressively decreasing (Fig. 3.17 A). Then calculating the first derivative of relative fluorescence intensity, one can get a curve about the first derivative of relative fluorescence intensity and concentration of NAA. When the first derivative of relative fluorescence intensity equals exactly 0.5, the NAA concentrations equals dissociation constant (Kd). In this study, the dissociation constant (Kd) of NAA was 47.8 nM.

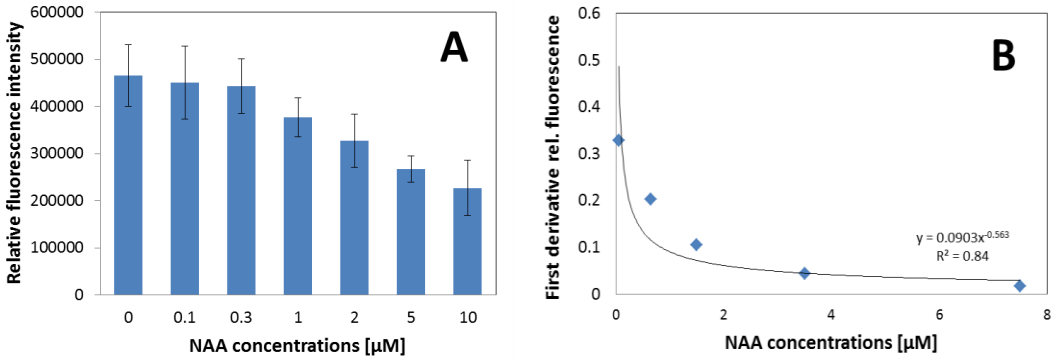

Fig. 3.17 Relative fluorescence intensity of NBD-NAA in responses to the increasing concentrations of NAA (A). The WT BY-2 cells were treated with 2 µM NBD-NAA, together with different concentrations of NAA for 20 min. Each point is based on at least 900 individual cells from three independent experimental series. The data were fitted using a Michaelis-Menten function and got the dissociation constant (Kd) (B).

3.3 Summary

Auxin is a relatively simple structure chemical substance, but has very complex effects on plant system. Some fundamental questions in auxin biology concern how plant cell senses auxin, how auxin involves in cell activities, where is auxin localization in the cell, and so on. There are some researches show that the developmental responses of suspension BY-2 cells are clearly under control of auxin in a very specific manner, such as the synchrony of cell division related to the actin-dependent polar auxin transport (Campanoni and Nick, 2005; Maisch and Nick, 2007).

In first part of this dissertation, potential link between auxin-responsiveness and actin dynamics was investigated. Wild type BY-2 cell line and transgenic GF11 line were exposed to different concentrations of auxin (IAA) during their cultivation cycle. The typical auxin responses in the different cultivation stages were analyzed. The presence of IAA (2μM, 8 μM and 16 μM) stimulated and prolonged the mitotic index in WT, whereas IAA caused a slight, but significant reduction of MI in the GF11 line. The cell division duration was independent on auxin in WT and GF11, with the exception that high level of auxin and overexpression of the GFP-FABD2 marker synergistically and dramatically slowed down the first cell division in GF11. In addition, the exit point from the cycling stage was delayed by auxin in both WT and GF11; for 32 μM of IAA, the cycling stage for the WT was strongly prolonged, whereas this response seems to be suppressed in the GF11 line. However, at the stationary phase of the cultivation cycle, auxin strongly accelerated the cell file disintegration. Interestingly, it was not suppressed but progressed to a more complete disintegration in the GF11 line. Furthermore, the organization of actin filaments were also observed in the GF11 line through the culture cycle and no detectable significant differences of the actin filaments were found in any of these treatments.

More details of auxin biology about auxin spatial distribution and binding

characteristic in the cell were probed in the second part of this dissertation. The fluorescent auxin analogs (NBD-NAA and NBD-IAA) were designed to mimic auxin, and could be transported by auxin transport system without activate auxin signaling. With application of fluorescent auxin analogs in WT BY-2 cell, it demonstrated that NBD-NAA was localized to the ER and the tonoplast, and NBD-IAA was localized to the ER. Then auxin (NAA, IAA, 2,4-D) were used to compete with fluorescent auxin analogs for their binding sites. It showed that only NAA could high efficiently compete with NBD-NAA and NBD-IAA. However, IAA and 2,4-D, though not as efficient as NAA, could also affect NBD-NAA binding to the binding sites. Further analysis colocalization of NBD-NAA with ER-Tracker, it turned out that IAA bind to the ER, while 2,4-D bind to the tonoplast, causing reduction of NBD-NAA signal although in different ways. Furthermore, the dissociation constant of NAA was calculated by quantification of fluorescence intensity of NBD-NAA.

4. Discussion

The naturally occurring auxin (IAA) plays a major role in coordination of many growth and developmental processes. Although auxin is a relatively simple structure chemical substance, plant cell have developed multiply mechanisms to integrate numerous stimuli into auxin signal pathway. Therefore, auxin itself can represent direct signal to trigger specific responsiveness. Intracellular auxin has close connection with actin-dependent auxin carrier localization. Thus, actin dynamics might involve in auxin-responsiveness. What are the differences of auxin-responsiveness between the wild type BY-2 cell and the transgenic cell line with modified actin dynamicity? Measuring the typical cell phenotypes, the experimental approaches led to a model on auxin sensing in respect to actin dynamics. Furthermore, visualize the auxin distribution in the single cell offer a deeper insight into auxin signal pathway.

4.1 Sensory role of actin in auxin-dependent responses

4.1.1 Cellular responses to auxin are modulated in the GFP-FABD2 overexpressor

To get insight into the role of actin for auxin-dependent developmental responses of walled plant cells, first step is to map the behavior of tobacco BY-2 cells in the presence of different concentrations of the natural auxin (IAA) and compare the response patterns of the non-transformed line with a line overexpressing a GFP fusion of the actin-binding domain 2 of plant fimbrin. This actin marker confers a slight stabilization of actin (Holweg, 2007; Zaban *et al*., 2013), which, upon overexpression in *Arabidopsis thaliana*, can also cause subtle changes of growth, such as a reduced elongation of root hairs (Wang *et al*., 2008).

Using this marker, it is now able to address the effect of slight actin stabilization on

the auxin responses in a tobacco suspension cell line by quantifying physiological readouts for actin-dependent responses. Since actin dynamicity can vary even between neighboring cells within a cell file (Eggenberger *et al*. 2017), such a physiological approach is useful, because it integrates over the entire cell population. The use of cells in suspension to address such "developmental" aspects may be surprising at first sight. Suspension cell cultures are widely used as model for biochemical and cell biological studies, and the tobacco cell line BY-2 has acquired a certain celebrity in this respect as "HeLa cell line" of plant biologists (Nagata *et al*., 1992), because cell suspensions represent a convenient system to accumulate "biomass". However, their potential as systems to address cellular aspects of development has been rarely exploited. Although suspension cells are often designated as "dedifferentiated", they still preserve certain characteristics of their origin. In case of the BY-2 line, these characteristics include the reduced recapitulation of a developmental program seen in a pith parenchymatic cell that is stimulated by auxin to differentiate into a vascular bundle (Opatrný *et al*., 2014). Whereas this developmental sequence can even reach to the formation of secondary cell wall thickenings in other, slower, cell strains derived from pith parenchyma (Nick *et al*., 2000), the selection of BY-2 for rapid division has resulted in a cell strain that cannot sustain the viability of the auxin-depleted state long enough to develop these hallmarks of differentiation. Nevertheless, even in BY-2, there is a distinct and reproducible sequence of developmental stages including proliferation, formation of pluricellular files, transition to cell expansion, and progressive disintegration of the files into smaller units and eventually individual cells (Fig. 3.1). By stringent standardization of culture conditions, it is possible to reach a degree of reproducibility that allows us to deduce quantitative data from this system. Doing so, it was able to derive the following conclusions on the effect of auxin and actin stability:

Auxin stimulated and prolonged mitotic activity (Fig. 3.2), and delayed the exit from the proliferation phase (Fig. 3.8). Both responses were prominent for high concentrations of auxin, and both responses were suppressed in the FABD2

overexpressor line.

In contrast to these features, the length of the cell cycle, as monitored by the doubling times, was generally independent of auxin and actin (Fig. 3.4). However, the first cycle after subcultivation, which was considerably slower than the subsequent division cycles, was extremely retarded in the FABD2 overexpressor, but only in presence of high auxin concentrations.

Auxin not only delayed the exit from proliferation (Fig. 3.8), but also the disintegration of files exiting from the proliferation phase (Fig. 3.5). Both phenomena were suppressed in the FABD2 overexpressor. On the other hand, when acting on the residual bicellular files persisting at the end of the cultivation cycle, auxin strongly accelerated the disintegration of these residual files (Fig. 3.9). While it is difficult to directly observe, whether an inclompletely decayed file already enters a new round of proliferation, it is possible to make a statistical statement: The time constant for the decrease of bicellular files was higher than that seen for proliferation. This means that the vast majority of bicellular files first decays before entering a new cycle of mitosis, although it cannot be excluded that a small number of files already initiates a new cell cycle prior to complete disintegration of the file. In the FABD2 overexpressor, the disintegration was not only resistant to the retarding effect of auxin, but was generally progressing to a more complete disintegration in the later phase of the cultivation cycle, such that the incidence of bicellular files was significantly reduced. Furthermore, the auxin-dependent acceleration of disintegration was even stronger as compared to the non-transformed BY-2 wild type.

In summary, while some auxin responses were found to be retarded or downmodulated in the FABD2 overexpressors, others were seen to be either unaltered or even more pronounced. Interestingly, only few of these auxin responses followed a bell-shaped dose response, where the highest concentration (32 µM) was loosing activity if compared to the lower concentration (2 µM). This bimodal behavior is

classically interpreted as manifestation of a receptor dimer (Foster *et al*., 1952; Foster *et al*., 1955). Interestingly, only the amplitude of mitotic index (Fig. 3.2) was following such a pattern, indicating that the activation of the cell cycle by auxin might differ from the activation of the other responses considered here.

It should be mentioned here that low concentrations (0.9 µM) of the non-transportable, artificial auxin (2,4-D) were added to probe for the function of transportable, natural auxin. This low background level of 2,4-D was required, because IAA is not completely stable over the entire cultivation cycle of 7 days. Over repeated cycles this degradation results in fluctuations of proliferation activity, which is avoided by 2,4-D. This non-transportable form of auxin has been shown to be inactive with respect to pattern formation and actin-dependent auxin transport (Maisch and Nick, 2007; Nick *et al*., 2009), but is required to sustain a stable basal level of proliferation (Campanoni and Nick, 2005). To probe for a potential influence of 2,4-D, it requires a comparison among the effect of a high (32 µM) concentration of exogenous auxin administered either completely in form of transportable IAA, of non-transportable 2,4-D, or a combination of a high (31.1 µM) concentration of IAA with the basal (0.9 µM) concentration of 2,4-D used in the experiments. Frequency distribution of cell number per file (as measure for division synchrony) was monitored as most sensitive readout (Fig. 3.7). The data show clearly that division synchrony was accentuated by supplementary IAA, while presence or absence of 2,4-D was irrelevant. The fact that even in absence of exogenous IAA, a certain level of division synchrony was observed, indicates that 2,4-D activates the synthesis of endogenous IAA, a conclusion that had already been drawn earlier (Qiao *et al*., 2010) in experiments with a light-sensitive tobacco cell line.

To integrate these findings into a working model, in a first step, the observations will be grouped into phenomena seen at the onset of a new culture cycle, when stationary cells are confronted with exogenous IAA, and phenomena seen at the transition from the proliferation in the subsequent expansion phase of the culture.

4.1.2 At the onset of proliferation, FABD2 renders auxin responses more sensitive

At the end of the culture cycle, cells are highly vacuolated after several days of expansion growth. The nucleus is located at the periphery of the cell in a cytoplasmic pocket, from where transvacuolar strands of cytoplasm emanate. When a new cultivation cycle is initiated by transfer into fresh medium, the nucleus first has to migrate to the cell center, before the first division can initiate correlated with a significant increase of doubling time for the first division compared to the subsequent cycles that start from a situation, where the nucleus is already central (Fig. 3.4). Nuclear migration has been extensively studied in fungal systems and shown to depend on both, plus-end kinesin and minus-end dynein motors (Meyerzon *et al*., 2009; Fridolfsson and Starr, 2010). However, higher plants lack dynein motors - here, premitotic nuclear migration depends on so called kinesins with a calponin-homology domain (KCH), a plant-specific group of minus-end directed class-XIV kinesins (Frey *et al*., 2010; Schneider and Persson, 2015). These kinesins exist in two functionally distinct subpopulations: either linked with actin filaments controlling premitotic nuclear movement, or uncoupled from actin in cell-wall related microtubule arrays, such as phragmoplast or cortical microtubules (Klotz and Nick, 2012). A link of nuclear migration with actin is not an exclusive acquisition of higher plants, but has also been observed in other organisms. For instance, actin-dependent tethering of the nucleus is a characteristic feature of cytoplasmic transport from nurse cells to the oocyte in the developing fruit fly follicle (Gutzeit, 1986). Moreover, several proteins responsible for the link between nuclear lamina and actin have been reported in mammalian cells (Razafsky and Hodzic, 2009). Although there is no nuclear lamina in plants, and although sequence homologues for some of these linker proteins seem to be absent, there exist functional analogues that convey the same function and link with plant-specific class-XI myosins (Tamura *et al*., 2013). The nuclear movement is associated with local contraction of a specific perinuclear actin basket at the leading

edge indicating a peristaltic mechanism of movement (Durst *et al.*, 2014). The extreme slow-down of the first cell cycle in response to 32 µM auxin was exclusively seen in the GFP-FABD2 overexpressor, indicating that the actin-dependent machinery driving nuclear movement is disrupted. When followed potential structural changes of actin in response to IAA based on the GFP reporter (Fig. 3.3), it was not able to detect any significant differences between control and IAA treatment. Specifically, there was no disruption of actin filaments to be seen. This indicates that the breakdown of nuclear movement caused by high concentrations of IAA in the GFP-FABD2 overexpressor is of functional, rather than of structural, nature. It should be mentioned here that the initial migration of the nucleus from the periphery towards the cell center requires that the cells have fully entered the expansion phase in the preceding cultivation cycle. This depends on the density in the inoculum - when the cells are cultivated at higher density, such that exit from proliferation is retarded and therefore the nucleus still not completely arrived at the cell periphery, this will mask the initial centripetal movement.

Not only was the nuclear movement at the initiation of a new culture cycle found to be sensitized against auxin upon overexpression of GFP-FABD2. Also the disintegration of the residual bicellular files had already progressed further in this cell strain, and this disintegration was further accelerated by exogenous auxin, and in the GFP-FABD2 strain, the amplitude of this acceleration was more pronounced (Fig. 3.9). This is remarkable, because file integrity depends on a different population of actin filaments that link neighboring cells through the plasmodesmata and are connected with a different class of plant specific class-VIII myosins that differ from the class-XI myosins involved in nuclear movement (Baluška *et al.*, 2001).

Thus, at the onset of the proliferation phase, overexpression of GFP-FABD2 causes a sensitization of auxin responses.

4.1.3 At the progression of proliferation, FABD2 renders auxin responses less sensitive

The structural role of actin in the division of plant cells extends beyond steering and tethering the nucleus during its premitotic migration. It also extends over the role actin plays as a so called matrix that surrounds the division spindle (Forer and Wilson, 1994), and organizes the myosin-dependent cleavage of daughter cells (Mabuchi, 1986). In plant cells, actin filaments also participate in the control of division ability and symmetry: Once the nucleus has reached its final position, the transvacuolar actin cables fuse into a structure that spans the cell like a Maltesian cross oriented perpendicular to the long axis of the cell. While the microtubular preprophase band heralding axis and symmetry of the ensuing cell division is of transient nature and disappears in the very moment, when the nuclear envelope disintegrates, this so called actin phragmosome persists and lines a central zone, where actin is depleted (Sano *et al*., 2005; Nick, 2008). After the separation of chromosomes, microtubules are organized into the interdigitating array of the phragmoplast and deliver vesicles containing cell wall material to the growing cell plate. The edge of the expanding cell plate is tethered to the zone of actin depletion, which had been previously occupied by the preprophase band. Thus, actin is considered to align the growth of the cell plate with the plane of symmetry (Kost and Chua, 2002). Exogenous auxin significantly stimulated mitotic activity and kept the cells in the proliferation phase, concomitantly with a delay of file disintegration (Figs. 3.5 and 3.8). Neither this delay, nor the stimulation of mitotic activity is seen in the GFP-FABD2 overexpressor, not even for the highest concentration of auxin (32 µM), indicating that, with progression into the proliferation phase, the responsiveness to auxin is reduced.

Thus, overexpression of GFP-FABD2 correlates with a desensitization of auxin responses (with progression into the proliferation phase), which is in sharp contrast seen to the increased sensitivity observed in stationary cells upon transition into the

new culture cycle. What shows here, is nothing else than a sign-reversal with respect to the role of actin in auxin-dependent developmental responses. It is difficult to explain this sign-reversal by the structural functions of actin, since these structural functions (tethering of the nucleus via a process depending on class-XI myosins, symplastic continuity of neighboring cells via a process depending on class-VIII myosins) are similar. When followed the GF11 line by spinning-disc microscopy over the culture cycle, it was not able to detect any significant difference in actin organization in response to different concentrations of exogenous IAA (Fig. 3.3). This means that the specific differences observed in the GFP-FABD2 strain must be linked with a function of actin that is not structural.

4.1.4 A role for actin in auxin sensing

One candidate for such a role of actin that extends beyond the canonical structural effect of the cytoskeleton is the link between auxin transport and actin (Zhu and Geisler, 2015). Even the mild stabilization of actin filaments mediated by the overexpression of GFP-FABD2 in Arabidopsis can cause a substantial reduction in polar auxin transport (Holweg, 2007). Also for rice, actin stabilization caused by overexpression of mouse talin could be shown to impair auxin transport by using donor blocks of agar doped with radioactively labeled IAA and quantifying the proportion of radioactivity arriving in the receiver block (Nick *et al*., 2009). However, this approach is not feasible in suspension cells. The activity of polar auxin transport can be inferred by considering division synchrony across a cell file. Especially the synchrony of the third division is under control of polar auxin transport (Campanoni *et al*., 2003; Maisch and Nick, 2007). In case of asynchrony, a cell with n = 4 will move on to n = 5, in case of synchrony, a file with n = 6 will be produced. If the stabilization of actin by overexpression of GFP-FABD2 would impair the polarity of auxin transport, this should be seen as a significant reduction in the ratio of hexacellular over pentacellular files. This is exactly, what have been observed (Fig. 3.6). By flooding the cell with extracellular IAA, the situation found in GF11 can be

phenocopied in the wild type: in the presence of 32 µM IAA, the synchrony of the third division cycle has dropped to the value seen in the GFP-FABD2 overexpressor. Thus, a (mild) stabilization of actin, or likewise the out-competition of endogenous auxin gradients by an excess of exogenous IAA, reduce division synchrony in the same manner, indicative for a reduced polarity of auxin transport. This is consistent with previous work, where actin was destabilized by overexpression of actin-depolymerization factor 2 (ADF2) leading to disturbed division synchrony. Here, a mild stabilization of actin by low concentrations of phalloidin or by addition of phosphatidylinositol 4,5-bisphosphate (PIP_2) sequestering the excess ADF2 was able to rescue the division synchrony (Durst *et al*., 2013). Therefore, division synchrony requires that actin dynamics has to be balanced within a certain extent.

That the stabilization of actin should impair the polarity of auxin transport, would be expected from the actin-auxin oscillator model (Nick, 2010), since the stabilized actin filaments would trap the auxin efflux carriers, and thus interfere with their integration into the plasma membrane. Why the auxin-sensitivity of actin-dependent responses should undergo a sign-reversal, when cells pass on from stationary phase into a new cycle of proliferation, cannot be predicted by this model, though. Since these responses (for instance file disintegration) overlap with respect to the responsible actin arrays, explanations based on differently responsive actin subpopulations do not appear to be feasible either.

A simple way to explain sign-reversals in the response to a signal are mechanisms where this signal is perceived by two different receptors that switch their activity depending on the situation. In fact, tobacco cells have been shown to harbor two signaling chains that can be triggered by IAA. These chains differ with respect to functionality, perception and signaling (Campanoni and Nick, 2005): One signal chain is preferentially binding the artificial auxin 1-naphthalene acetic acid (NAA), is not sensitive to the G-protein inhibitor pertussis toxin, not activated by the G-protein activator aluminum tetrafluoride, and activates preferentially cell expansion. The

other signal chain is preferentially binding the artificial auxin 2,4-D, is sensitive to pertussis toxin, activated by aluminum tetrafluoride, and activates preferentially cell division. There is also evidence for a differential interaction of these signaling chains with actin: treatment 2,3-butanedione monoxime (BDM), a generic inhibitor of myosins, not only causes a disorganization of cortical actin, but also delays the onset of cell division to auxin, while leaving cell expansion unaffected (Holweg *et al*., 2003). Moreover, different species of auxin differ in their ability to trigger a detachment of actin cables into fine filaments (Maisch and Nick, 2007; Nick *et al*., 2009): the natural auxin IAA, as well as its artificial analogue NAA are both transported in a polar manner are able to debundle actin. In contrast, 2,4-D, which only shows a poor polar transport, is also not effective in actin debundling.

The findings of this part study along with the concept of different auxin-signaling pathways can be integrated into the following working model (Fig. 4.1): In cells that have progressed into the proliferation phase, auxin activates a signal chain that activates the cell cycle and at the same time is linked with polar transport. This signaling requires dynamic actin and is therefore impaired, when actin is stabilized by overexpression of the GFP-FABD2 marker (auxin-actin oscillator, Fig. 4.1, left). If actin dynamics would drive a cycling of this receptor in a similar way as it does with the PIN proteins, bundling of actin should trap the receptor in a membrane-bound, intracellular and inactive state resulting in a desensitization of auxin signaling. In cells that have completed their proliferation phase, the cell-cycle related auxin signaling is expected to be down modulated, partitioning auxin signaling to cell expansion, dismantling of plasmodesmata-related actomyosin (leading to file disintegration), and nuclear migration to the cell periphery (Fig. 4.1, right). When this auxin signal chain competes with actin-dependent signaling for a common factor (common auxin signaling factor, Fig. 4.1, CAF) that is limiting, the desensitization of actin-dependent auxin signaling caused by the GFP-FABD2 marker might lead to a sensitization of this alternative actin-independent signaling chain.

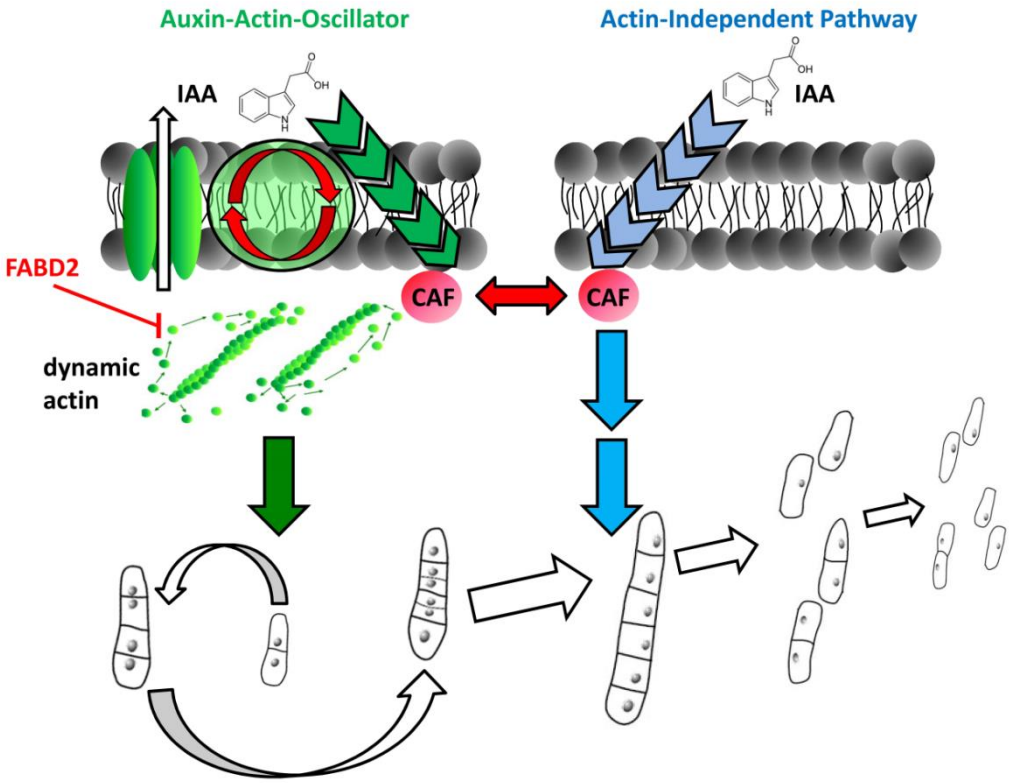

Fig. 4.1 Working model to explain the different actin-dependency of auxin responses in cycling versus stationary cells. The model is based upon the assumption of two different auxin signaling pathways. One pathway depends on dynamic actin and is active in proliferating cells (green) and is inhibited by overexpression of the fimbrin actin binding domain (FABD). Since dynamic actin also controls auxin efflux, an oscillatory circuit is established. The alternative pathway (blue) is active in stationary cells, is independent of actin dynamics and drives cell expansion, file disintegration, and nuclear positioning to the periphery. Auxin-actin oscillator and the actin independent auxin signaling compete for a common factor (operationally defined as common auxin signaling factor, CAF). As a consequence, activation of the actin-independent pathway by recruitment of the CAF will inhibit the auxin-actin oscillator.

This working model is admittedly speculative, but leads to clear predictions that can be tested in future experiments: since the auxin signal driving the cell cycle is dependent on actin dynamics as well, the GF11 line is expected to show a specific response to compounds that interfere with G-proteins, and it is also expected to produce different dose-response relations, if treated with NAA versus 2,4-D.

Furthermore, if actin-dependent auxin signaling depends on the polar flux of auxin, inhibitors of auxin transport should not only cause a bundling of actin (Dhonukshe et al., 2008), but they should also reduce the sensitivity of the treated cell to exogenous auxin.

4.2 Muitiple auxin binding sites within the cytoplasm

Until recent years, it is possible to visualize details of auxin distribution due to the advances of available method to directly trace auxin. To get insight into auxin distribution in plant, Hayashi *et al*. (2014) synthesize fluorescently labeled auxin analogs by conjugating small fluorophores NBD to auxins, which retain to be active for auxin transport system but inactive for auxin signaling and metabolism. Using these fluorescent auxin analogs, it is now able to address the auxin spatial distribution at subcellular level, and probe auxin binding property in tobacco BY-2 cells.

4.2.1 Fluorescent auxin analogs subcellular distribution in tobacco BY-2 cell

The two fluorescent auxin analogs are highly specific for auxin transport system, providing the potential to detect auxin distribution with high spatial resolution. Application of NBD-NAA and NBD-IAA to BY-2 cells, the first impression of these two fluorescent auxin analogs distributions in the cell is distinct (Fig. 3.10). Comparing short time (1 min) with long time (20 min) incubation, NBD-NAA distribution patterns shift from dot-like to membrane-like pattern. In contrast, NBD-IAA distribution patterns remain dot-like pattern with either short time (1 min) or long time (20 min) incubation. These findings indicate the differences of cellular and physiological property between NBD-NAA and NBD-IAA, which might due to the structural differences of NAA and IAA. IAA includes an indole ring; as for NAA, it is a naphthalene ring instead of an indole ring. It has revealed that the IAA binds to the auxin receptor TIR1 involving its indole ring and its side-chain carboxyl group.

NAA can bind to TIR1 in a similar way as IAA, but compared with the indole ring of IAA, the naphthalene ring occupies more space in the binding cavity of the TIR1 receptor (Tan *et al.* 2007). The physiological property differences between NAA and IAA have also been displayed by the auxin transport carriers. The influx carrier membranes of AUX1, LAX1, and LAX3 promote uptake of IAA, but not NAA (Yamamoto and Yamamoto, 1998; Yang *et al*., 2006; Swarup *et al*., 2008; Péret *et al.*, 2012). As for efflux carrier PIN family, every known PIN protein member can transport IAA, but only PIN4 and PIN7 can efflux NAA, while PIN1 and PIN2 do not exhibit this capacity (Petrášek *et al*., 2006; Blakeslee *et al*., 2007).

Further experiment of colocalization of fluorescent auxin analogs with specific fluorescent markers tagged to specific organelles, it confirmed that NBD-NAA was distributed to the ER and the tonoplast, whereas NBD-IAA was localized to the ER (Fig. 3.11 and Fig. 3.12). These results are partly consistent with the report form Hayashi *et al*., (2014): NBD-NAA and NBD-IAA localized to the ER. However, in their experiment result, NBD-NAA and NBD-IAA did not colocalized with tonoplast marker VHA-a3-mRFP, expressing in the *Arabidopsis thaliana* root. In current work of tonoplast marker NtTPC1A-GFP, NtTPC1A-GFP was colocalized with NBD-NAA. The different results might be due to the different experimental systems. Taking together with results of NBD-NAA and NBD-IAA distribution patterns (Fig. 3.10), it implies that when NBD-NAA entered the cytoplasm, it was first localized to the ER in a very short period of time, and then moved to the tonoplast; however, NBD-IAA was directly localized to the ER after it was taken into the cell. It should be mentioned that the fluorescent signal shift of NBD-NAA from the ER to the tonoplast, whether it happens by the movement of NBD-NAA or vesicle trafficking from the ER to vacuole (Viotti *et al*., 2013; Pedrazzini *et al.*, 2013; Viotti, 2014) requires further investigation.

4.2.2 Auxin subcellular distribution in tobacco BY-2 cell and auxin binding sites with distinct characteristics

One critical point need to be emphasized here: the fluorescent auxin analogs cannot completely represent auxin. Thus, it is necessary to test the similarity of fluorescent auxin analogs and auxins. Coincubation of NBD-NAA with NAA (or NBD-IAA with IAA) in the cell, it showed some unexpected findings (Fig. 3.13 and Fig. 3.15): NBD-NAA shared the common binding sites with NAA, but NBD-IAA did not display the similar result with IAA. The possible reason might be the conjugation of IAA with NBD moiety changed molecular structure and chemical characteristic, affecting binding capability of IAA moiety to the IAA binding sites. NBD-IAA has been proved to be inactive to auxin signaling and metabolism in *Arabidopsis* root (Hayashi *et al.*, 2014); however, another report suggested IAA in the form of a conjugate with fluorescein isothiocyanate (FITC) or rhodamine isothiocyanate (RITC) could still remain IAA-like activity in Arabidopsis root (Sokolowska *et al*., 2014). Thus, the different nature of conjugated moiety could have different influence on auxin characteristic. But, at least, NBD-NAA can represent NAA very well; therefore it can conclude that NAA is localized to the ER and the tonoplast.

With more combinations of NBD-NAA and auxin (IAA and 2,4-D) were tested (Fig. 3.16), the values of colocalization coefficients of NBD-NAA were reduced by IAA, but increased by 2,4-D. It indicated IAA could bind to some binding sites at the ER which were occupied by NBD-NAA, and 2,4-D replaced NBD-NAA to bind to some binding sites at the tonoplast. Compare the results of combination of NBD-NAA and auxin (NAA, IAA, and 2,4-D) (see Fig. 3.13 and Fig. 3.14), the reduction of NBD-NAA fluorescent signal was less in the presence of IAA or 2,4-D. Therefore, it implied that part amount of IAA molecules were localized to ER and part of 2,4-D molecules were localized to the tonoplast. Some “short” PIN proteins, including PIN5, PIN6, and PIN8, localize to the ER and transport IAA and NAA from the cytoplasm

in to the ER (Petrášek *et al*., 2006; Mravec *et al.*, 2009; Ganguly *et al*., 2010; Dal Bosco *et al*., 2012; Sawchuk *et al*., 2013). But, the "long" PIN proteins (PIN1-4 and PIN7) show polar plasma membrane-localization, and display polar auxin transport (Petrášek *et al*. 2006; Tanaka *et al.* 2006; Vieten *et al*. 2007; Zažímalová *et al*. 2007; Yang and Murphy, 2009). Indeed, the localization of NBD-NAA did not exhibit on plasma membrane (Fig. 3.12). Thus, these "long" PIN proteins could not be binding sites for the NBD-NAA, whereas it seems likely that these "short" PIN proteins may conduct the localization of NBD-NAA and IAA to the ER. Besides, major portion of Auxin Binding Protein 1 (ABP1) is also localized to the ER, indicating perhaps some cooperation between ABP1 with "short" PIN proteins to regulate IAA transport through ER (Mravec *et al.*, 2009; Ganguly *et al*., 2010). Interestingly, it has revealed that unlike IAA, 2,4-D is not a good substrate for ABP1 (Löbler and Klämbt, 1985). Furthermore, a previous study proposed there were two auxin binding sites, site I at the ER and site II at the tonoplast (Dohrmann et al., 1978). This has also been proved in the current study: 2,4-D is localized to the tonoplast, instead of the ER (Fig. 3.16).

The findings of the current study along with the concept of different auxin binding sites can be integrated into a working model (Fig. 4.2): In the cytoplasm, fluorescent auxin analog NBD-NAA displays to two organelles, including the ER and the tonoplast. Because of NAA as a highly efficient competitor to NBD-NAA, the localization of NAA is overlapped with NBD-NAA. Thus, NAA is also localized to these two organelles. Coincubation of NBD-NAA with IAA, some auxin binding sites at the ER is preferentially binding IAA, but also can bind to NBD-NAA if there is only NBD-NAA. Similarly, some auxin binding sites existing at the tonoplast choose 2,4-D as prioritized substrate. Though providing very high concentration (100 µM) of IAA or 2,4-D, these auxin molecules cannot completely occupy auxin binding sites, removing NBD-NAA from its binding sites. In short, the binding sites at the ER can precisely bind NAA or bind both NAA and IAA; at the tonoplast, the binding sites can accurately bind NAA or bind both NAA and 2,4-D. Due to vesicle trafficking from the ER to vacuole (Viotti *et al*., 2013; Pedrazzini *et al*., 2013; Viotti, 2014), it is not clear

whether the auxin binding sites, only precisely binding to NAA, belong to the same group. But, what is clear is that NAA, IAA, and 2,4-D have been separated to two different organelles. This compartment process of auxin causes an intracellular auxin gradient, which is important for auxin signaling and auxin metabolism (Woodward and Bartel, 2005; Mravec *et al*., 2009; Ganguly *et al*., 2010). This study has revealed the subcellular distribution of auxin at the ER and the tonoplast. Some of these auxin binding sites display the capability to recognize subtle structural differences among three types of auxins in a specific manner. This might imply a cue to potential auxin receptor in the cytoplasm, which needs further investigation.

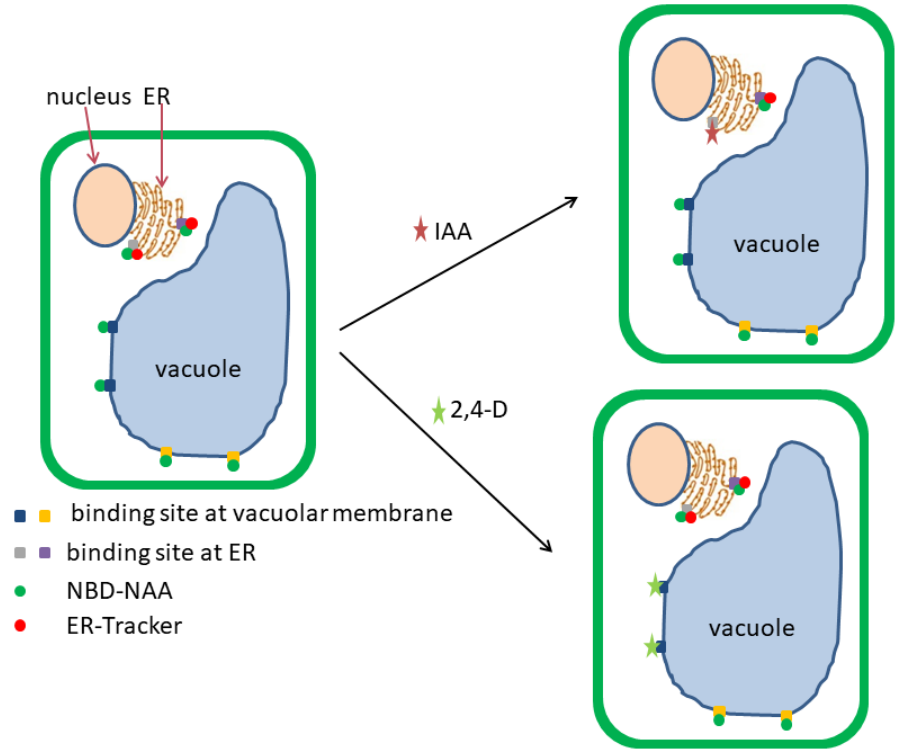

Fig. 4.2 Working model to explain the different auxin binding sites in cytoplasm. The NBD-NAA distributions are targeted to the ER and the tonoplast. With the application of IAA, some auxin binding sites at the ER once were binding with NBD-NAA, now associating with IAA. The left auxin binding sites at the ER, which probably different from former mentioned auxin binding sites, are still associated with NBD-NAA. The alternative situation is application of 2,4-D, causing some auxin binding sites at the tonoplast choose to bind 2,4-D, instead of NBD-NAA. Some distinct auxin binding sites at the tonoplast exhibit the specificity binding characteristic to NBD-NAA.

4.3 Conclusion

This actin-auxin oscillator model displays auxin, actin, and auxin efflux carriers' interaction in a feedback loop (Nick, 2010). Change any element in this feedback loop will affect the other elements. In the current study, two cell lines (WT and GF11) with different actin dynamicity were used to probe the interaction with auxin. The reaction turned out to be morphogenesis built, due to the auxin-induced responsiveness. Therefore, it is necessary to monitor cell developmental responses during the cultivation. Application IAA to the wild type BY-2 cell, the cell division activity was enhanced in amplitude and time. Additionally, the transition from cell proliferation to cell elongation was also delayed. However, once cell left proliferation stage, namely enter stationary phase, auxin promoted cell file disintegration. We could conclude that IAA promoted cellular activities in WT along the whole cell cultivation. In contrast, the GF11 was repressed in proliferation phase, but reinforce cell file disintegration with IAA treatment. Furthermore, actin filament structure was always intact in GF11. Thus, the function shift from repression to reinforcement supports a sensory role of actin filaments.

To get more insight into the auxin signal, fluorescent auxin analogs were used as a marker for auxin binding sites in a single cell. One fluorescent auxin analogy (NBD-NAA) could successfully recognize the same binding sites for NAA. With some markers tagged to specific organelles, it revealed the localization of auxin included ER and tonoplast. We could also conclude there were distinct auxin binding sites to recognize NAA, IAA, and 2,4-D. This might provide another direction to explain the different but partly overlapped auxin-induced responsiveness.

4.4 Outlook

Auxin biology has been one of the central points in plant research. Auxin structure is not complex, but auxin has incredible complicated regulation network. Auxin polar transport is unique property for auxin among plant hormones. But this polar transport behavior could provide a means of regulate plant growth by integrating signal into auxin movement. In this work, the specific distribution positions of fluorescent auxin analogs after a relative short time treatment have been identified. It can provide a powerful tool to explore some interesting questions about auxin signal behavior in suspension cells and plant organism, which will be in focus of future research:

Though BY-2 cell can conduct polarity of auxin fluxes (Maisch and Nick, 2007), it is still not clear the intracellular auxin distribution in each along the cell file. Now, with fluorescent auxin analogs, direct evidence about auxin gradient in the cell file is possible. If the treatment of fluorescent auxin analogs covers the whole cell cultivation, we could get deeper understanding about auxin gradient distribution pattern at distinct stages. For the single cell, it will also provide information about the situation of auxin distribution pattern in a long time period. In addition, treatment with specific chemical drug, such as Latrunculin B to disrupt actin structure, we could probe how actin filaments affect auxin spatial distribution.

Besides cell file, regeneration of protoplast has the rebuilt process of cell polarity using auxin efflux to explore environment (Zaban *et al*. 2014). How cell polarity is set up is still a mystery. It is a continuous procedure to build cellular polarity, but it is difficult to identify the initial cue which finally leads to cell polarity. It might be auxin roadman distribution, or auxin carrier PIN protein roadman distribution. Intensive studies about auxin distribution during protoplast regeneration are required, which will greatly enrich our understanding to the nature of cell.

5. References

Andersson B, Sandberg G. 1982. Identification of endogenous N-(3-indolacetyl) aspartic acid in Scots pine (Pinus sylvestris L.) by combined gas chromatography–mass spectrometry, using highperformance liquid chromatography for quantification. *J. Chromatogr.* **238:** 151-156.

Amador-Vargas S, Dominguez M, Leon G, Maldonado B, Murillo J, Vides GL. 2014. Leaf-folding response of a sensitive plant shows context-dependent behavioral plasticity. *Plant Ecol.* **215:** 1445-1454.

Aus ín I, Alonso-Blanco C, Mart ínez-Zapater J. 2005. Environmental regulation of flowering. *Int. J. Dev. Biol.* **49:** 689-705.

Bajguz A, Piotrowska A. 2009. Conjugates of auxin and cytokinin. *Phytochemistry* **70:** 957-969.

Baluška F, Cvrčková F, Kendrick-Jones J, Volkmann D. 2001. Sink plasmodesmata as gateways for phloem unloading. Myosin VIII and calreticulin as molecular determinants of sink strength? *Plant Physiol.* **126:** 39-46.

Baluška F, Šamaj J, Wojtaszek P, Volkmann D, Menzel D. 2003. Cytoskeleton-plasma membrane-cell wall continuum in plants. Emerging links revisited. *Plant Physiol.* **133:** 482-491.

Balzan S Johal GS Carraro N. 2014. The role of auxin transporters in monocots development. *Front. Plant Sci.* **5:** 393.

Barnett MW, Larkman PM. 2007. The action potential. *Pract. Neurol.* **7:** 192-197.

Bartel B. 1997. Auxin biosynthesis. *Annu. Rev. Plant Physiol. Plant Mol. Biol.* **48:** 51-66.

Bartel B, Fink GR. 1995. ILR1, an amidohydrolase that releases active indole-3-acetic acid from conjugates. *Science* **268:** 1745-1748.

Benkov á E, Michniewicz M, Sauer M, Teichmann T, Seifertov á D, Jürgens G, Friml J. 2003. Local, efflux-dependent auxin gradients as a common module for plant organ formation. *Cell* **115:** 591-602.

Beyer EM, Morgan PW. 1970. Effect of ethylene on the uptake, distribution, and metabolism of indoleacetic acid-1–14C and -2–14C and naphthaleneacetic acid-1–14C. *Plant Physiol.* **46:** 157-162.

Bhalerao RP, Eklöf J, Ljung K, Marchant A, Bennett M, Sandberg G. 2002. Shoot-derived auxin is essential for early lateral root emergence in *Arabidopsis* seedlings. *Plant J.* **29:** 325-332.

Bialek K, Cohen JD. 1986. Isolation and partial characterization of the major amide-linked conjugate of indole-3-acetic acid from *Phaseolus vulgaris* L, *Plant Physiol.* **80:** 99-104.

Blakeslee JJ, Bandyopadhyay A, Lee OR, Mravec J, Titapiwatanakun B, Sauer M, Makam SN, Cheng Y, Bouchard R, Adamec J, Geisler M, Nagashima A, Sakai T, Martinoia E, Friml J, Peer WA, Murphy AS. 2007. Interactions among PIN-FORMED and P-glycoprotein auxin transporters in *Arabidopsis*. *Plant Cell* **19:** 131-147.

Blazquez MA, Green R, Nilsson O, Sussman MR, Weigel D. 1998. Gibberellins promote flowering of *Arabidopsis* by activating the LEAFY promoter. *Plant Cell* **10:** 791-800.

Blilou I, Xu J, Wildwater M, Willemsen V, Paponov I, Friml J, Heidstra R, Aida M, Palme K, Scheres B. 2005. The PIN auxin efflux facilitator network controls growth and patterning in *Arabidopsis* roots. *Nature* **433:** 39-44.

Boer DR, Freire-Rios A, van den Berg WA, Saaki T, Manfield IW, Kepinski S, Lopez-Vidrieo I, Franco-Zorrilla JM, de Vries SC, Solano R, Weijers D, Coll M. 2014. Structural basis for DNA binding specificity by the auxin-dependent ARF transcription factors. *Cell* **156:** 577-589.

Bonner J, Bandurski RS. 1952. Studies of the physiology, pharmacology, and biochemistry of the auxins. *Annu. Rev. Plant Physiol.* **3:** 59-86.

Bosco CD, Dovzhenko A, Liu X, Woerner N, Rensch T, Eismann M, Eimer S, Hegermann J, Paponov IA, Ruperti B, Heberle-Bors E, Touraev A, Cohen JD, Palme K. 2012. The endoplasmic reticulum localized PIN8 is a pollen specific auxin carrier involved in intracellular auxin homeostasis. *Plant J.* **71:** 860-870.

Brochhausen L, Maisch J, Nick P. 2016. Break of symmetry in regenerating tobacco protoplasts is independent of nuclear positioning. *J. Integr. Plant Biol.* **58:** 799-812.

Buschmann H, Green P, Sambade A, Doonan JH, Lloyd CW. 2011. Cytoskeletal dynamics in interphase, mitosis and cytokinesis analysed through *Agrobacterium*-mediated transient transformation of tobacco BY-2 cells. *New Phytol.* **190:** 258-267.

Calderón-Villalobos LI, Lee S, De Oliveira C, Ivetac A, Brandt W, Armitage L, Sheard LB, Tan X, Parry G, Mao H, Zheng N, Napier R, Kepinski S, Estelle M. 2012. A combinatorial TIR1/AFB-Aux/IAA co-receptor system for differential sensing of auxin. *Nat. Chem. Biol.* **8:** 477-485.

Campanoni P, Blasius B, Nick P. 2003. Auxin transport synchronizes the pattern of cell division in a tobacco cell line. *Plant Physiol.* **133:** 1251-1260.

Campanoni P, Nick P. 2005. Auxin-dependent cell division and cell elongation: NAA and 2,4-D activate different pathways. *Plant Physiol*. **137:** 939-948.

Carraro N, Tisdale-Orr TE, Clouse RM, Knöller AS, Spicer R 2012. Diversification and expression of the PIN, AUX/LAX, and ABCB families of putative auxin transporters in *populus*. *Front. Plant Sci*. **3:** 17.

Carrier DJ, Abu Bakar NT, Swarup R, Callaghan R, Napier RM, Bennett MJ, Kerr ID. 2008. The binding of auxin to the *Arabidopsis* auxin influx transporter AUX1. *Plant Physiol.* **148:** 529-535.

Casal JJ, Candia AN, Sellaro R. 2014. Light perception and signalling by phytochrome A. *J. Exp. Bot.* **65:** 2835-2845.

Casimiro I, Marchant A, Bhalerao RP, Beeckman T, Dhooge S, Swarup R, Graham N, Inzé D, Sandberg G, Casero PJ, Bennett M. 2001. Auxin transport promotes *Arabidopsis* lateral root initiation. *Plant Cell* **13:** 843-852.

Chang XL, Riemann M, Liu Q, Nick P. 2015. Actin as deathly switch? How auxin can suppress cell-death related defence. *PLoS ONE* **10**, e0125498.

Chapman EJ, Estelle M. 2009. Mechanism of auxin-regulated gene expression in plants. *Annu. Rev. Genet*. **43:** 265-285.

Chattopadhyay A. 1990. Chemistry and biology of N-(7-nitrobenz-2-oxa-1,3-diazol-4-yl)-labeled lipids: fluorescent probes of biological and model membranes. *Chem. Phys. Lipids* **53:** 1-15.

Chen R, Hilson P, Sedbrook J, Rosen E, Caspar T, Masson PH. 1998. The *Arabidopsis thaliana* AGRAVITROPIC 1 gene encodes a component of the polar-auxin-transport efflux carrier. *Proc. Natl. Acad. Sci. USA* **95:** 15112-15117.

Cheng Y, Dai X, Zhao Y. 2006. Auxin biosynthesis by the YUCCA flavin monooxygenases controls the formation of floral organs and vascular tissues in *Arabidopsis*. *Genes Dev*. **20:** 1790-1799.

Cheong JJ, Hahn MG. 1991. A specific, high-affinity binding-site for the hepta-beta-glucoside elicitor exists in soybean membranes. *Plant Cell* **3:** 137-147.

Choi J, Choi D, Lee S, Ryu CM, Hwang I. 2011. Cytokinins and plant immunity: old foes or new friends? *Trends Plant Sci*. **16:** 388-394.

Colebrook EH, Thomas SG, Phillips AL, Hedden P. 2014. The role of gibberellin signalling in plant responses to abiotic stress. *J. Exp. Bot.* **217:** 67-75.

Dai X, Mashiguchi K, Chen Q, Kasahara H, Kamiya Y, Ojha S, Dubois J, Ballou D, Zhao Y. 2013. The biochemical mechanism of auxin biosynthesis by an *Arabidopsis* YUCCA flavin-containing monooxygenase. *J. Biol. Chem.* **288:** 1448-1457.

Dal Bosco C, Dovzhenko A, Liu X, Woerner N, Rensch T, Eismann M, Eimer S, Hegermann J, Paponov IA, Ruperti B, Heberle-Bors E, Touraev A, Cohen JD, Palme K. 2012. The endoplasmic reticulum localized PIN8 is a pollen-specific auxin carrier involved in intracellular auxin homeostasis. *Plant J*. **71:** 860-870.

Darwin C. 1880. The power of movement in plants. John Murray, London

Dello Ioio R, Nakamura K,Moubayidin L, Perilli S, Taniguchi M, Morita MT, Aoyama T, Costantino P, Sabatini S. 2008. A genetic framework for the control of cell division and differentiation in the root meristem. *Science* **322:** 1380-1384.

Devlin PF, Christie JM, Terry MJ. 2007. Many hands make light work. *J. Exp. Bot.* **58:** 3071-3077.

Dharmasiri N, Dharmasiri S, Estelle M. 2005a. The F-box protein TIR1 is an auxin receptor. *Nature* **435:** 441-445.

Dharmasiri N, Dharmasiri S, Jones AM, Estelle M. 2003. Auxin action in a cell-free system. *Curr. Biol.* **13:** 1418-1422.

Dharmasiri N, Dharmasiri S, Weijers D, Lechner E, Yamada M, Hobbie L, Ehrismann JS, Jurgens G, Estelle M. 2005b. Plant development is regulated by a family of auxin receptor F box proteins. *Dev. Cell* **9:** 109-119.

Dhonukshe P, Aniento F, Hwang I, Robinson DG, Mravec J, Stierhof Y-D, Friml J. 2007. Clathrin-mediated constitutive endocytosis of PIN auxin efflux carriers in *Arabidopsis*. *Curr. Biol.* **17:** 520-527.

Dhonukshe P, Grigoriev I, Fischer R, Tominaga M, Robinson DG, Hašek J, Paciorek T, Petrašek J, Seifertová D, Tejos R, Meisel LA, Zažímalová E, Gadella TWJ, Stierhof YD, Ueda T, Oiwa K, Akhmanova A, Brocke R, Spang A, Friml J. 2008. Auxin transport inhibitors impair vesicle motility and actin cytoskeleton dynamics in diverse eukaryotes. *Proc. Natl. Acad. Sci. USA* **105:** 4489-4494.

Doherty GJ, McMahon HT. 2008. Mediation, modulation and consequences of membrane-cytoskeleton interactions. *Annu. Rev. Biophys.* **37:** 65-95.

Dohrmann U, Hertel R, Kowalik H. 1978. Properties of auxin binding sites in different subcellular fractions from maize coleoptiles. *Planta* **140:** 97-106.

Dreher KA, Brown J, Saw RE, Callis J. 2006. The *Arabidopsis* Aux/IAA protein family has diversified in degradation and auxin responsiveness. *Plant Cell* **18:** 699-714.

Durst S, Nick P, Maisch J. 2013. *Nicotiana tabacum* actin-depolymerizing factor 2 is involved in actin-driven, auxin-dependent patterning. *J. Plant Physiol.* **170:** 1057-1066.

Durst S, Hedde PN, Brochhausen L, Nick P, Nienhaus GU, Maisch J. 2014. Organization of perinuclear actin in live tobacco cells observed by PALM with optical sectioning. *J. Plant Physiol.* **141:** 97-108.

Eggenberger K, Sanyal P, Hundt S, Wadhwani P, Ulrich AS, Nick P. 2017. Challenge Integrity: The Cell-Penetrating Peptide BP100 Interferes with the Auxin–Actin Oscillator. *Plant Cell Physiol.* **58:** 71-85.

Enders TA, Strader LC. 2015. Auxin activity: past, present, and future. *Am. J. Bot.* **102:** 180-196.

Ezratty EJ, Partridge MA, Gundersen GG. 2005. Microtubule-induced focal adhesion disassembly is mediated by dynamin and focal adhesion kinase. *Nat. Cell Biol.* **7:** 581-590.

Finkelstein RR, Gampala SS, Rock CD. 2002. Abscisic acid signaling in seeds and seedlings. *Plant Cell* **14:** 15-45.

Flamant F, Baxter JD, Forrest D, Refetoff S, Samuels H, Scanlan TS, Vennstrom B, Samarut J. 2006. International Union of Pharmacology. LIX. The pharmacology and classification of the nuclear receptor superfamily: thyroid hormone receptors. *Pharmacol. Rev.* **58:** 705-711.

Forer A, Wilson PJ. 1994. A model for chromosome movement during mitosis. *Protoplasma* **179:** 95-105.

Foster RJ, McRae DH, Bonner J. 1952. Auxin induced growth inhibition a natural consequence of two point attachment. *Proc. Natl. Acad. Sci. USA* **38:** 1012-1022.

Foster RJ, McRae DH, Bonner J. 1955. Auxin-antiauxin interaction at high auxin concentrations. *Plant Physiol.* **80:** 323-327.

Frey N, Klotz J, Nick P. 2010. A kinesin with calponin-homology domain is involved in premitotic nuclear migration. *J. Exp. Bot.* **61:** 3423-3437.

Fridolfsson HN, Starr DA. 2010. Kinesin-1 and dynein at the nuclear envelope mediate the bidirectional migrations of nuclei. *J. Cell. Biol.* **191:** 115-128.

Friml J. 2010. Subcellular trafficking of PIN auxin efflux carriers in auxin transport. *Eur. J. Cell Biol.* **89:** 231-235.

Friml J, Vieten A, Sauer M, Weijers D, Schwarz H, Hamann T, Offringa R, Jürgens G. 2003. Efflux-dependent auxin gradients establish the apical-basal axis of *Arabidopsis*. *Nature* **426:** 147-153.

Friml J, Wiśniewska J, Benková E, Mendgen K, Palme K. 2002. Lateral relocation of auxin efflux regulator PIN3 mediates tropism in *Arabidopsis*. *Nature* **415:** 806-809.

Gaff DF, Okong'O-Ogola O. 1971. The Use of Non-permeating Pigments for Testing the Survival of Cells. *J. Exp. Bot.* **22:** 756-758.

Gälweiler L, Guan C, Müller A, Wisman E, Mendgen K, Yephremov A, Palme K. 1998. Regulation of polar auxin transport by AtPIN1 in *Arabidopsis* vascular tissue. *Science* **282:** 2226-2230.

Ganguly A, Lee SH, Cho M, Lee OR, Yoo H, Cho HT. 2010. Differential auxin-transporting activities of PIN-FORMED proteins in *Arabidopsis* root hair cells. *Plant Physiol.* **153:** 1046-1061.

Garner WW. Allard HA. 1920. Effect of the relative length of day and night and other factors of the environment on growth and reproduction in plants. *J. Agric. Res.* **18:** 553-606.

Gazarian IG, Lagrimini LM, Mellon FA, Naldrett MJ, Ashby GA, Thorneley RN. 1998. Identification of skatolyl hydroperoxide and its role in the peroxidase-catalysed oxidation of indol-3-yl acetic acid. *Biochem. J.* **333:** 223-232.

Geldner N, Friml J, Stierhof Y-D, Jürgens G, Palme K. 2001. Auxin transport inhibitors block PIN1 cycling and vesicle trafficking. *Nature* **413:** 425-428.

Gens JS, Fujiki M, Pickard BG. 2000. Arabinogalactan protein and wall-associated kinase in a plasmalemma reticulum with specialized vertices. *Protoplasma* **212:** 115-134.

Gomez-Gomez L, Boller T. 2000. FLS2: An LRR receptor–like kinase involved in the perception of the bacterial elicitor flagellin in *Arabidopsis*. *Mol. Cell* **5:** 1003-1011.

Gomi K, Matsuoka M. 2003. Gibberellin signalling pathway. *Curr. Opin. Plant Biol.* **6:** 489-493.

Gourlay CW, Ayscough KR. 2005. The actin cytoskeleton: a key regulator of apoptosis and ageing? *Nat. Rev. Mol. Cell Biol.* **6:** 583-589.

Gray WM, Kepinski S, Rouse D, Leyser O, Estelle M. 2001. Auxin regulates SCF^{TIR1}-dependent degradation of AUX/IAA proteins. *Nature* **414:** 271-276.

Grieneisen VA, Xu J, Mar ée AF, Hogeweg P, Scheres B. 2007. Auxin transport is sufficient to generate a maximum and gradient guiding root growth. *Nature* **449:** 1008-1013.

Grossmann K. 2010. Auxin herbicides: current status of mechanism and mode of action. *Pest Manag. Sci.* **66:** 113-120.

Guan X, Buchholz G, Nick P. 2013. The cytoskeleton is disrupted by the bacterial effector HrpZ, but not by the bacterial PAMP flg22 in tobacco BY-2 cells. *J. Exp. Bot.* **64:** 1805-1816.

Guilfoyle TJ, Hagen G. 2007. Auxin response factors. *Curr. Opin. Plant Biol.* **10:** 453-460.

Gutzeit H.O., 1986. The role of microfilaments in cytoplasmic streaming in *Drosophila* follicles. *J. Cell Sci.* **80:** 159-169.

Hamaker JW, Johnston H, Martin RT, Redemann CT. 1963. A picolinic acid derivative: a plant growth regulator. *Science* **141:** 363.

Hamner KC. 1940. Interrelation of light and darkness in photoperiodic induction. *Bot. Gaz.* **101:** 658-687.

Hamner KC, Bonner J. 1938. Photoperiodism in relation to hormones as factors in floral initiation and development. *Bot. Gaz.* **100:** 388-431.

Hayashi KI, Nakamura SI, Fukunaga S, Nishimura T, Jenness MK, Murphy AS, Motose H, Nozaki H, Furutani M, Aoyama T. 2014. Auxin transport sites are visualized in planta using fluorescent auxin analogs. *Proc. Natl. Acad. Sci. USA* **111:** 11557-11562.

Hejnowicz Z. 1961. The response of the different parts of the cell elongation zone in root to external β-indolylacetic acid. *Acta Soc. Bot. Polon.* **30:** 25-42.

Hodgkin AL, Huxley AF. 1939. Action potentials recorded from inside a nerve fibre. *Nature* **144:** 710-711.

Holweg C. 2007. Living markers for actin block myosin-dependent motility of plant organelles and auxin. *Cell Motil. Cytoskeleton* **64:** 69-81.

Holweg C, Honsel A, Nick P. 2003. A myosin inhibitor impairs auxin-induced cell division. *Protoplasma* **222:** 193-204.

Holweg C, Susslin C, Nick P. 2004. Capturing in vivo dynamics of the actin cytoskeleton stimulated by auxin or light. *Plant Cell Physiol.* **45:** 855-863.

Hošek P, Kubeš Laňková M, Dobrev PI, Klima P, Kohoutová M, Petrášek J, Hoyerová K, Jiřina M, Zažimalová E. 2012. Auxin transport at cellular level: new insights supported by mathematical modeling. *J. Exp. Bot.* **63:** 3815-3827.

Hou G, Mohamalawari DR, Blancaflor EB. 2003. Enhanced gravitropism of roots with a disrupted cap actin cytoskeleton. *Plant Physiol.* **131:** 1360-1373.

Ikeda Y, Men S, Fischer U, Stepanova AN, Alonso JM, Ljung K, Grebe M. 2009. Local auxin biosynthesis modulates gradient directed planar polarity in *Arabidopsis*. *Nat. Cell Biol.* **11:** 731-738.

Ingber DE. 2003. Tensegrity: II. How structural networks influence cellular information-processing networks. *J. Cell Sci.* **116:** 1397-1408.

Ishida T, Fujiwara S, Miura K, Stacey N, Yoshimura M, Schneider K, Adachi S, Minamisawa K, Umeda M, Sugimoto K. 2009. SUMOE3 ligaseHIGHPLOIDY2 regulates endocycle onset and meristem maintenance in *Arabidopsis*. *Plant Cell* **21:** 2284-2297.

Jain M, Kaur N, Garg R, Thakur JK, Tyagi AK, Khurana JP. 2006. Structure and expression analysis of early auxin-responsive Aux/IAA gene family in rice (*Oryza sativa*). *Funct. Integr. Genomics* **6:** 47-59.

James TW, Crescitelli F, Loew ER, McFarland WN. 1992. The eyespot of *euglena gracilis*: a microspectrophotometric study. *Vision Res.* **32:** 1583-1591.

Jones JD, Dangl JL. 2006. The plant immune system. *Nature* **444:** 323-329.

Kadota Y, Furuichi T, Ogasawara Y, Goh T, Higashi K, Muto S, Kuchitsu K. 2004. Identification of putative voltage-dependent Ca^{2+}-permeable channels involved in cryptogein-induced Ca^{2+} transients and defense responses in tobacco BY-2 cells. *Biochem.Biophys.Res.Commun.* **317:** 823-830.

Kaku H, Nishizawa Y, Ishii-Minami N, Akimoto-Tomiyama C, Dohmae N, Takio K, Minami E, Shibuya N. 2006. Plant cells recognize chitin fragments for defense signaling through a plasma membrane receptor. *Proc. Natl. Acad. Sci. USA* **103:** 11086-11091.

Kepinski S, Leyser O. 2004. Auxin-induced SCFTIR1-Aux/IAA interaction involves stable modification of the SCF–TIR1 complex. *Proc. Natl. Acad. Sci. USA* **101:** 12381-12386.

Kepinski S, Leyser O. 2005. The *Arabidopsis* F-box protein TIR1 is an auxin receptor. *Nature* **435:** 446-451.

Kermode AR. 2005. Role of abscisic acid in seed dormancy. *J. Plant Growth Regul.* **24:** 319-344.

Klotz J, Nick P. 2012. A novel actin-microtubule cross-linking kinesin, NtKCH, functions in cell expansion and division. *New Phytologist* **193:** 576-589.

Korasick DA, Enders TA, Strader LC. 2013. Auxin biosynthesis and storage forms. *J. Exp. Bot.* **64:** 2541-2555.

Kost B, Chua NH. 2002. The plant cytoskeleton: Vacuoles and cell walls make the difference. *Cell* **108:** 9-12.

Kramer EM, Bennett MJ. 2006. Auxin transport: a field in flux. *Trends Plant Sci.* **11:** 382-386.

Kurusu T, Nishikawa D, Yamazaki Y, Gotoh M, Nakano M, Hamada H, Yamanaka T, Iida K, Nakagawa Y, Saji H, Shinozaki K, Iida H, Kuchitsu K. 2012b. Plasma membrane protein OsMCA1 is involved in regulation of hypo-osmotic shock-induced Ca^{2+} influx and modulates generation of reactive oxygen species in cultured rice cells. *BMC Plant Biol.* **12:** 11.

Kuss-Wymer CL, Cyr RJ. 1992. Tobacco protoplasts differentiate into elongate cells without net microtubule depolymerization. *Protoplasma* **168:** 64-72.

Lace B, Prandi C. 2016. Shaping small bioactive molecules to untangle their biological function: a focus on fluorescent plant hormones. *Mol. Plant* **9:** 1099-1118.

Lee S, Sundaram S, Armitage L, Evans JP, Hawkes T, Kepinski S, Ferro N, Napier RM. 2014. Defining binding efficiency and specificity of auxins for $SCF^{TIR1/AFB}$-Aux/IAA co-receptor complex formation. ACS Chem. Biol. **9:** 673-682.

Leivar P, Quail PH. 2011. PIFs: Pivotal components in a cellular signaling hub. *Trends Plant Sci.* **16:** 19-28.

Li SD, Lei L, Yingling YG, Gu Y. 2015. Microtubules and cellulose biosynthesis: the emergence of new players. *Curr. Opin. Plant Biol.* **28:** 76-82.

Liscum E, Reed JW. 2002. Genetics of Aux/IAA and ARF action in plant growth and development. *Plant Mol. Biol.* **49:** 387-400.

Liu X, Barkawi L, Gardner G, Cohen JD. 2012. Transport of indole-3-butyric acid and indole-3-acetic acid in Arabidopsis hypocotyls using stable isotope labeling. *Plant Physiol.* **158:** 1988-2000.

Ljung K, Bhalerao RP, Sandberg G. 2001. Sites and homeostatic control of auxin biosynthesis in *Arabidopsis* during vegetative growth. *Plant J.* **28:** 465-474.

Ljung K, Hull AK, Celenza J, Yamada M, Estelle M, Normanly J, Sandberg G. 2005. Sites and regulation of auxin biosynthesis in *Arabidopsis* roots. *Plant Cell* **17:** 1090-1104.

Ljung K, Hull AK, Kowalczyk M, Marchant A, Celenza J, Cohen JD, Sandberg G. 2002. Biosynthesis, conjugation, catabolism and homeostasis of indole-3-acetic acid in *Arabidopsis thaliana*. *Plant Mol. Biol*. **49:** 249-272.

Löbler M, Klämbt D. 1985. Auxin-binding protein from coleoptile membranes of corn (Zea mays L.). I. Purification by immunological methods and characterization. *J. Biol. Chem.* **260:** 9848-9853.

Lorenzo O, Piqueras R, Sanchez-Serrano JJ, Solano R. 2003. ETHYLENE RESPONSE FACTOR1 integrates signals from ethylene and jasmonate pathways in plant defense. *Plant Cell* **15:**165-178.

Los DA, Murata N. 2004. Membrane fluidity and its roles in the perception of environmental signals. *Biochim. Biophys. Acta.* **1666:** 142-157.

Ludwig-Müller J. 2011. Auxin conjugates: their role for plant development and in the evolution of land plants. *J. Exp. Bot.* **62:** 1757-1773.

Mabuchi I. 1986. Biochemical aspects of cytokinesis. *Int. Rev. Cytol.* **101:** 175-213.

Maisch J, Nick P. 2007. Actin is involved in auxin-dependent patterning. *Plant Physiol.* **143:** 1695-1704.

Marchant A, Kargul J, May ST, Muller P, Delbarre A, Perrot-Rechenmann C, Bennett MJ. 1999. AUX1 regulates root gravitropism in *Arabidopsis* by facilitating auxin uptake within root apical tissues. *EMBO J.* **18:** 2066-2073.

Mashiguchi K, Tanaka K, Sakai T, Sugawara S, Kawaide H, Natsume M, Hanada A, Yaeno T, Shirasu K, Yao H, McSteen P, Zhao Y, Hayashi K, Kamiya Y, Kasahara H. 2011. The main auxin biosynthesis pathway in *Arabidopsis*. *Proc. Natl. Acad. Sci. USA* **108:** 18512-18517.

Mattsson J, Sung ZR, Berleth T. 1999. Responses of plant vascular systems to auxin transport inhibition. *Development* **126:** 2979-2991.

McCloy RA, Rogers S, Caldon CE, Lorca T, Castro A, Burgess A. 2014. Partial inhibition of Cdk1 in G2 phase overrides the SAC and decouples mitotic events. *Cell Cycle* **13:** 1400-1412.

Meudt WJ, Gaines TP. 1967. Studies on the oxidation of indole-3-acetic acid by peroxidase enzymes. I. Colorimetric determination of indole-3-acetic acid oxidation products. *Plant Physiol.* **42:** 1395-1399.

Meyerzon M, Fridolfsson HN, Ly N, McNally FJ, Starr DA. 2009. UNC-83 is a nuclear-specific cargo adaptor for kinesin-1-mediated nuclear migration. *Development* **136:** 2725-2733.

Mikkelsen MD, Hansen CH, Wittstock U, Halkier BA. 2000. Cytochrome P450 CYP79B2 from *Arabidopsis* catalyzes the conversion of tryptophan to indole-3-acetaldoxime, a precursor of indole glucosinolates and indole-3-acetic acid. *J. Biol. Chem.* **275:** 33712-33717.

Mishra RC, Ghosh R, Bae H. 2016. Plant acoustics: in the search of a sound mechanism for sound signaling in plants. *J. Exp. Bot.* **67:** 4483-4494.

Mravec J, Kubeš M, Bielach A, Gaykova V, Petrášek J, Skupa P, Chand S, Benková E, Zažímalová E, Friml J. 2008. Interaction of PIN and PGP transport mechanisms in auxin distribution-dependent development. *Development* **135:** 3345-3354.

Mravec J, Skůpa P, Bailly A, Hoyerová K, Krecek P, Bielach A, ,Petrásek J, Zhang J, Gaykova V, Stierhof YD, Dobrev PI, Schwarzerová K, Rolc ĸ J, Seifertová D, Luschnig C, Benková E, Zaz ímalová E, Geisler M, Friml J. 2009. Subcellular homeostasis of phytohormone auxin is mediated by the ER-localized PIN5 transporter. *Nature* **459:** 1136-1140.

Murashige T, Skoog F. 1962. A revised medium for rapid growth and bioassays with tobacco tissue cultures. *Physiol. Plant.* **15:** 473-497.

Nagata T, Kumagai F. 1999. Plant cell biology through the window of the highly synchronized tobacco BY-2 cell line. *Methods Cell Sci.* **21:** 123-127.

Nagata T, Nemoto Y, Hasezawa S. 1992. Tobacco BY-2 cell line as the "Hela" cell in the cell biology of higher plants. *Int. Rev. Cytol.* **132:** 1-30.

Nick P. 2008. Control of cell axis. *Plant Cell Monographs* **143:** 3-46.

Nick P. 2010. Probing the actin-auxin oscillator. *Plant Signal Behav.* **5:** 94-98.

Nick P. 2013. Microtubules, signaling and abiotic stress. *Plant J.* **75:** 309-323.

Nick P, Han M, An G. 2009. Auxin stimulates its own transport by actin reorganization. *Plant Physiol.* **151:** 155-167.

Nick P, Heuing A, Ehmann B. 2000. Plant chaperonins: a role in microtubule-dependent wall-formation? *Protoplasma* **211:** 234-244.

Normanly J, Cohen JD, Fink GR. 1993. *Arabidopsis thaliana* auxotrophs reveal a tryptophan-independent biosynthetic pathway for indole-3-acetic acid. *Proc. Natl. Acad. Sci. USA* **90:** 10355–10359.

Okada K, Ueda J, Komaki MK, Bell CJ, Shimura Y. 1991. Requirement of the auxin polar transport system in early stages of *Arabidopsis* floral bud formation. *Plant Cell* **3:** 677-684.

Opatrný Z, Nick P, Petrášek J. 2014. Plant Cell Strains in Fundamental Research and Applications. *Plant Cell Monographs* **22:** 455-481.

Oppenheimer JH, Koerner K, Schwartz HL, Surks MI. 1972. Specific nuclear triiodothyronine binding sites in rat liver and kidney. *J. Clin. Endocrinol. Metab.* **35:** 330-333.

Östin A, Kowalczyk M, Bhalerao RP, Sandberg G. 1998. Metabolism of indole-3-acetic acid in *Arabidopsis*. *Plant Physiol.* **118:** 285-296.

Östin A, Moritz T, Sandberg G. 1992. Liquid chromatography/mass spectrometry of conjugates and oxidative metabolites of indole-3-acetic acid. *Biol. Mass. Spectrom.* **21:** 292-298.

Ottenschläger I, Wolff P, Wolverton C, Bhalerao RP, Sandberg G, Ishikawa H, Evans M, Palme K. 2003. Gravity-regulated differential auxin transport from columella to lateral root cap cells. *Proc. Natl. Acad. Sci. USA* **100:** 2987-2991.

Pacifici E, Polverari L, Sabatini S. 2015. Plant hormone cross-talk: the pivot of root growth. *J. Exp. Bot.* **66:** 1113-1121.

Pagnussat GC, Alandete-Saez M, Bowman JL, Sundaresan V. 2009. Auxin-dependent patterning and gamete specification in the *Arabidopsis* female gametophyte. *Science* **324:** 1684-1689.

Paponov IA, Teale WD, Trebar M, Blilou I, Palme K. 2005. The PIN auxin efflux facilitators: evolutionary and functional perspectives. *Trends Plant Sci.* **10:** 170-177.

Park S, Cohen JD, Slovin JP. 2006. Strawberry fruit protein with a novel indole-acyl modification. *Planta* **224:** 1015-1022.

Parry G, Calderón-Villalobos LI, Prigge M, Peret B, Dharmasiri S, Itoh H, Lechner E, Gray WM, Bennett M, Estelle M. 2009. Complex regulation of the TIR1/AFB family of auxin receptors. *Proc. Natl. Acad. Sci. USA* **106:** 22540-22545.

Pedrazzini E, Komarova NY, Rentsch D, Vitale A. 2013. Traffic routes and signals for the tonoplast. *Traffic* **14:** 622-628.

Peer WA. 2013. From perception to attenuation: auxin signalling and responses. *Curr. Opin. Plant Biol.* **16:** 561-568.

Peng J, Richards DE, Hartley NM, Murphy GP, Devos KM, Flintham JE, Beales J, Fish LJ, Worland AJ, Pelica F, Sudhakar D, Christou P, Snape JW, Gale MD, Harberd NP. 1999. 'Green revolution' genes encode mutant gibberellin response modulators. *Nature* **400:** 256-261.

Péret B, Swarup K, Ferguson A, Seth M, Yang YD, Dhondt S, James N, Casimiro I, Perry P, Syed A, Yang HB, Reemmer J, Venison E, Howells C, Perez-Amador MA, Yun J, Alonso J, Beemster G, Laplaze L, Murphy A, Bennett MJ, Nielsen E, Swarup R. 2012. AUX/LAX genes encode a family of auxin influx transporters that perform distinct functions during *Arabidopsis* development. *Plant Cell* **24:** 2874-2885.

Petrášek J, Mravec J, Bouchard R, Blakeslee JJ, Abas M, Seifertová D, Wiśniewska J, Tadele Z, Kubeš M, Čovanová M, Dhonukshe P, Skůpa P, Benková E, Perry L, Křeček P, Lee R, Fink GR, Geisler M, Murphy AS, Luschnig C, Zažímalová E, Friml J. 2006. PIN proteins perform a rate-limiting function in cellular auxin efflux. *Science* **312:** 914-918.

Pollmann S, Duchting P, Weiler EW. 2009. Tryptophan-dependent indole-3-acetic acid biosynthesis by 'IAA-synthase' proceeds via indole-3-acetamide. *Phytochemistry* **70:** 523-531.

Pont-Lezica RF, McNally JG, Pickard BG. 1993. Wall-to-membrane linkers in onion epidermis: some hypotheses. *Plant Cell Environ.* **16:** 111-123.

Qiao F, Chang XL, Nick P. 2010. The cytoskeleton enhances gene expression in the response to the Harpin elicitor in grapevine. *J. Exp. Bot.* **61:** 4021-4031.

Rahman A, Bannigan A, Sulaman W, Pechter P, Blancaflor EB, Baskin TI. 2007. Auxin, actin and growth of the *Arabidopsis thaliana* primary root. *Plant J.* **50:** 514-528.

Ramos JA, Zenser N, Leyser O, Callis J. 2001. Rapid degradation of auxin/indoleacetic acid proteins requires conserved amino acids of domain II and is proteasome dependent. *Plant Cell* **13:** 2349-2360.

Rashotte AM, Poupart J, Waddell CS, Muday GK. 2003. Transport of the two natural auxins, indole-3-butyric acid and indole-3-acetic acid, in *Arabidopsis*. *Plant Physiol.* **133:** 761-772.

Rayle DL, Cleland RE. 1992. The Acid Growth Theory of auxin-induced cell elongation is alive and well. *Plant Physiol*. **99:** 1271-1274.

Razafsky D, Hodzic D. 2009. Bringing KASH under the SUN: the many faces of nucleo-cytoskeletal connections. *J. Cell Biol.* **186:** 461-472.

Reed RC, Brady SR, Muday GK. 1998. Inhibition of auxin movement from the shoot into the root inhibits lateral root development in Arabidopsis. *Plant Physiol.* **118:** 1369-1378.

Reid JB. 1993. Plant hormone mutants. *J. Plant Growth Regul.* **12:** 207-226.

Reinhardt D, Pesce ER, Stieger P, Mandel T, Baltensperger K, Bennett M, Traas J, Friml J, Kuhlemeier C. 2003. Regulation of phyllotaxis by polar auxin transport. *Nature* **426:** 255-260.

Rhen T, Cidlowski JA. 2005. Antiinflammatory action of glucocorticoids - new mechanisms for old drugs. *N. Engl. J. Med.* **353:** 1711-1723.

Robert HS, Friml J. 2009. Auxin and other signals on the move in plants. *Nat. ChemBiol.* **5:** 325-332.

Robert HS, Grones P, Stepanova AN, Robles LM, Lokerse AS, Alonso JM, Weijers D, Friml J. 2013. Local auxin sources orient the apical-basal axis in *Arabidopsis* embryos. *Curr. Biol.* **23:** 2506-2512.

Ron M, Avni A. 2004. The receptor for the fungal elicitor ethylene-inducing xylanase is a member of a resistance-like gene family in tomato. *Plant Cell* **16:** 1604-1615.

Sabatini S, Beis D, Wolkenfelt H, Murfett J, Guilfoyle T, Malamy J, Benfey P, Leyser O, Bechtold N, Weisbeek P, Scheres B. 1999. An auxin-dependent distal organizer of pattern and polarity in the Arabidopsis root. *Cell* **99:** 463-472.

Sano T, Higaki T, Oda Y, Hayashi T, Hasezawa S. 2005. Appearance of actin microfilament 'twin peaks' in mitosis and their function in cell plate formation, as visualized in tobacco BY-2 cells expressing GFP-fimbrin. *Plant J.* **44:** 595-605.

Sasaki A, Ashikari M, Ueguchi-Tanaka M, Itoh H, Nishimura A, Swapan D, Ishiyama K, Saito T, Kobayashi M, Khush GS, Kitano H, Matsuoka M. 2002. Green revolution: A mutant gibberellin-synthesis gene in rice. *Nature* **416:** 701-702.

Sawchuk MG, Edgar A, Scarpella E. 2013. Patterning of leaf vein networks by convergent auxin transport pathways. *PLoS Genet.* **9:** e1003294.

Schneider R, Persson S. 2015. Connecting two arrays: the emerging role of actin-microtubule cross-linking motor proteins. *Front Plant Sci.* **6:** 415.

Schroeder JI, Kwak JM, Allen GJ. 2001. Guard cell abscisic acid signalling and

engineering drought hardiness in plants. *Nature* **410:** 327-330.

Sharp WR, Gunckel JE. 1969. Physiological comparisons of pith callus with crown-gall and genetic tumors of *Nicotiana glauca*, *N. langsdorffii*, and *N. glauca-langsdorffii* grown *in vitro.* II. Nutritional Physiology. *Plant Physiol.* **44:** 1073-1079.

Shimizu-Sato S, Tanaka M, Mori H. 2009. Auxin–cytokinin interactions in the control of shoot branching. *Plant Mol. Biol.* **69:** 429-435.

Shoji K, Addicott FT, Swets WA. 1951. Auxin in relation to leaf blade abscission. *Plant Physiol.* **26:** 189-191.

Sidler M, Hassa P, Hasan S, Ringli C, Dudler R. 1998. Involvement of an ABC transporter in a developmental pathway regulating hypocotyl cell elongation in the light. *Plant Cell* **10:** 1623-1636.

Simon S, Petrášek J. 2011. Why plants need more than one type of auxin. *Plant Sci.* **180:** 454-460.

Skoog F, Miller CO. 1957. Chemical regulation of growth and organ formation in plant tissues cultured in vitro. *Symp. Soc. Exp. Biol.* **11:** 118-131.

Smertenko A, Franklin-Tong VE. 2011. Organisation and regulation of the cytoskeleton in plant programmed cell death. *Cell Death Differ.* **18:** 1263-1270.

Sokolowska K, Kizinska J, Szewczuk Z, Banasiak A. 2014. Auxin conjugated to fluorescent dyes - a tool for the analysis of auxin transport pathways. *Plant Biol.* doi: 10.1111/plb.12144.

Song Y. 2014. Insight into the mode of action of 2,4-dichlorophenoxyacetic acid (2,4-D) as an herbicide. *J. Integr. Plant Biol.* **56:** 106-113.

Sonner JM, Purves WK. 1985. Natural occurrence of indole-3-acetyl aspartate and indole-3-acetyl glutamate in cucumber shoot tissue. *Plant Physiol.* **77:** 784-785.

Stals H, Inze D. 2001. When plant cells decide to divide. *Trends Plant Sci.* **6:** 359-364.

Stepanova AN, Robertson-Hoyt J, Yun J, Benavente LM, Xie DY, Dolezal K, Schlereth A, Jürgens G, Alonso JM. 2008. TAA1-mediated auxin biosynthesis is essential for hormone crosstalk and plant development. *Cell* **133:** 177-191.

Strader LC, Culler AH, Cohen JD, Bartel B. 2010. Conversion of endogenous indole-3-butyric acid to indole-3-acetic acid drives cell expansion in *Arabidopsis* seedlings. *Plant Physiol.* **153:** 1577-1586.

Sun H, Basu S, Brady SR, Luciano RL, Muday GK. 2004. Interactions between auxin transport and the actin cytoskeleton in developmental polarity of Fucus distichus embryos in response to light and gravity. *Plant Physiol.* **135:** 266-278.

Swarup R, Friml J, Marchant A, Ljung K, Sandberg G, Palme K, Bennett M. 2001. Localization of the auxin permease AUX1 suggests two functionally distinct hormone transport pathways operate in the *Arabidopsis* root apex. *Genes Dev.* **15:** 2648-2653.

Swarup R, Kargul J, Marchant A, Zadik D, Rahman A, Mills R, Yemm A, May S, Williams L, Millner P, Tsurumi S, Moore I, Napier R, Kerr ID, Bennett MJ. 2004. Structure-function analysis of the presumptive *Arabidopsis* auxin permease AUX1. *Plant Cell* **16:** 3069-3083.

Swarup R, Kramer EM, Perry P, Knox K, Leyser HM, Haseloff J, Beemster GT, Bhalerao R, Bennett MJ. 2005. Root gravitropism requires lateral root cap and epidermal cells for transport and response to a mobile auxin signal. *Nat. Cell Biol.* **7:** 1057-1065.

Swarup R, Péret B. 2012. AUX/LAX family of auxin influx carriers: an overview. *Front. Plant Sci.* **3:** 225.

Szerszen JB, Szczyglowski K, Bandurski RS. 1994. *iaglu*, a gene from Zea mays involved in conjugation of growth hormone indole-3-acetic acid. *Science* **265:** 1699-1701.

Tamura K, Iwabuchi K, Fukao Y, Kondo M, Okamoto K, Ueda H, Nishimura M, Hara-Nishimura I. 2013. Myosin XI-i links the nuclear membrane to the cytoskeleton to control nuclear movement and shape in *Arabidopsis*. *Curr. Biol.* **23:** 1776-1781.

Tan X, Calderon-Villalobos LIA, Sharon M, Zheng CX, Robinson CV, Estelle M, Zheng N. 2007. Mechanism of auxin perception by the TIR1 ubiquitin ligase. *Nature* **446:** 640-645.

Tanaka H, Dhonukshe P, Brewer PB, Friml J. 2006. Spatiotemporal asymmetric auxin distribution: a means to coordinate plant development. *Cell. Mol. Life Sci.* **63:** 2738-2754.

Tao Y, Ferrer JL, Ljung K, Pojer F, Hong FX, Long JA, Li L, Moreno JE, Bowman ME, Ivans LJ, Cheng YF, Lim J. 2008. Rapid synthesis of auxin via a new tryptophan-dependent pathway is required for shade avoidance in plants. *Cell* **133:** 164-176.

Tiwari SB, Hagen G, Guilfoyle TJ. 2003. The roles of auxin response factor domains in auxin-responsive transcription. *Plant Cell* **15:** 533-543.

Tiwari SB, Hagen G, Guilfoyle TJ. 2004. Aux/IAA proteins contain a potent transcriptional repression domain. *Plant Cell* **16:** 533-543.

Ueda M, Zhang Z, Laux T. 2011. Transcriptional activation of *Arabidopsis* axis patterning

genes WOX8/9 links zygote polarity to embryo development. *Dev. Cell* **20:** 264-270.

Ulmasov T, Murfett J, Hagen G, Guilfoyle T. 1997. Aux/IAA proteins repress expression of reporter genes containing natural and highly active synthetic auxin response elements. *Plant Cell* **9:** 1963-1971.

Umemoto N, Kakitani M, Iwamatsu A, Yoshikawa M, Yamaoka N, Ishida I. 1997. The structure and function of a soybean b-glucan-elicitor-binding protein. *Proc. Natl. Acad. Sci. USA* **94:** 1029-1034.

Vanneste S, Friml J. 2009. Auxin: a trigger for change in plant development. *Cell* **136:** 1005-1016.

Vieten A, Sauer M, Brewer PB, Friml J. 2007. Molecular and cellular aspects of auxin-transport-mediated development. *Trends Plant Sci*. **12:** 160-168.

Viotti C. 2014. ER and vacuoles: never been closer. *Front. Plant Sci.* **5:** 20.

Viotti C, Falco K, Krebs M, Neubert C, Fink F, Lupanga U, Scheuring D, Boutté Y, Frescatada-Rosa M, Wolfenstetter S, Sauer N, Hillmer S, Grebe M, Schumacher K. 2013. The endoplasmic reticulum is the main membrane source for biogenesis of the lytic vacuole in *Arabidopsis*. *Plant Cell* **25:** 3434-3449.

Waller F, Riemann M, Nick P. 2002. A role for actin-driven secretion in auxin-induced growth. *Protoplasma* **219:** 72-81.

Wang D, Pei K, Fu Y, Sun Z, Li S, Liu H, Tang K, Han B, Tao Y. 2007. Genome-wide analysis of the auxin response factors (ARF) gene family in rice (*Oryza sativa*). *Gene* **394:** 13-24.

Wang QY, Nick P. 1998. The auxin response of actin is altered in the rice mutant Yin-Yang. *Protoplasma* **204:** 22-33.

Wang R, Estelle M. 2014. Diversity and specificity: auxin perception and signaling through the TIR1/AFB pathway. *Curr. Opin. Plant Biol.* **21:** 51-58.

Wang YS, Yoo CM, Blancaflor EB. 2008. Improved imaging of actin filaments in transgenic *Arabidopsis* plants expressing a green fluorescent protein fusion to the C- and N-termini of the fimbrin actin-binding domain 2. *New Phytol*. **177:** 525-536.

Weijers D, Schlereth A, Ehrismann JS, Schwank G, Kientz M, Jürgens G. 2006. Auxin triggers transient local signaling for cell specification in *Arabidopsis* embryogenesis. *Dev. Cell* **10:** 265-270.

Werner T, Motyka V, Strnad M, Schmülling T. 2001. Regulation of plant growth by cytokinin. *Proc. Natl. Acad. Sci. USA* **98:** 10487-10492.

Winkler M, Niemeyer M, Hellmuth A, Janitza P, Christ G, Samodelov SL, Wilde V, Majovsky P, Trujillo M, Zurbriggen MD, Hoehenwarter W, Quint Q, Calderón-Villalobos LI. 2017. Variation in auxin sensing guides AUX/IAA transcriptional repressor ubiquitylation and destruction. *Nat. Commun.* **8:** 15706.

Wisniewska J, Xu J, Seifertova D, Brewer PB, Ruzicka K, Blilou I, Rouquie D, Benkova E, Scheres B, Friml J. 2006. Polar PIN localization directs auxin flow in plants. *Science* **312:** 883.

Woodward AW, Bartel B. 2005. Auxin: regulation, action, and interaction. *Ann. Bot. (London)* **95:** 707-735.

Wright AD, Sampson MB, Neuffer MG, Michalczuk L, Slovin JP, Cohen JD. 1991. Indole-3-acetic acid biosynthesis in the mutant maize orange pericarp, a tryptophan auxotroph. *Science* **254:** 998-1000.

Wyatt SE, Carpita NC. 1993. The plant cytoskeleton - cell wall continuum. *Trends Cell Biol.* **3:** 413-417.

Wymer CL, Wymer SA, Cosgrove DJ, Cyr RJ. 1996. Plant cell growth responds to external forces and the response requires intact microtubules. *Plant Physiol.* **110:** 425-430.

Yamada M, Greenham K, Prigge MJ, Jensen PJ, Estelle M. 2009. The TRANSPORT INHIBITOR RESPONSE2 (TIR2) gene is required for auxin synthesis and diverse aspects of plant development. *Plant Physiol.* **151:** 168-179.

Yamamoto M, Yamamoto KT. 1998. Differential effects of 1-naphthaleneacetic acid, indole-3-acetic acid and 2,4-dichlorophenoxyacetic acid on the gravitropic response of roots in an auxin-resistant mutant of Arabidopsis, *aux1*. *Plant Cell Physiol.* **39:** 660-664.

Yang H, Murphy AS. 2009. Functional expression and characterization of *Arabidopsis* ABCB, AUX 1 and PIN auxin transporters in Schizosaccharomyces pombe. *Plant J.* **59:** 179-191.

Yang Y, Hammes UZ, Taylor CG, Schachtman DP, Nielsen E. 2006. High-affinity auxin transport by the AUX1 influx carrier protein. *Curr. Biol.* **16:** 1123-1127.

Yang Y, Xu R, Ma CJ, Vlot AC, Klessig DF, Pichersky E. 2008. Inactive methyl indole-3-acetic acid ester can be hydrolyzed and activated by several esterases belonging to the AtMES esterase family of *Arabidopsis*. *Plant Physiol.* **147:** 1034-1045.

Yang ZB, Liu GC, Liu JJ, Zhang B, Meng WJ, Müller B, Hayashi K, Zhang XS, Zhao Z, Smet ID, Ding ZJ. 2017. Synergistic action of auxin and cytokinin mediates aluminum-induced root growth inhibition in *Arabidopsis*. *EMBO Rep.* **18:** 1213-1230.

Zaban B, Maisch J, Nick P. 2013. Dynamic actin controls polarity induction *de novo* in protoplasts. *J. Integr. Plant Biol.* **55:** 142-159.

Zaban B, Liu W, Jiang X, Nick P. 2014. Plant cells use auxin efflux to explore geometry. *Sci. Rep.* **4:** 5852.

Zažímalová E, Křeček P, Skůpa P, Hoyerová K, Petrášek J. 2007. Polar transport of the plant hormone auxin - the role of PIN-FORMED (PIN) proteins. *Cell. Mol. Life Sci.* **64:** 1621-1637.

Zenser N, Ellsmore A, Leasure C, Callis J. 2001. Auxin modulates the degradation rate of Aux/IAA proteins. *Proc. Natl. Acad. Sci. USA* **98:** 11795-11800.

Zhang NG, Hasenstein KH. 1999. Initiation and elongation of lateral roots in *Lactuca sativa*. *Int. J. Plant Sci.* **160:** 511-519.

Zhao Y. 2010. Auxin biosynthesis and its role in plant development. *Annu. Rev. Plant Biol*. **61:** 49-64.

Zhao Y. 2012. Auxin biosynthesis: a simple two-step pathway converts tryptophan to indole-3-acetic acid in plants. *Mol. Plant* **5:** 334-338.

Zhao Y, Hull AK, Gupta NR, Goss KA, Alonso J, Ecker JR, Normanly J, Chory J, Celenza JL. 2002. Trp-dependent auxin biosynthesis in *Arabidopsis*: involvement of cytochrome P450s CYP79B2 and CYP79B3. *Genes Dev.* **16:** 3100-3112.

Zhu JK. 2002. Salt and drought stress signal transduction in plants. *Annu. Rev. Plant Biol*. **53:** 247-273.

Zhu JS, Geisler M. 2015. Keeping it all together: auxin-actin crosstalk in plant development. *J. Exp. Bot.* **66:** 4983-4998.

Zipfel C, Kunze G, Chinchilla D, Caniard A, Jones JD, Boller T, Felix G. 2006. Perception of the bacterial PAMP EF-Tu by the receptor EFR restricts *Agrobacterium*-mediated transformation. *Cell* **125:** 749-760.

6. Appendix

PUBLICATIONS

Xiang Huang, Jan Maisch, Peter Nick. **2017.** Sensory role of actin in auxin-dependent responses of tobacco BY-2. *Journal of Plant Physiology* 218: 6-15.